

ICE PLASMON POLARITONS AND DETERMINATIO  
X DIELECTRIC PERMITTIVITY AND THICKNESS  
THIN METAL (SEMICONDUCTOR) FILMS

By

ABDURAHMAN AHMED

A Thesis

Presented to the  
School of Graduate Studies  
and  
The Faculty of Science  
Addis Ababa University

In Partial Fulfillment of the  
Requirement for the Degree  
Master of Science in Physics

June, 1989

ADDIS ABABA UNIVERSITY  
SCHOOL OF GRADUATE STUDIES

Surface Plasmon Polaritons and Determination of  
Complex Dielectric Permittivity and Thickness  
Of Thin Metal (Semiconductor) Films

By

Abdurahman Ahmed  
Faculty of Science

Approved By the Examining Board:

Dr. V.S. Varma  
External Examiner

Vijaya Varma

Dr. D. Letov  
Advisor

Letov

Dr. J. Jelen  
Examiner

J. Jelen

Dr. P. Hruska  
Examiner

P. Hruska

## Abstract

Surface plasmon-polaritons (SPP) which can be excited on dielectric/metal (dielectric/semiconductor) interface can be used as highly sensitive non destructive probe for the determination of the dielectric constant  $\epsilon(\omega) = \epsilon'(\omega) + i\epsilon''(\omega)$  and thickness  $h$  of a metal (semiconductor) film without a preset expression for  $\epsilon(\omega)$ .

The theoretical background of the method [3] is based on the solution of the Maxwell's equations which provides the dispersion equation of SPP at the surface of a thin metal (semiconductor) film and its interpretation in terms of attenuated total reflection (ATR) characteristics. The physical sense of the solution is demonstrated through the power flows and the field distributions of SPP and other possible excitations.

It is shown that for strong absorbing metals (semiconductors) low radiative SPP can exist at frequencies higher than the plasma frequency  $\omega_p$ . The analysis of the approximate solution of the approximate solution of dispersion equation for thin metal (semiconductor) film [3] established a well-defined limited frequency range of its applicability. It was found that the upper frequency limit depends upon the thickness of the film and falls down from  $\omega_p/\sqrt{2}$  to  $\sim 0.35 \omega_p$  as  $h \rightarrow 0$ .

A computer model simulating realistic experimental conditions of measurement ATR characteristics is discussed. The accuracy of  $\epsilon'(\omega)$ ,  $\epsilon''(\omega)$  and  $h$  determination is established.

### ACKNOWLEDGEMENT

I would like to express my deepest gratitude and respect to my advisor and instructor Dr. D.A. Letov for paying series attention to the work accomplished, and his persistent assistance and guidance in the computer program. In addition, I owe a debt to him who aroused my interest, for further research (in this field, and from whose lectures I benefited much.

I am also grateful to Dr. P. Hurshka for his guidance in applying numerical analysis and the basic knowledge of a computer. My gratitude also goes to W/O Shenaz Ahmed who undertook to type this paper work in devoting her valuable time.

Introduction.....	i
Chapter 1 Surface plasmon-polaritons on the interface of metal (semiconductor) with a dielectric medium....	1
1.1 Derivation of SPlP dispersion equation semi-infinite case.....	1
1.2 The analysis of the dispersion equation.....	8
1.3 Dispersion equation for strong absorption case.....	30
Chapter 2 Surface plasmon polaritons analysis through the phenomena of attenuated total reflection.....	33
2.1 Derivation of SPlP for dielectric medium 1-metal film-dielectric medium 3.....	33
2.2 Approximate solution for the dispersion equation.....	36
2.3 Excitation of SPlP by attenuated total reflection technique.....	42
2.4 ATR model.....	49
2.5 Typical results.....	53
Chapter 3 Applied theory of surface plasmon polaritons.....	59
3.1 Use of SPlP for determination of the thickness and optical constants of thin metallic film....	59
3.2 A suggested modification of the method for the determination of $\epsilon(\omega)$ and $h$ .....	60
3.3 The accuracy of the method.....	62
3.4 The computer program.....	64
3.5 Analysis of the methods accuracy.....	67
Summary.....	75
References.....	77
Appendix A	
Appendix B	

The internal degrees of freedom of a medium generally excited by the passage through it of an electromagnetic wave. Infact because of the medium, the electromagnetic wave becomes a new type of wave in which the original electromagnetic field is modified by the induced polarization of the medium. This new mode of excitation is known as a polariton. For example, a photon coupled to the elementary excitation of an electron plasma in metals or semiconductors is called a plasmon polariton. A photon coupled to the lattice vibration in a crystal is called a phonon polariton, and so on.

Under certain conditions plasmon polariton propagates along the boundary of metals or semi-conductors with dielectric medium (discussed in Chapter I).

This type of elementary excitations is called a surface plasmon polariton (SP1P). The electric and magnetic fields of SP1P are taking maximum values at the interface metal or semiconductor/dielectric medium and are exponentially decaying with distance from a boundary in the direction of normal.

Concentration of the electromagnetic field near the metal or semiconductor surface makes SP1P very sensitive to minor changes in characteristic quantities of interfacing media (like complex dielectric permittivity  $\epsilon = \epsilon' + i\epsilon''$ ) and to the state of roughness of the boundary.

Therefore SP1P constitutes a highly sensitive non-destroying probe for measuring purposes, particularly in the optical and infra-red range of frequencies.

Practical implementation of this possibility relates with the techniques of attenuated total reflection (ATR) through which SPlP is excited in the specified range of frequencies. The demands of this technique is based on the fundamental properties of SPlP which is the subject of investigation in Chapter I.

Excitation of SPlP is also possible when we deal with metal or semi-conductor thin film bounding dielectric media.

Particularities brought about by a finite thickness  $H$  of the film are discussed in Chapter II.

The approximate dispersion equation of SPlP at a thin metal or semi-conductor film and the approximate theory of ATR, showing the relationship between the reflected radiation and  $\epsilon'$ ,  $\epsilon''$ ,  $H$  of the thin film are the subject of Chapter II.

Chapter II is also dedicated to the exact theory of ATR, showing how the dispersion equation of SPlP can be interpreted in terms of the resonant angle of ATR.

The equations derived in Chapter II form the theoretical basis of the method for the determination of  $\epsilon'$ ,  $\epsilon''$  and  $H$  of metal and semi-conductor films via SPlP excitation using ATR technique.

In Chapter III a computer model simulating realistic experimental conditions of measurement ATR characteristics is discussed. The accuracy of  $\epsilon'$ ,  $\epsilon''$  and  $H$  determination is established.

## Chapter I

### 1.1 Derivation of SPLP dispersion equation semiinfinite media case.

Suppose a TM polarization  $\vec{H} = H_z \hat{z}$  wave is incident on the interface  $n_1/n_2$  of two media as shown in Fig. (1.1).

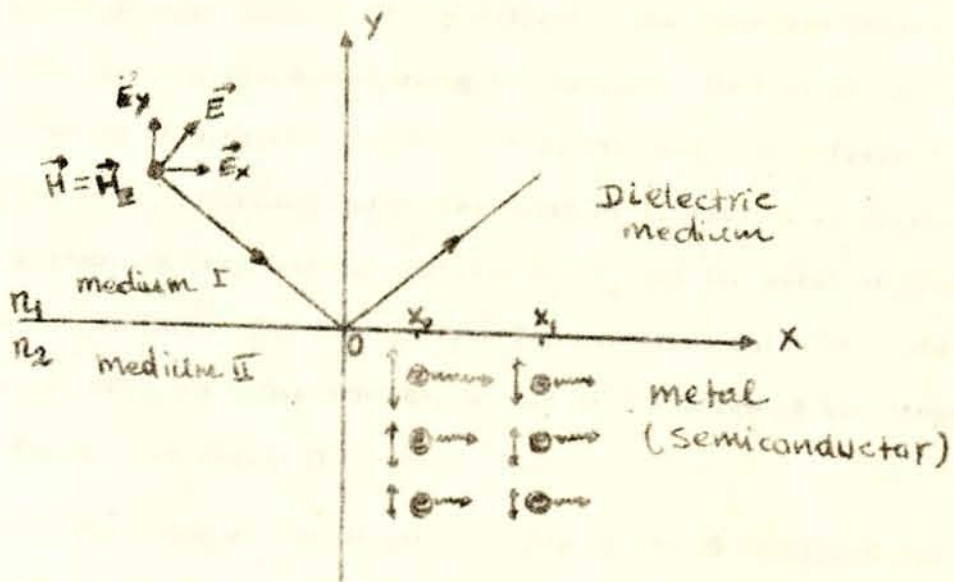


Fig. (1.1) General view of a boundary between semi-infinite dielectric medium and semi-infinite metal or semiconductor.

$$\vec{H} = \langle 0, 0, H_z \rangle \text{ ----- (1)}$$

Maxwell's Curl equations and equation (1) yield in

$$\vec{E} = \vec{E}_x + \vec{E}_y \text{ ----- (2)}$$

where  $E_x$  is parallel to the interface, and  $E_y$  is perpendicular to the interface. It is known from the electromagnetic theory that an accelerating charge radiates a secondary electromagnetic wave in the direction perpendicular to the direction of the charges motion. This implies that the  $E_x$  component of the incident primary radiation sets up the oscillation of an electron at metal or semiconductor surface

$X = X_0$  in the OX direction. The secondary radiation is in the OY direction. The radiation in the  $y > 0$  direction adds up to the radiation reflected from the  $n_1/n_2$  interface. The radiation in the  $y < 0$  direction is absorbed by the und medium.

The EY component of the electric field produces oscillation of the electron perpendicular to the surface. The secondary radiation from the electron propagates along the surface. Part of the secondary radiation in OX direction contributes to the radiation reflected from the  $n_1/n_2$  interface and another part of it sets up oscillations of electrons in neighbouring position  $X = X_1$  and the metal or semiconductor surface. The same is true for electrons which are situated below the metal or semiconductor surface at distances of the range of skin depth. See Fig. (1.1)

Transmittance of the OY oscillations in the OX direction via secondary radiation represent a new mode of excitation called surface plasmon polariton (SPP).

Now, let us see the electric and magnetic fields of the guided SPP.

Suppose the  $H_z$  in medium II can be described as:

$$H_{z2}^P = A_2 e^{-iK_{2y}y} e^{i(K_x X - \omega t)} \quad (1.3)$$

where  $K_{2y} = K_{2y}' + iK_{2y}''$  ;  $K_x = K_x' + iK_x''$  (the wave vectors) are describing propagation along OY direction and OX direction (along the surface) respectively.

But from the boundary condition,  $H_{2t} - H_{1t} = \hat{J}$  (where  $H_{it}$ ,  $(i=1,2)$  is the tangential component of the magnetic field, and  $J$  is linear density of the current flowing parallel to the interface), if there is no external source,  $\hat{J} = 0$  then

then

$$H_{2t} = H_{1t} \text{-----} \quad (4a)$$

equation (4a) implies that there must be some distribution of magnetic field in medium I. Supposing that, magnetic field distribution in medium I is of the same nature as in medium II,

$$H_{Z1}^P = A_1 e^{ik_{1y}Y} e^{i(K_X X - wt)} \text{-----} \quad (4b)$$

where  $K_{1y} = K_{1y}^{\parallel} + iK_{1y}^{\perp}$  is wave vector that describes propagation along OY direction in medium I. The value of  $K_X$  must be universal for both medium, since the electric and magnetic fields in medium I and in medium II are to be matched at  $Y = 0$ , at any arbitrary value of  $X$ .

From the boundary condition

$$H_{Z2}^P (Y=0) = H_{Z1}^P (Y = 0)$$

which results  $A_2 = A_1 = A$ , where  $A$  is the amplitude. Now let us consider the boundary condition for tangential components of the electric field,  $E_x$  component in this case

$$E_{x2} = E_{x1} \quad \text{at } Y = 0.$$

From Maxwell's curl equation we can express  $E_x$  through  $H_z$ , that is

$$\nabla \times \vec{H}_z = \epsilon \frac{\partial \vec{E}}{\partial t} + \vec{J}, \text{ but } \vec{J} = 0$$

or

$$\begin{vmatrix} i & j & k \\ \frac{\partial}{\partial x} & \frac{\partial}{\partial y} & 0 \\ 0 & 0 & H_z \end{vmatrix} = -i\omega\epsilon(\vec{E}_x + \vec{E}_y)$$

$$H_{Z2}^P = A e^{-ik_{2y}Y} e^{i(k_x X - wt)}$$

$$H_{Z1}^P = A e^{i k_{1y} Y} e^{i(k_x X - wt)}$$

$$\frac{\partial H_z}{\partial y} = -i\omega E_x ; E_x = -\frac{i}{\omega\epsilon} \frac{\partial H_z}{\partial y}$$

$$\frac{\partial H_z}{\partial x} = i\omega E_y ; E_y = -\frac{i}{\omega\epsilon} \frac{\partial H_z}{\partial x}$$

then it follows

$$E_{x1} = -\frac{K_{1y}}{i\omega\epsilon_1} H_{z1}^P$$

$$E_{x2} = +\frac{K_{2y}}{i\omega\epsilon_2} H_{z2}^P$$

$$\text{At } Y = 0 ; -\frac{K_{1y}}{\epsilon_1} = +\frac{K_{2y}}{\epsilon_2}$$

$$\text{Or } \frac{K_{1y}}{k_{2y}} = -\frac{\epsilon_1}{\epsilon_2} \quad \text{or} \quad \frac{K_{1y}}{k_{2y}} = -\frac{\epsilon_{r1}}{\epsilon_{r2}} \quad \text{-----} \quad (16)$$

where  $\epsilon_{r1}$  and  $\epsilon_{r2} = \epsilon_{r2}' + i\epsilon_{r2}''$  are relative dielectric permittivities of medium I and medium II respectively. From now on we shall operate with relative dielectric permittivities only. Therefore, for short writtining representation we shall denote again  $\epsilon_{r1}$  as  $\epsilon_1$ , and  $\epsilon_{r2}$  as  $\epsilon_2$ .

Now let us find the relationship between  $K_{1y}$  and  $K_1$  using the wave equation.

$$\nabla^2 H_z = \frac{\epsilon_1}{c^2} \frac{\partial^2 H_z}{\partial t^2} \quad \text{-----} \quad (17)$$

Since we assume that  $H_{z1}^P = e^{i(k_1 x + k_{1y} Y - \omega t)} = e^{i(k_x x + k_{1y} Y - \omega t)}$  equation (17) can be written as

$$\vec{K}_1 \cdot \vec{K}_1 = K_0^2 \epsilon_1 \text{ ----- (1.8)}$$

$$K_1'^2 - K_1''^2 + 2iK_1' K_1'' \cos(\angle K_1' K_1'') = K_0^2 \epsilon_1 \text{ ----- (1.8a)}$$

Resolving equation (1.8) into real and imaginary parts, we get:

$$K_1'^2 - K_1''^2 = K_0^2 \epsilon_1 \text{ ----- (1.9)}$$

$$2K_1' K_1'' \cos(\angle K_1' K_1'') = \text{----- (1.10)}$$

equation (1.10) indicates that in dielectric medium I  $\vec{K}_1' \perp \vec{K}_1''$

Next let us resolve  $K'$  and  $K''$  into components

$$\vec{K}_1' = K_{1x}' + K_{1y}' = K_x' + K_{1y}' \text{ ----- (1.11)}$$

$$\vec{K}_1'' = K_{1x}'' + K_{1y}'' = K_x'' + K_{1y}'' \text{ ----- (1.12)}$$

On the other hand let us consider

$$\begin{aligned} K_x'^2 + K_{1y}'^2 &= (K_x' + iK_x'')^2 + (K_{1y}' + iK_{1y}'')^2 \\ &= K_x'^2 - K_x''^2 + K_{1y}'^2 + 2i[K_x' K_x'' + K_{1y}' K_{1y}''] + K_{1y}''^2 \\ &= K_x'^2 + K_{1y}'^2 - K_x''^2 - K_{1y}''^2 + 2iK_1' K_1'' \cos(\angle K_1' K_1'') \\ &\cong K_1'^2 - K_1''^2 + 2iK_1' K_1'' \cos(\angle K_1' K_1'') \text{ ---- (1.13)} \end{aligned}$$

Comparison of equation (1.13) with equation (1.8a) gives results

$$\vec{K}_1 \cdot \vec{K}_1 = K_x^2 + K_{1y}^2 = K_0^2 \epsilon_1 \text{ ----- (1.14)}$$

Hence

$$K_{1y} = \sqrt{K_0^2 \epsilon_1 - K_x^2} \text{ ----- (1.15)}$$

Similar consideration for the conducting medium II, with

$$H_{z2}^p \sim e^{i(K_2 \cdot r - \omega t)} = e^{i(K_x x - K_{2y} y - \omega t)}$$

gives

$$\vec{K}_2 \cdot \vec{K}_2 = K_0^2 \epsilon_2 \text{ ----- (1.16)}$$

Or

$$K_2'^2 - K_2''^2 + 2iK_2' K_2'' \cos(\vec{K}_2' \wedge \vec{K}_2'') = K_0^2 \epsilon_2' + iK_0^2 \epsilon_2'' \text{ ----}$$

Resolving equation (1.17) into real and imaginary parts we get

$$K_2'^2 - K_2''^2 = K_0^2 \epsilon_2' \text{ ----- (1.18)}$$

$$2K_2' K_2'' \cos(\vec{K}_2' \wedge \vec{K}_2'') = K_0^2 \epsilon_2'' \text{ ---- (1.19)}$$

Equation (1.19) indicates that the angle between  $\vec{K}_2'$  and  $\vec{K}_2''$  is less than  $\pi/2$ , since  $\epsilon_2'' > 0$ .

On the other hand, let us consider the following

$$\begin{aligned} K_x^2 + K_{2y}^2 &= (K_x^1 + iK_x'')^2 + (K_{2y}' + iK_{2y}'')^2 \\ &= K_x^1{}^2 - K_x''^2 + K_{2y}'^2 - K_{2y}''^2 + 2i[K_x' K_x'' + K_{2y}' K_{2y}''] \\ &= K_2'^2 - K_2''^2 + 2iK_2' K_2'' \cos(\vec{K}_2' \wedge \vec{K}_2'') \text{ ---- (1.20)} \end{aligned}$$

Comparison of equation (1.20) with equations (1.18) and (1.19) results

$$\vec{K}_2 \cdot \vec{K}_2 = K_x^2 + K_{2y}^2 = K_0^2 \epsilon_2 \text{ ----- (1.21)}$$

Hence

$$K_{2y} = \sqrt{K_0^2 \epsilon_2 - K_x^2} \text{ ----- (1.22)}$$

The graphical representation for the components of  $\vec{K}_1$  and  $\vec{K}_2$  is shown at fig. (1.2) below.

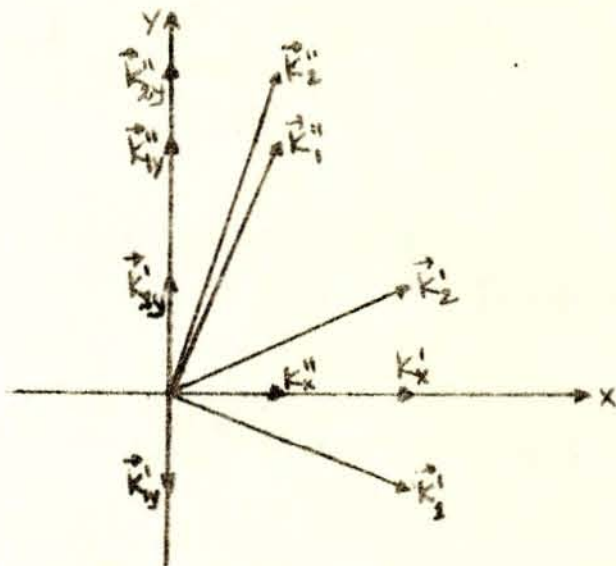


Fig.(1.2) The graph of  $\vec{K}_1$  and  $\vec{K}_2$  and their components in cartesian representation.

Substitution of equations (1.15) and (1.22) into equation (1.6) results

$$\sqrt{K_0^2 \epsilon_1 - K_x^2} = - \frac{\epsilon_1}{\epsilon_2} \quad (1.23)$$

$$\sqrt{K_0^2 \epsilon_2 - K_x^2}$$

Resolving equation (1.23) for  $K_x$  we receive

$$K_x = K_0 \sqrt{\frac{\epsilon_1 \epsilon_2}{\epsilon_1 + \epsilon_2}} \quad (1.24a)$$

Equation (1.24a) describes the dispersion equation of SP1P

where  $K_0 = \frac{W}{C}$  is the wave vector in vacuum

For metals the dielectric permittivity function of a free electron model is given by (1.24b) [1]. A medium with a positive dielectric function is often termed a 'passive medium', and commonly used examples of such media include air, vacuum, glass, etc. A medium with a negative dielectric function is called an 'active medium', and include metals and semiconductors at frequencies below the plasma frequency  $\omega_p$  [1].

$$\epsilon_2(\omega) = 1 - \frac{\omega_p^2}{\omega(\omega + i\tau^{-1})} = \epsilon_2' + i\epsilon_2'' \quad (1.24b)$$

$$= 1 - \frac{\omega_p^2}{(\omega^2 + \tau^{-2})} + i \frac{\omega_p^2}{\omega\tau} \cdot \frac{1}{(\omega^2 + \tau^{-2})}$$

which results

$$\epsilon_2'(\omega) = 1 - \frac{\omega_p^2}{(\omega^2 + \tau^{-2})} ; \quad \epsilon_2''(\omega) = \frac{\omega_p^2}{\omega\tau} \cdot \frac{1}{(\omega^2 + \tau^{-2})}$$

$$\omega_p^2 = \frac{N e^2}{\epsilon_0 m^*}$$

Where  $N$  is the free electron density,  $e$  is the electronic charge,  $\epsilon_0$  is permittivity of free space,  $m^*$  is the effective 'mass' and  $\tau$  is the relaxation time describes electron photon collision.

The dependence of  $\epsilon_2'$  and  $\epsilon_2''$  on the angular frequency  $\omega$  is seen at figure (1.7).

## 1.2 The Analysis of the Dispersion Equation

The simplest case in the analysis of the dispersion equation is, the case in which the absorbing part in the expression of  $\epsilon_2$  is zero tha

is  $\epsilon_2'' = 0$ . Under this case the whole range of frequencies could be separated into three sub ranges.

In the first subrange;  $0 < \omega < \frac{\omega_p}{\sqrt{\epsilon_1 + 1}}$  from equation (1.24a) we have;

$$\epsilon_2' < 0, \quad \epsilon_1 + \epsilon_2' < 0 \text{ and } K_x' > 0; \quad K_x'' = 0 \quad \text{-----} \quad (1.25)$$

From equation (1.15) and equation (1.22)

$$\begin{aligned} K_{1y}' &= 0; & K_{1y}'' &> 0 \\ K_{2y}' &= 0; & K_{2y}'' &> 0 \end{aligned} \quad \text{-----} \quad (1.26)$$

which means that a non radiative plasmon exists.

Let us support this conclusion from the general consideration of the energy flow.

Time average poynting vector component along OX direction is given in air at X=0 and Y=0 by

$$S_x^I = \frac{1}{2} R_e E_{oy}^I H_{oz}^{I*} = \frac{K_x'}{2\omega\epsilon_0\epsilon_1} \quad \text{-----} \quad (1.27)$$

in metal at X=0, and y=0

$$S_x^{II} = \frac{1}{2} R_e E_{oy}^{II} H_{oz}^{II*} = \frac{1}{2} \frac{[\epsilon_2' K_x' + \epsilon_2'' K_x'']}{\omega\epsilon_0 [\epsilon_2'^2 + \epsilon_2''^2]} \quad \text{-----} \quad (1.28)$$

Time average Poynting vector component along OY direction is given by, in air, at X=0, and y=0 by

$$S_y^I = -\frac{1}{2} R_e E_{ox}^I H_{oz}^{I*} = \frac{K_{ly}'}{2\omega\epsilon_0\epsilon_1} \quad \text{-----} \quad (1.29)$$

Similarly in metal at  $X=0$ , and  $Y=0$

$$S_y^{II} = -\frac{1}{2} R_e E_{ox}^{II} H_{oz}^{II} = -\frac{1}{2} \frac{[\epsilon_2' K_{2y}' + \epsilon_2'' K_{2y}'' ]}{W_o [\epsilon_2' / 2 + \epsilon_2'' / 2]} \quad (1.30)$$

The non absorbing case  $\epsilon_2'' = 0$  will be demonstrated as a limiting case of derived general formulas.

Suppose that

$$\epsilon_2'' < |\epsilon_2'|, \quad \epsilon_2'' < |(\epsilon_1 + \epsilon_2)|$$

Under these assumptions for  $0 < W < \frac{W_p}{\sqrt{\epsilon_1 + 1}}$

From equation (1.24a)

$$K_x' = K_o \sqrt{\frac{\epsilon_1 \epsilon_2'}{\epsilon_1 + \epsilon_2'}} > 0 \quad (1.31)$$

$$K_x'' = K_o \sqrt{\frac{\epsilon_1 \epsilon_2'}{\epsilon_1 + \epsilon_2}} \cdot \frac{\epsilon_1 \epsilon_2''}{2 \epsilon_2' (\epsilon_1 + \epsilon_2')} > 0 \quad (1.32)$$

See Fig. (1.3a) and Fig. (1.4a).

(Note that letter "a" corresponds to  $\tau = 10^{125} \text{ sec}$ )

From equation (1.15)

$$K_{ly}' = -\frac{K_x' K_x''}{K_{ly}''} = -\frac{K_o \epsilon_1 \epsilon_2'' \sqrt{-(\epsilon_1 + \epsilon_2')}}{2(\epsilon_1 + \epsilon_2')^2} < 0 \quad (1.33)$$

$$K_{ly}'' = \sqrt{K_x'^2 - K_o^2 \epsilon_1^2} = K_o \frac{\epsilon_1}{\sqrt{-(\epsilon_1 + \epsilon_2')}} > 0 \quad (1.34)$$

From equation (1.22)

$$K_{2y} = \frac{K_o^2 \epsilon_2'' - 2K_x' K_x''}{2K_{2y}''} = -K_o \frac{\epsilon_2'' (2\epsilon_1 + \epsilon_2') \sqrt{-(\epsilon_1 + \epsilon_2')}}{2(\epsilon_1 + \epsilon_2')^2} \quad (1.35)$$

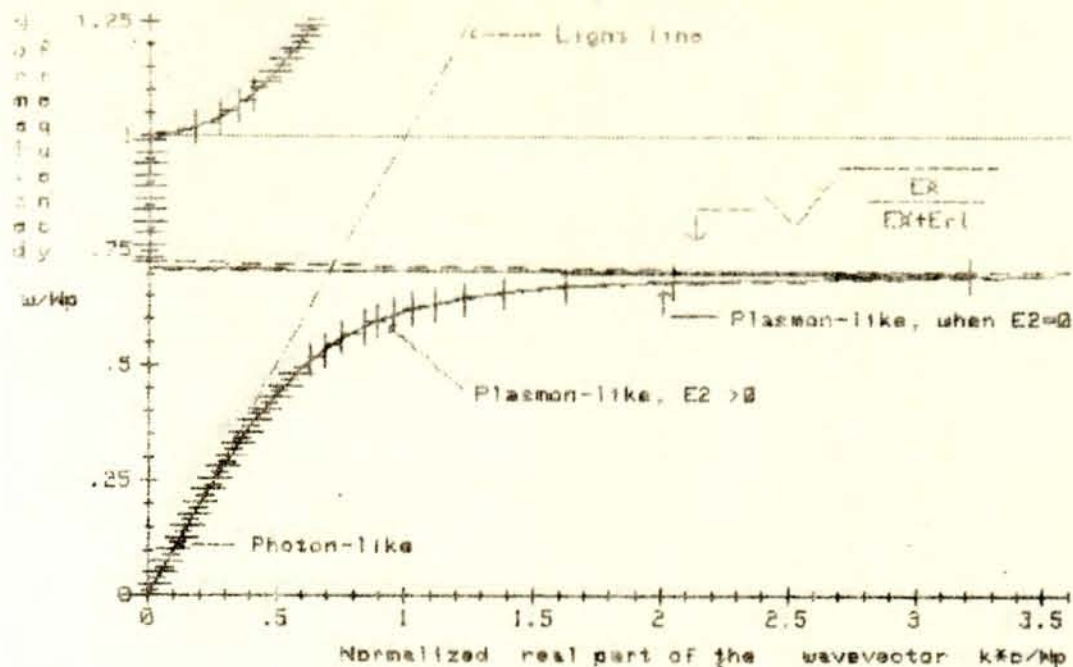


Fig (3a) Surface plasmon-polariton dispersion curve for a free electron metal plotted for: (a) real  $k$ , real  $\omega$  - (solid curve); (b) real  $\omega$ , real part of complex  $k$  - (broken line). The curves are plotted in dimensionless units.  $\omega_p = 1.E+15$  rad/e ;  $\tau = 1.E+125$  s

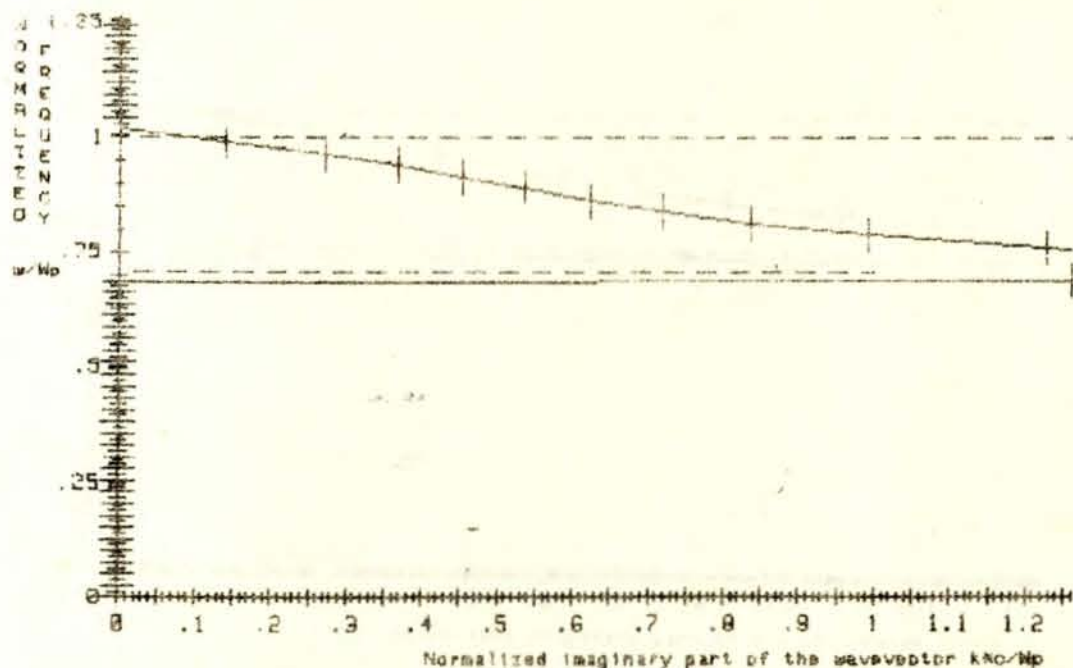
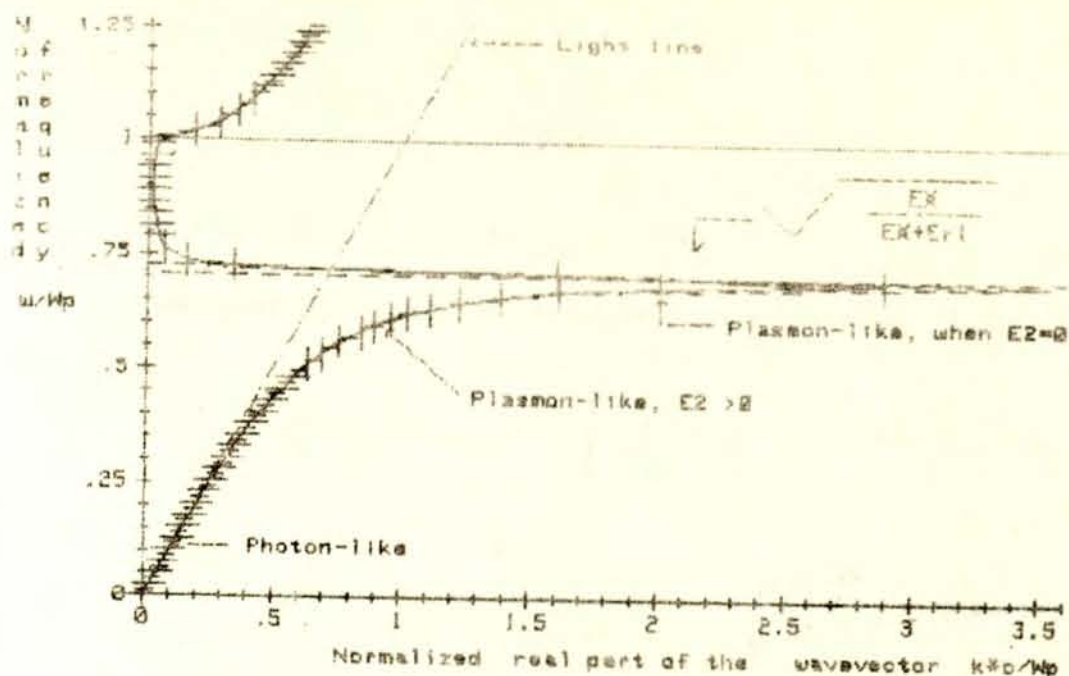
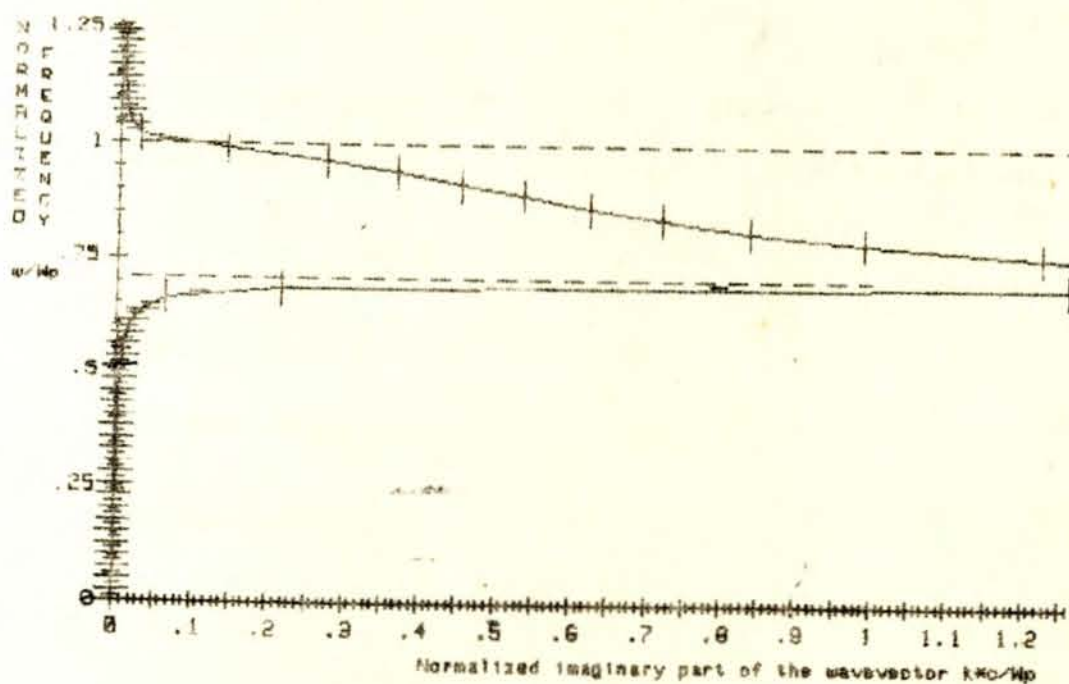


Fig (4a) Surface plasmon-polariton dispersion curve for imaginary part of complex  $k$  versus real  $\omega$ : (a) exact numerical solution - (||||| - line); (b) approximate analytical solution - (IIIII line).  $\omega_p = 1.E+15$  rad/e ;  $\tau = 1.E+125$  s



Fig(3b) Surface plasmon-polariton dispersion curve for a free electron metal plotted for: (a) real  $k$ , real  $\omega$  - (solid curve); (b) real  $\omega$ , real part of complex  $k$  - (dashed line). The curves are plotted in dimensionless units.  $\omega_p = 1.E+15$  rad/s ;  $\tau = 1.E-13$  s



Fig(4b) Surface plasmon-polariton dispersion curve for imaginary part of complex  $k$  versus real  $\omega$ : (a) exact numerical solution - (solid line); (b) approximate analytical solution - (dashed line).  $\omega_p = 1.E+15$  rad/s ;  $\tau = 1.E-13$  s

$$K_{2y}'' = K_0 \frac{\epsilon_2'}{\sqrt{-(\epsilon_1 + \epsilon_2')}} > 0 \text{ ----- (1.36)}$$

See Fig. (1.5a) and Fig. (1.5b)

From equations (1.27) to (1.30) and using equations (1.31) to (1.36)

$$S_x^I = \frac{K_0}{2W\epsilon_0} \frac{1}{\epsilon_1} \sqrt{\frac{\epsilon_1 \epsilon_2'}{\epsilon_1 + \epsilon_2'}} > 0 \text{ ---- (1.37)}$$

$$S_x^{II} = \frac{1}{2W\epsilon_0} \frac{K_x'}{\epsilon_2'} = \frac{K_0}{2W\epsilon_0 \epsilon_2'} \sqrt{\frac{\epsilon_1 \epsilon_2'}{\epsilon_1 + \epsilon_2'}} < 0 \text{ ---- (1.38)}$$

$$S_y^I = -\frac{K_0}{2W\epsilon_0} \left( \frac{\epsilon_2'' \sqrt{-(\epsilon_1 + \epsilon_2')}}{2(\epsilon_1 + \epsilon_2')^2} \right) < 0 \text{ ----- (1.39)}$$

$$S_y^{II} = -\frac{K_0}{2W\epsilon_0} \left( \frac{\epsilon_2'' \sqrt{-(\epsilon_1 + \epsilon_2')}}{2(\epsilon_1 + \epsilon_2')^2} \right) < 0 \text{ ----- (1.40)}$$

Let us normalize the power flows in equations (1.37) to (1.40) to the total power flow in both media. Since  $S_x'' < 0$ , we shall take it as follows:

$$S_{tot} = \sqrt{(S_x^I + |S_x^{II}|)^2 + S_y^2} \text{ ----- (1.41)}$$

where  $S_y = S_y^I = S_y^{II}$

For frequencies  $0 < \omega < \frac{\omega_p}{\sqrt{\epsilon_1 + 1}}$ ,  $S_y^2 \ll (S_x^I + |S_x^{II}|)^2$

therefore,

$$S_{tot} = S_x^I + |S_x^{II}|$$

$$K_0 \frac{\sqrt{\frac{\epsilon_1 \epsilon_2'}{\epsilon_1 + \epsilon_2'}}}{2W\epsilon_0} \left[ \frac{\epsilon_1 + |\epsilon_2'|}{\epsilon_1 \cdot |\epsilon_2'|} \right] \text{ ----- (1.42)}$$

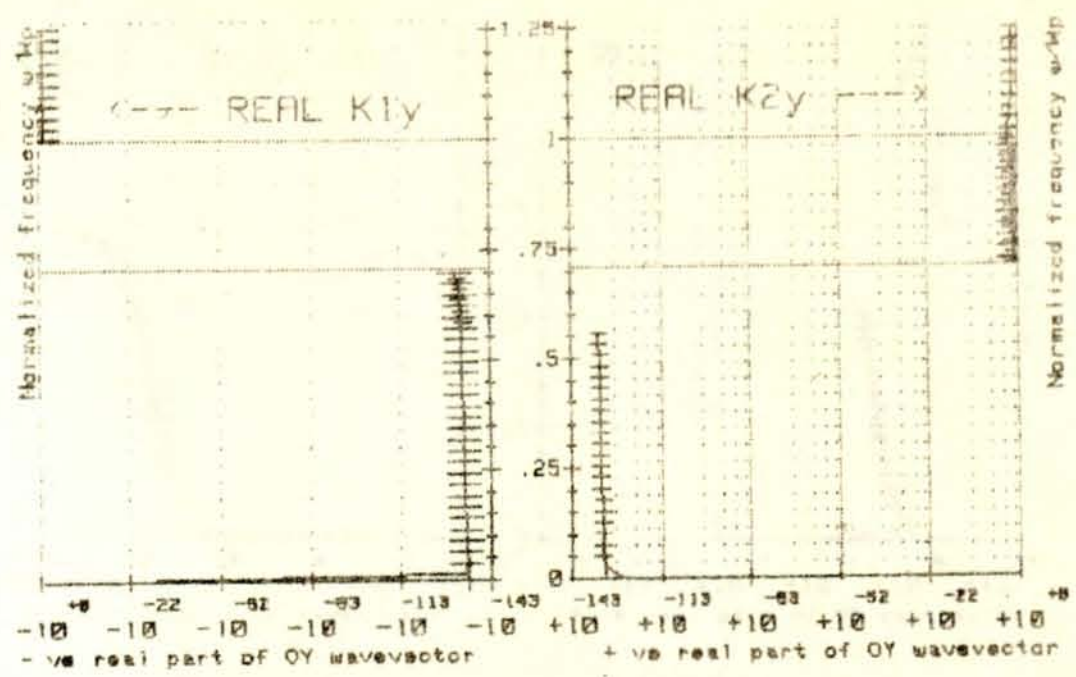


Fig (105a) REAL parts of the  $K_y$  wave vectors: (a) in dielectric medium 1 - ( |||| - line); (b) in metal - ( ||||| - line)  
 $\omega_p = 1.E+15$  rad/s;  $\tau = 1.E+125$  s<sup>-1</sup>

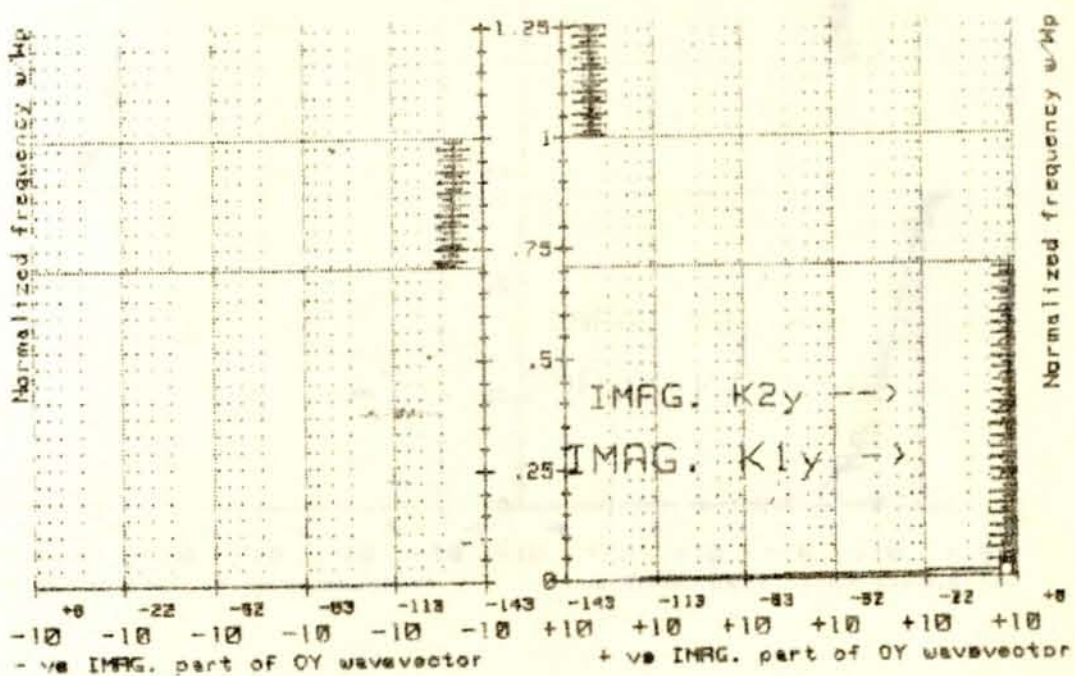


Fig (106a) Imaginary parts of the  $K_y$  wave vectors: (a) in dielectric medium 1 - ( |||| - line); (b) in metal - ( ||||| - line)  
 $\omega_p = 1.E+15$  rad/s;  $\tau = 1.E+125$  s<sup>-1</sup>

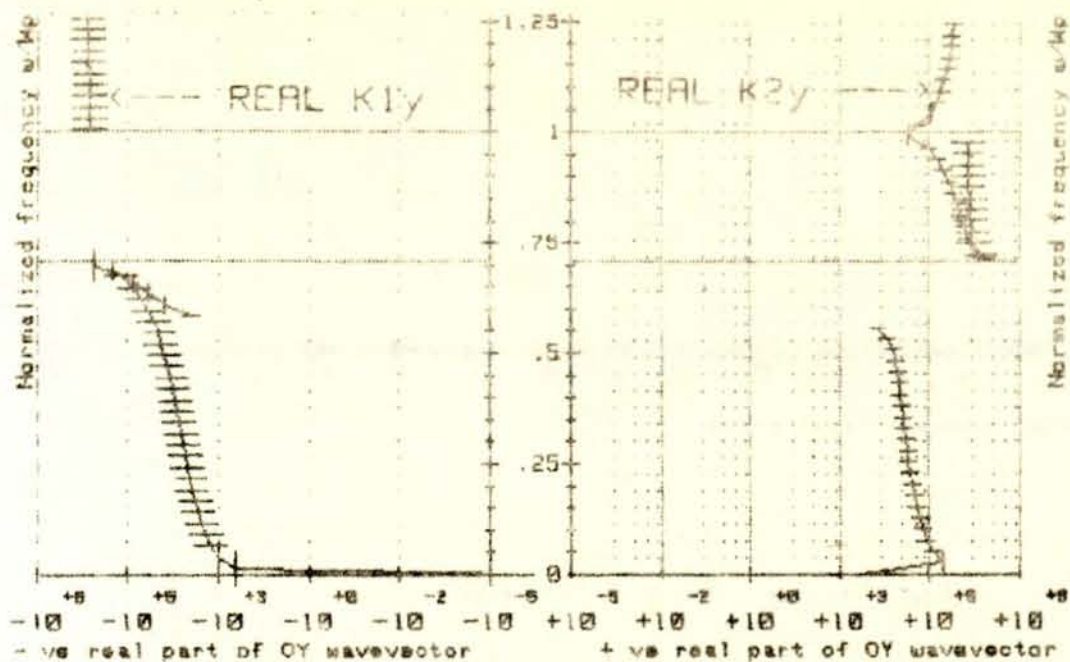


Fig (15b) REAL parts of the  $K_y$  wave vectors: (a) in dielectric medium 1 - ( |||| - line); (b) in metal - ( ||||| - line)  
 $\omega_p = 1.E+15$  rad/s;  $\tau = 1.E-13$  s

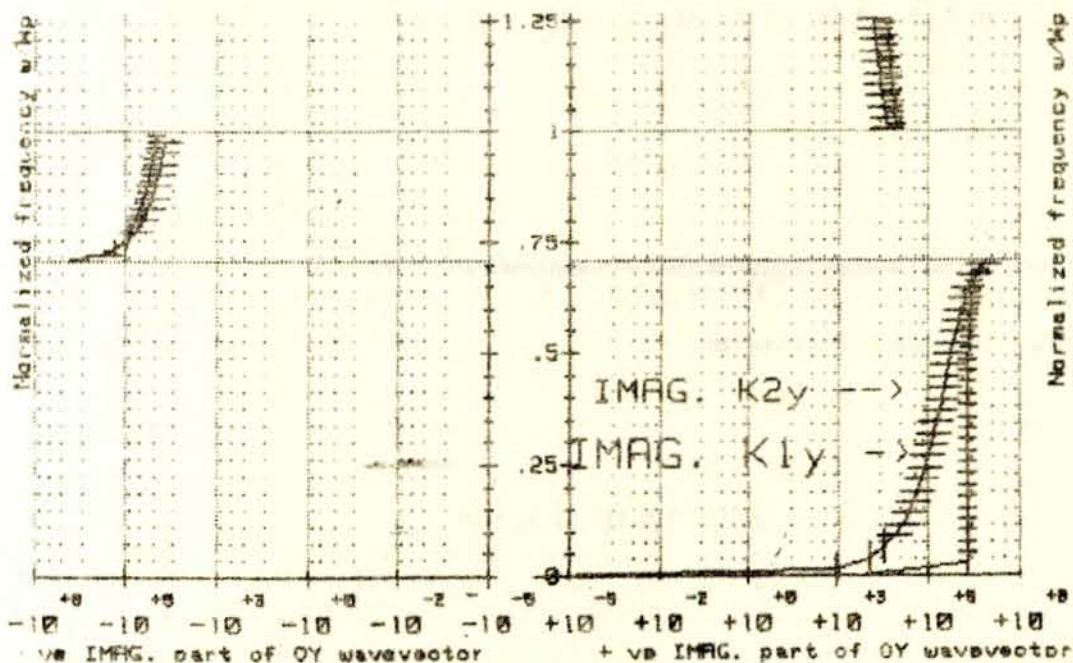


Fig (16b) Imaginary parts of the  $K_y$  wave vectors: (a) in dielectric medium 1 - ( |||| - line); (b) in metal - ( ||||| - line)  
 $\omega_p = 1.E+15$  rad/s;  $\tau = 1.E-13$  s

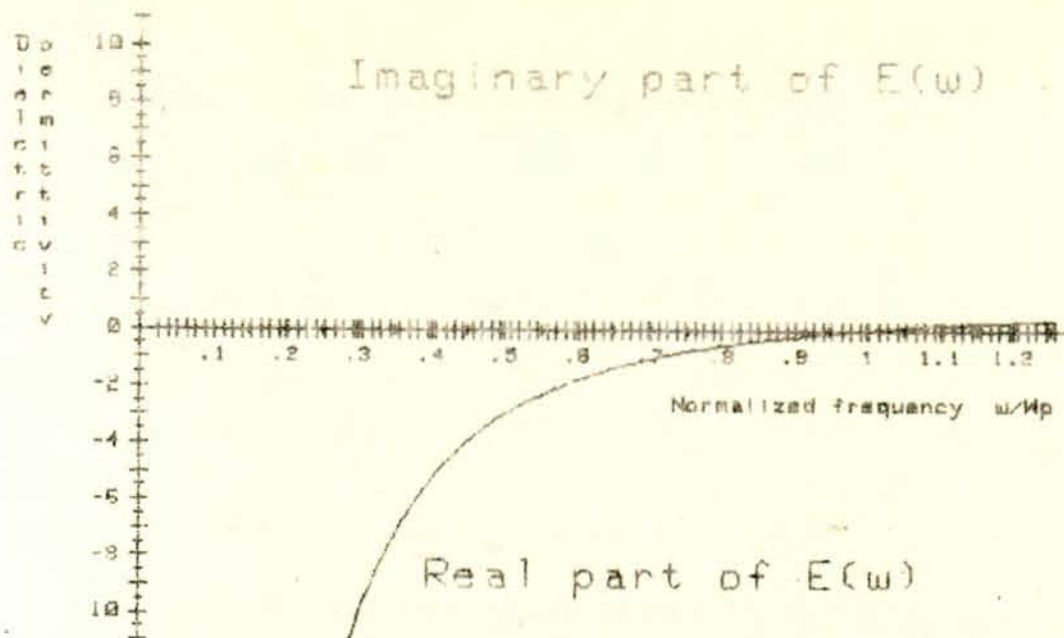


Fig. (a) Graph of dielectric permittivity versus normalized frequency: (a) real part of  $E(\omega)$  - (solid line) ; (b) imaginary part of  $E(\omega)$  - (broken line).  $\omega_p = 1.E+15 \text{ rad/s}$  ;  $\tau = 1.E+12 \text{ s}$

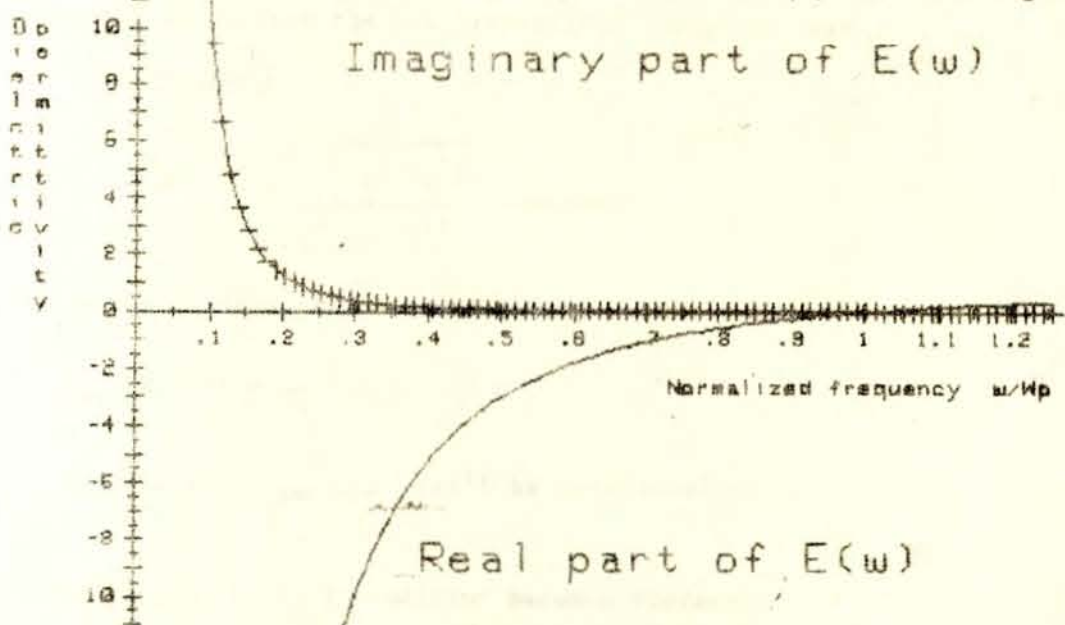


Fig. (b) Graph of dielectric permittivity versus normalized frequency: (a) real part of  $E(\omega)$  - (solid line) ; (b) imaginary part of  $E(\omega)$  - (broken line).  $\omega_p = 1.E+15 \text{ rad/s}$  ;  $\tau = 1.E-13 \text{ s}$

The normalized power flow can be expressed as:

$$S_{xn}^I = \frac{S_x^I}{S_{tot}} = \frac{|\epsilon_2'|}{\epsilon_1 + |\epsilon_2'|} \quad (1.43)$$

$$S_{xn}^{II} = \frac{S_x^{II}}{S_{tot}} = - \frac{\epsilon_1}{\epsilon_1 + |\epsilon_2'|} \quad (1.44)$$

In the limiting cases

$$S_{xn}^I (W = 0) = 1 \text{ and } S_{xn}^{II} (W = 0) = 0$$

which means that the whole energy is transmitted through dielectric medium I.

$$S_{xn}^I \left( W = \frac{W_p}{\sqrt{\epsilon_1 + 1}} \right) = \frac{1}{2}, \text{ and } S_{xn}^{II} \left( W = \frac{W_p}{\sqrt{\epsilon_1 + 1}} \right) = -\frac{1}{2}$$

which means that the net transmitted energy is zero.

(See Fig. 10a)

$$S_{yn} = \frac{\epsilon_2'' \sqrt{\epsilon_1 (-\epsilon_2')}}{2(\epsilon_1^2 - \epsilon_2'^2)} \quad (1.45)$$

In the limiting case (for  $\tau \rightarrow \infty$ )

$$S_{yn} (W = 0) = \frac{1}{2W_p \tau}$$

The case  $W = \frac{W_p}{\sqrt{\epsilon_1 + 1}}$  can't be considered since

$\epsilon_2'' \ll (\epsilon_1 + \epsilon_2')$  condition becomes violated.

The general behavior of  $S_{yn}$  can be seen from figures 9a and 10a

The field distribution of the plasmon describe by equations (1.3), (1.33) - (1.36) is shown at Fig. 10a.

The second subrange is,  $\frac{W_p}{\sqrt{\epsilon_1 + 1}} < W < W_p$ . In this subrange  $\epsilon_2' < 0$ ; and

$$\epsilon_2' + \epsilon_1 > 0.$$

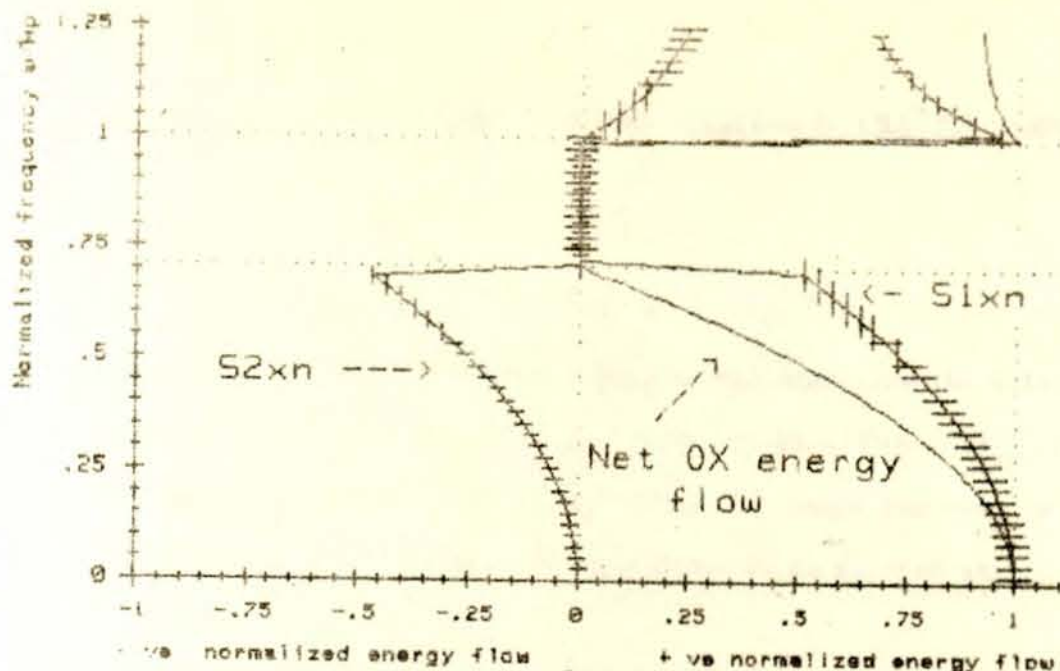


Fig (10a) Graph of normalized energy flow in OX direction as a function of normalized frequency: (a) - for medium 1 ( | | | | - line ), (b) - for medium 2 ( - - - - - line ), (c) - total energy flow in both media (solid line).  $\omega_p = 1.E+15$  rad/s ;  $\tau_{ou} = 1.E+125$  s

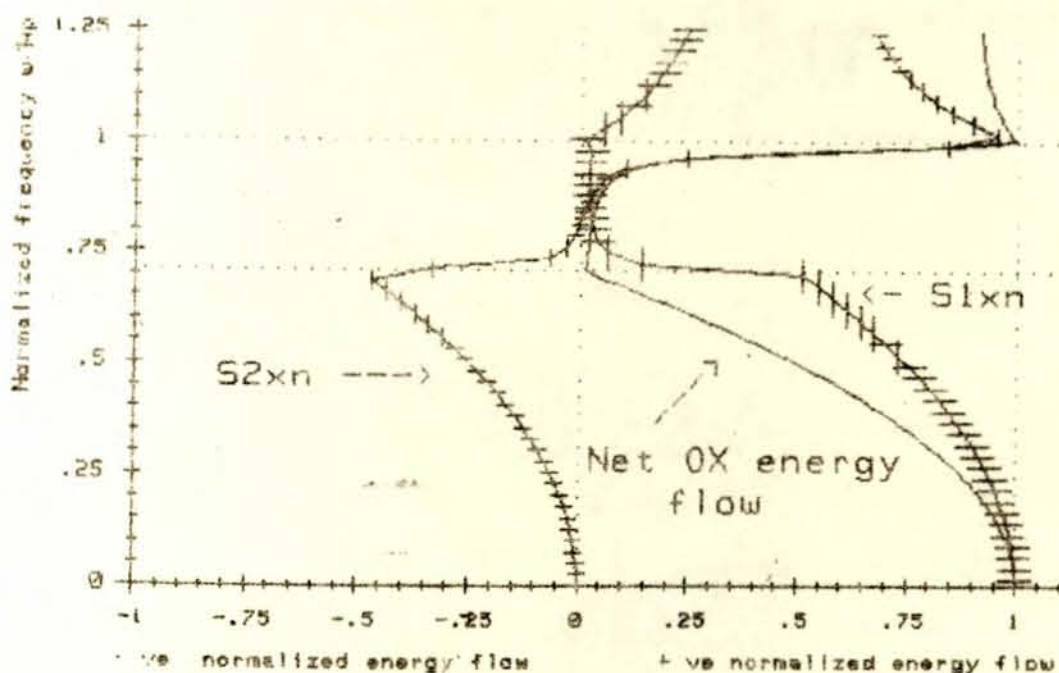


Fig (10b) Graph of normalized energy flow in OX direction as a function of normalized frequency: (a) - for medium 1 ( | | | | - line ), (b) - for medium 2 ( - - - - - line ), (c) - total energy flow in both media (solid line).  $\omega_p = 1.E+15$  rad/s ;  $\tau_{ou} = 1.E+13$  s.

$$S_{tot} = \frac{K_0}{2W\epsilon_0 \sqrt{\epsilon_1 + \epsilon_2'}} \quad (1.56)$$

Therefore the normalized power flow can be expressed as:

$$S_{yn}^I = S_{yn}^{II} = \pm 1 \quad (1.57)$$

$$S_{xn}^I = \frac{\epsilon_2'' \cdot \sqrt{\epsilon_1 \cdot (-\epsilon_2')}}{4 \cdot (-\epsilon_2') \cdot (\epsilon_1 + \epsilon_2')} > 0 \quad (1.58)$$

( $S_{xn}^I$  is the order of  $10^{-3}$  in the middle of the subrange)

$$S_{xn}^{II} = \frac{\epsilon_2'' \sqrt{\epsilon_1 (-\epsilon_2')} \cdot (\epsilon_1 + 2\epsilon_2')}{4\epsilon_2' (\epsilon_1 + \epsilon_2')} = S_{xn}^I \cdot \frac{(\epsilon_1 + 2\epsilon_2')}{(-\epsilon_2')} \quad (1.59)$$

The sign of  $S_{xn}^{II}$  depends upon the sign of  $(\epsilon_1 + 2\epsilon_2')$  term. For  $\frac{W}{W_p} < W < \frac{W_p}{\sqrt{\epsilon_1 + 1}}$  it is negative, elsewhere it is positive.

The results discussed in equations (1.57) - (1.59) are shown at figures (18a), (19a) and (19\*a).

The field distribution of the excitation that exists in the second subrange is shown at figures 14a and 14\*a. They correspond to the same frequency  $\frac{W}{W_p} = 0.70732$  but different in scale in the direction normal to the surface.

Third subrange is  $W > W_p$  in this subrange  $\epsilon_2' > 0$  and  $\epsilon_1 + \epsilon_2' > 0$ .

For ideal case  $\epsilon_2'' = 0$  from equations (1.15), (1.22) and (1.24a)

we get

$$K_x' > 0 ; K_x'' = 0$$

$$K_{ly}' < 0 ; K_{ly}'' = 0$$

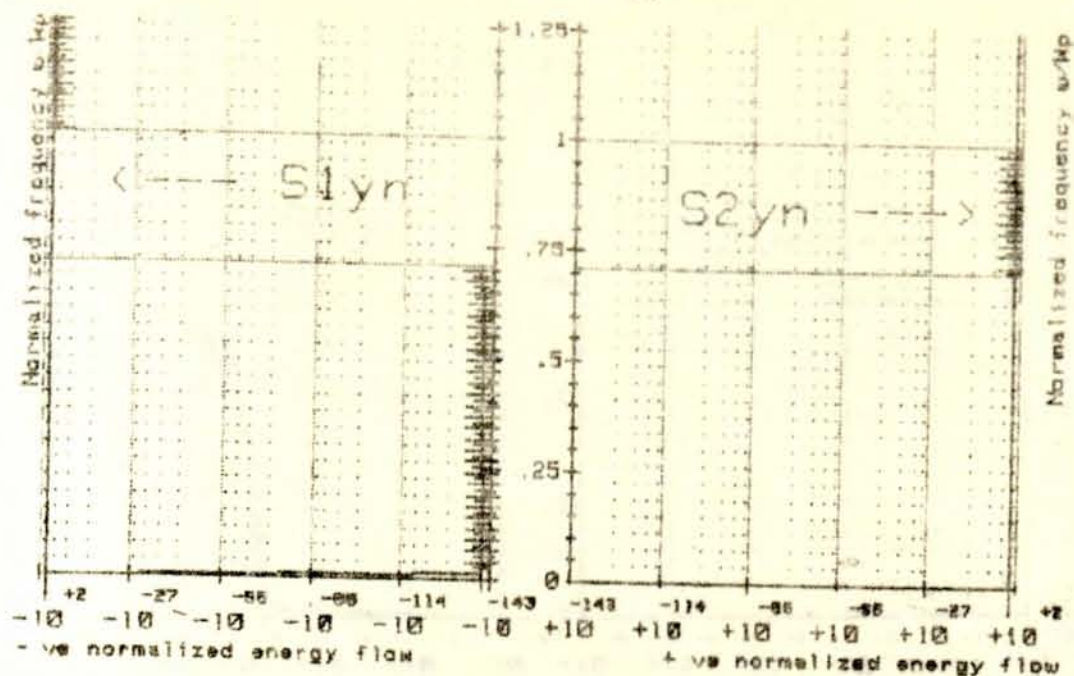


Fig. (18a) Graph of normalized energy flow along OY direction as a function of normalized frequency: (a) - for medium 1 (||||| - line), (b) - for medium 2 (IIIII - line).  
 $\omega_p = 1.E+15 \text{ rad/s}$  ;  $\tau = 1.E+125 \text{ s}$ .

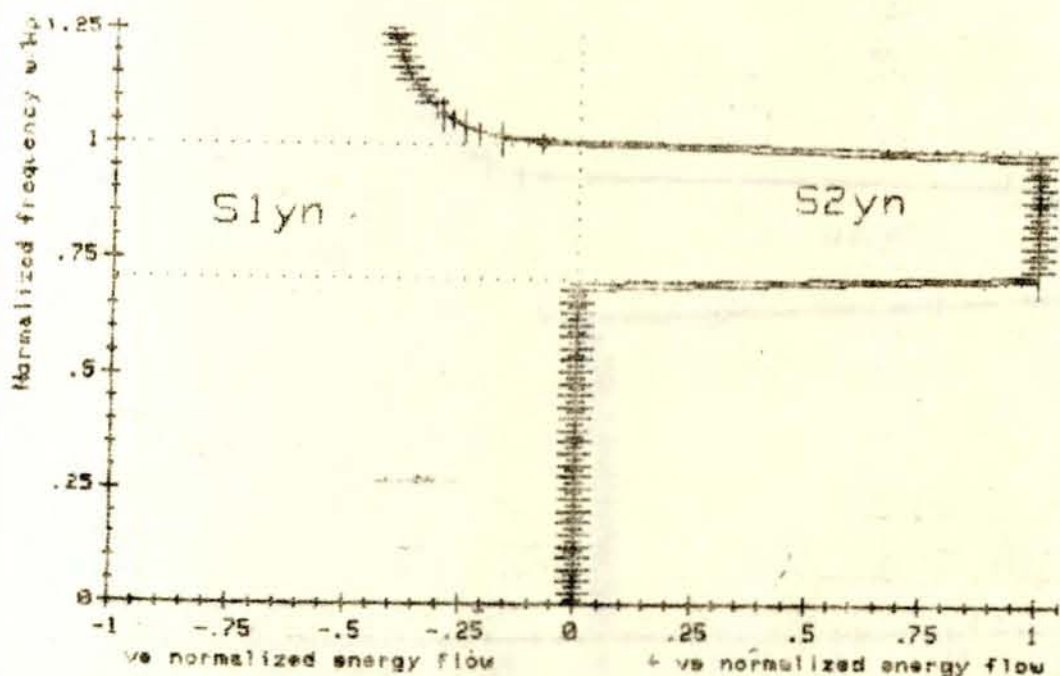


Fig. (18\*a) Graph of normalized energy flow along OY direction as a function of normalized frequency: (a) - for medium 1 (||||| - line), (b) - for medium 2 (IIIII - line).  
 $\omega_p = 1.E+15 \text{ rad/s}$  ;  $\tau = 1.E+125 \text{ s}$ .

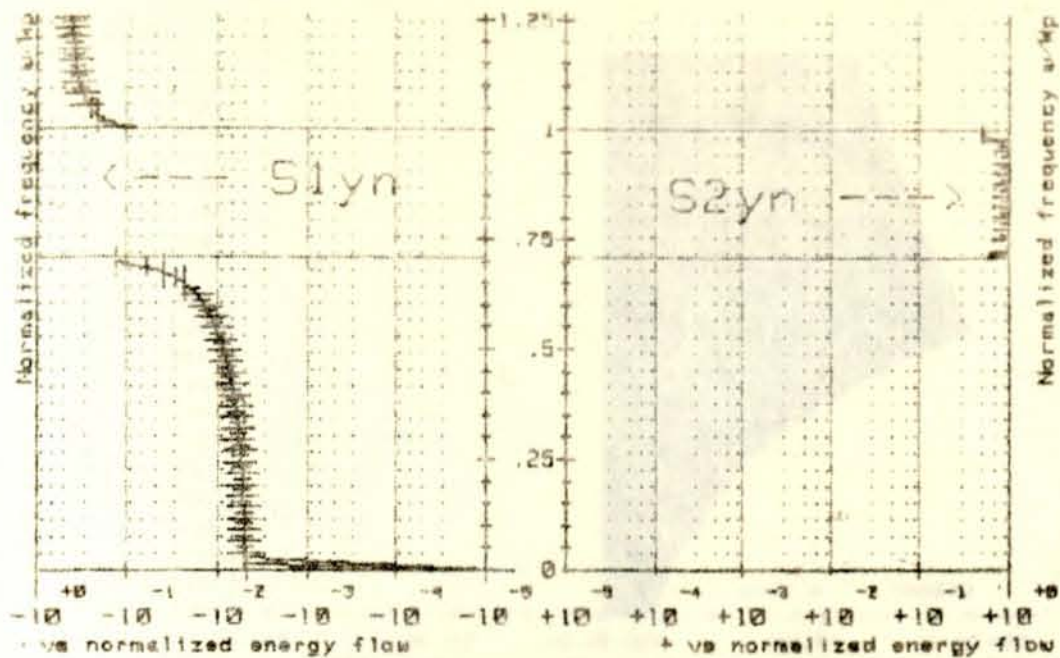


Fig. (8a) Graph of normalized energy flow along OY direction as a function of normalized frequency: (a) - for medium 1 (||||| - line), (b) - for medium 2 (||||| - line).  
 $\omega_p = 1.E+15 \text{ rad/s}$  ;  $\tau = 1.E-13 \text{ s}$ .

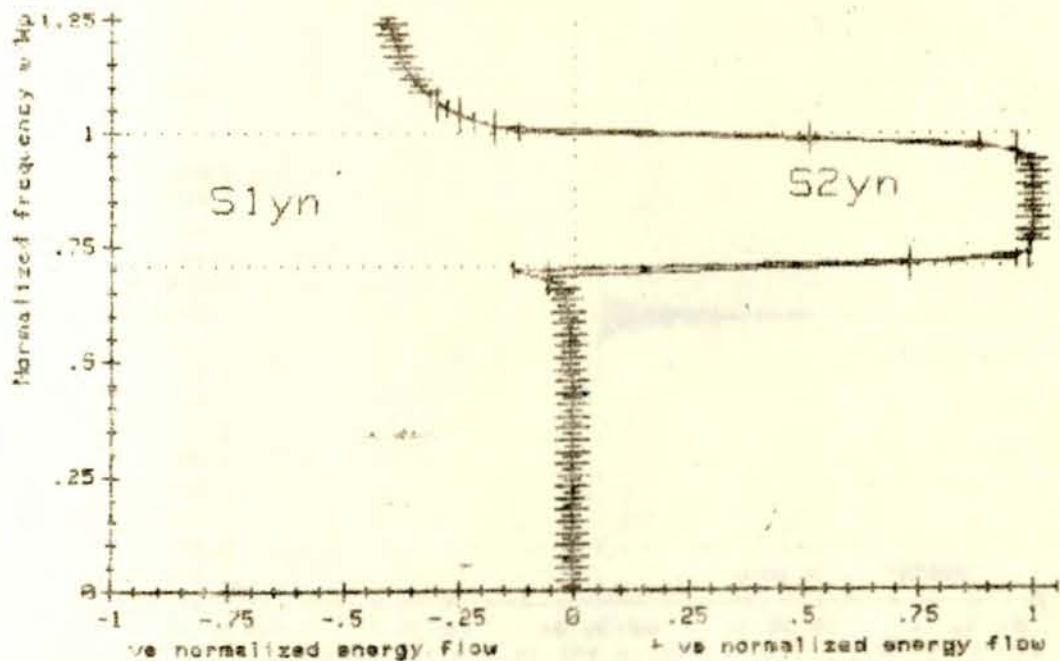
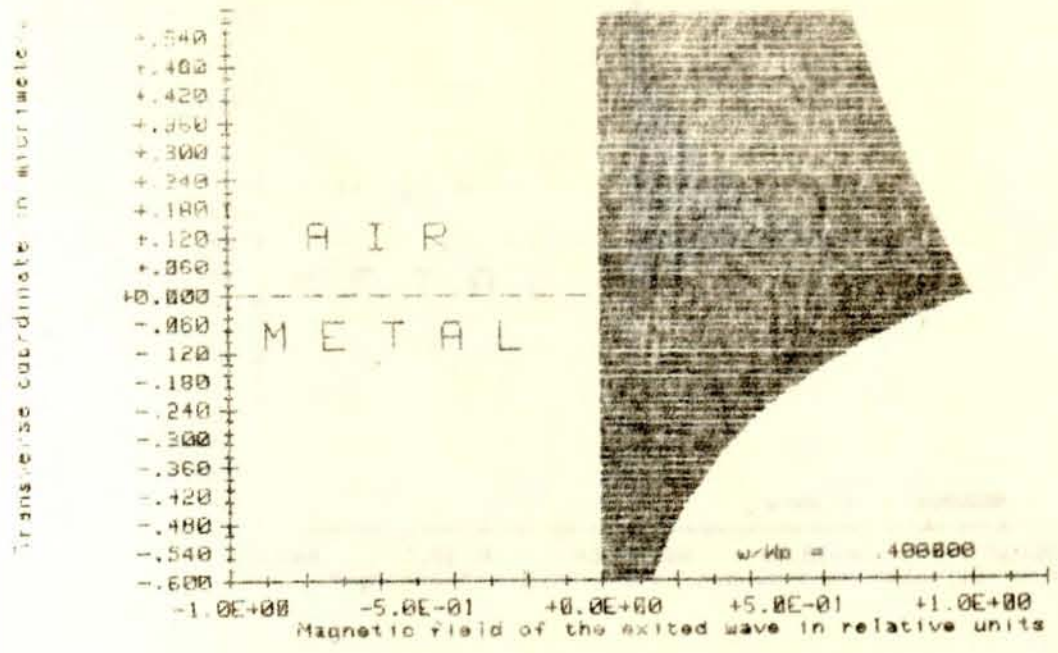
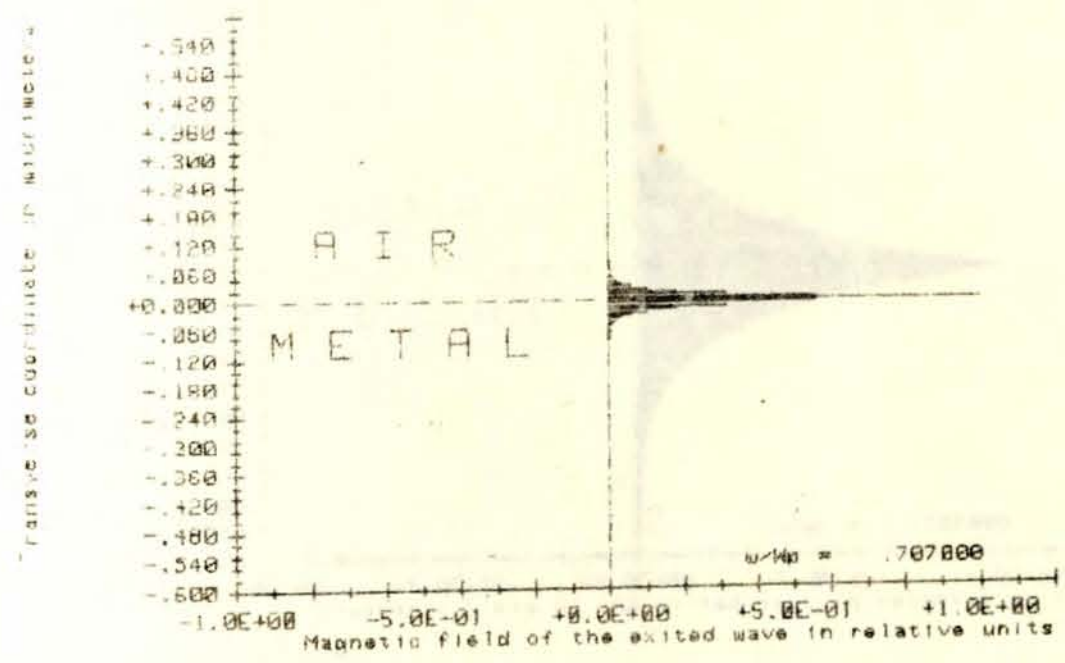


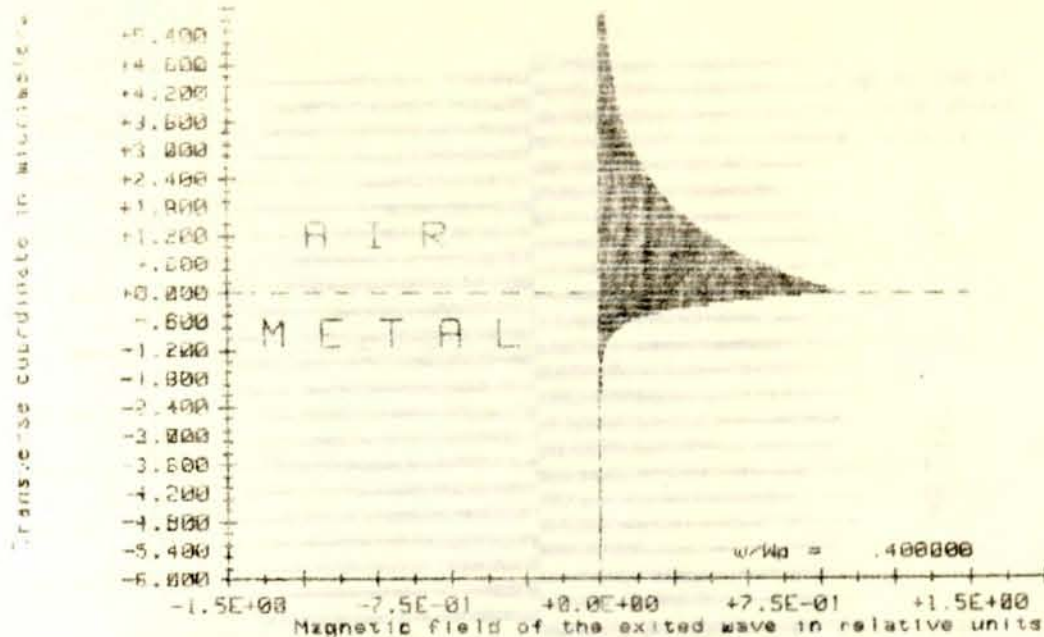
Fig. (8b) Graph of normalized energy flow along OY direction as a function of normalized frequency: (a) - for medium 1 (||||| - line), (b) - for medium 2 (||||| - line).  
 $\omega_p = 1.E+15 \text{ rad/s}$  ;  $\tau = 1.E-13 \text{ s}$ .



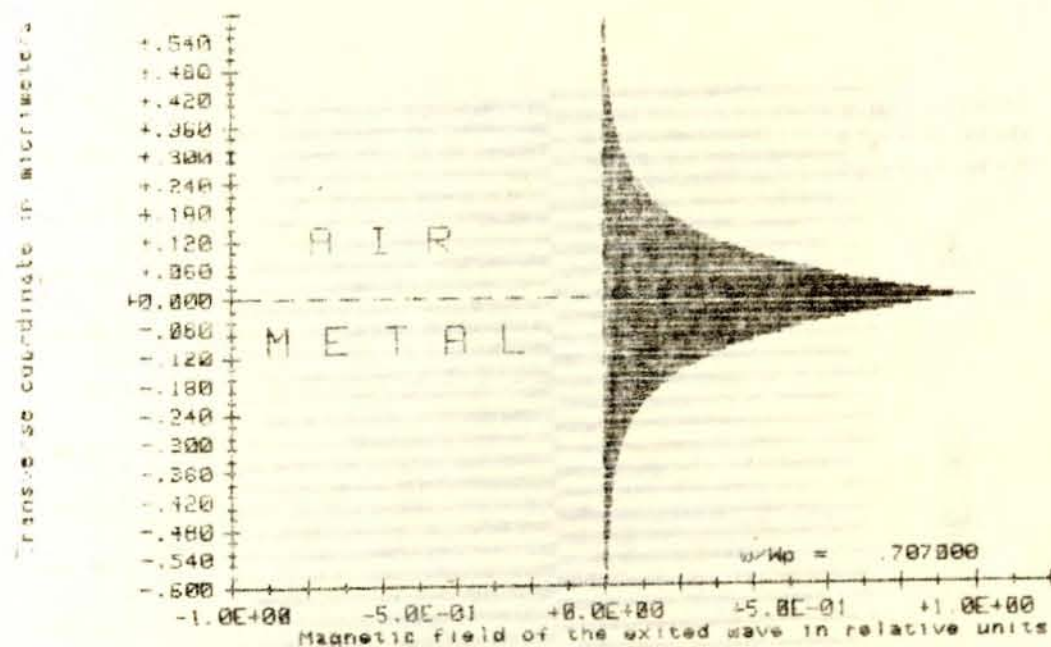
Fig(10a). Magnetic field (Z - component) distribution of the excited wave near the metal surface with respect to transverse Y - coordinate. (small frequency range).  $\omega_p = 1.E+15$  rad/s;  $\tau = 1.E+125$  s \*



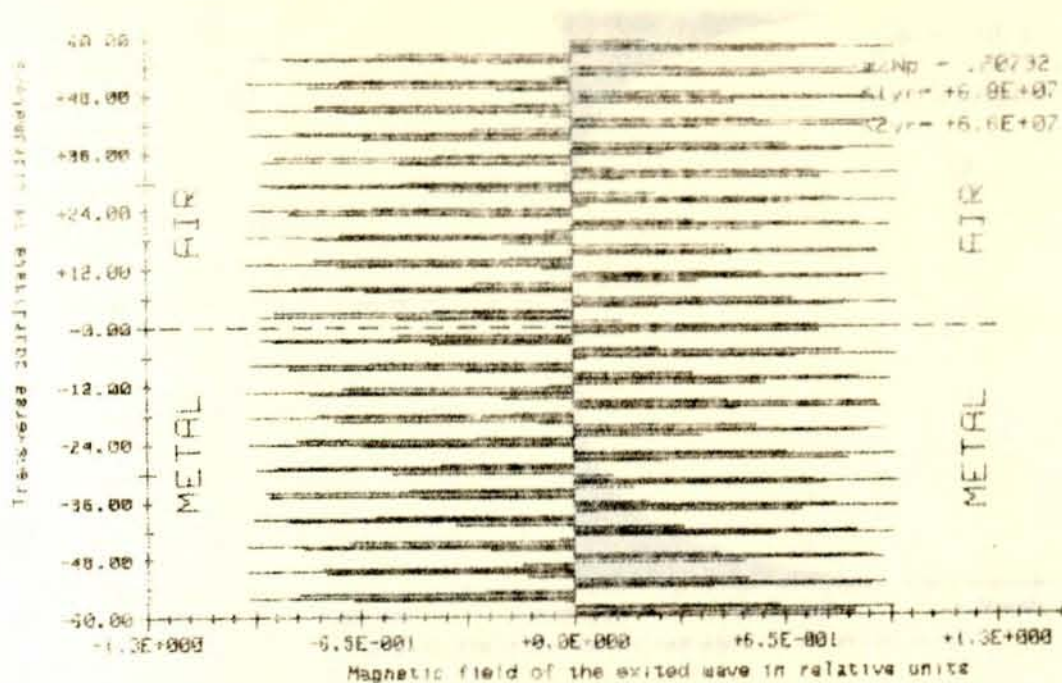
Fig(10b). Magnetic field (Z - component) distribution of the excited wave near the metal surface with respect to transverse Y - coordinate. (small frequency range).  $\omega_p = 1.E+15$  rad/s;  $\tau = 1.E+125$  s \*



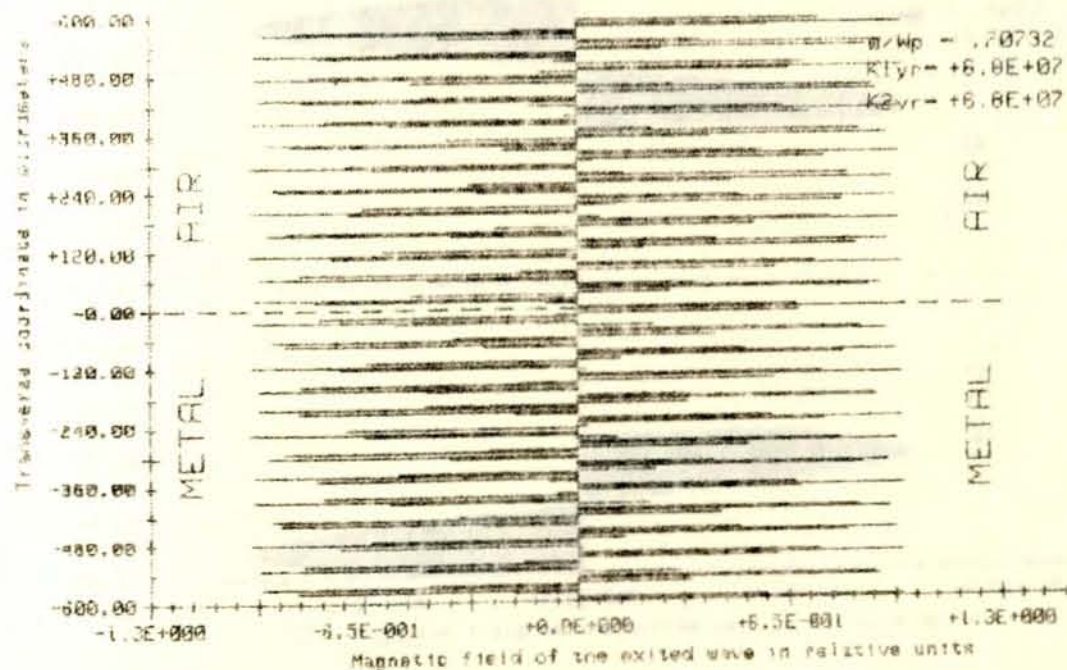
Fig(14ob) . magnetic field ( Z - component ) distribution of the excited wave near the metal surface with respect to transverse Y - coordinate, (small frequency range).  $\omega_p = 1.E+15$  rad/s;  $\tau = 1.E-13$  s \*



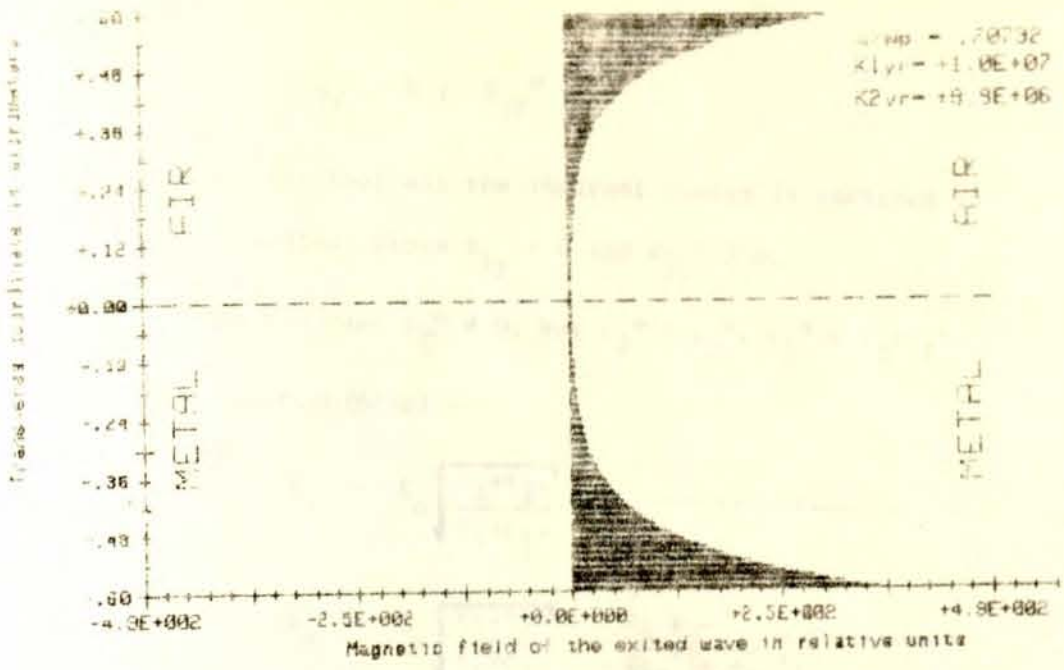
Fig(14ob) . magnetic field ( Z - component ) distribution of the excited wave near the metal surface with respect to transverse Y - coordinate, (small frequency range).  $\omega_p = 1.E+15$  rad/s;  $\tau = 1.E-13$  s \*



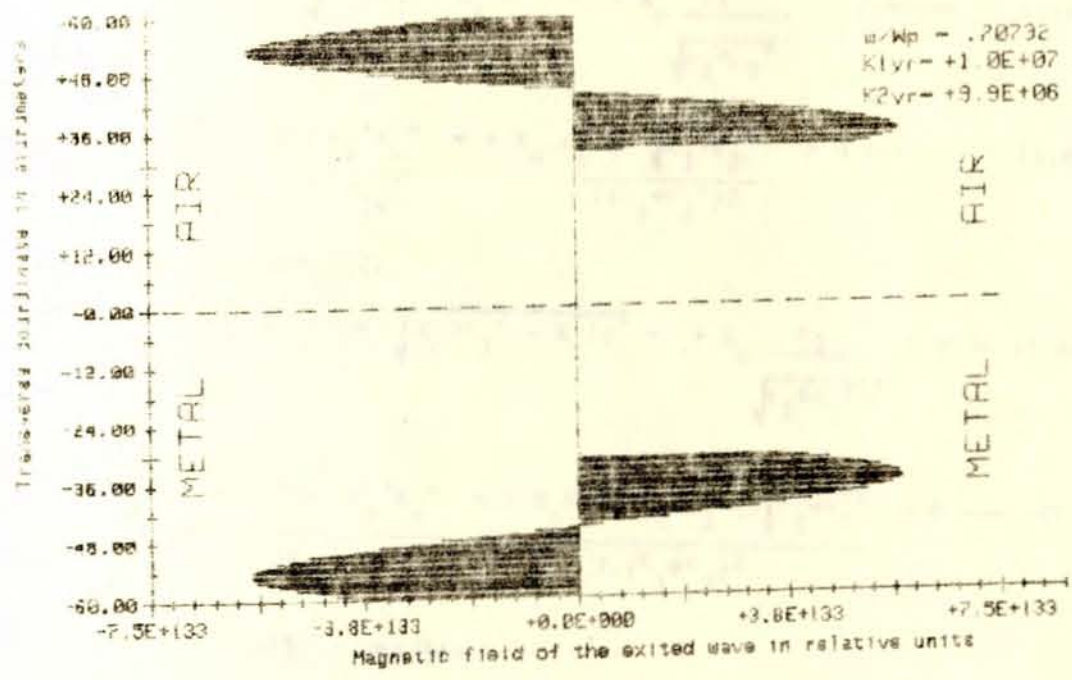
Fig(11a) Magnetic field (Z-component) distribution of the excited wave near the metal surface with respect to Y - coordinate (Medium frequency range) ;  $\omega_p = 1.E+15$  rad/s ;  $\tau = 1.E+125$  s



Fig(11a) Magnetic field (Z-component) distribution of the excited wave near the metal surface with respect to Y - coordinate (Medium frequency range) ;  $\omega_p = 1.E+15$  rad/s ;  $\tau = 1.E+125$  s



Fig(41b) Magnetic field (Z-component) distribution of the excited wave near the metal surface with respect to Y - coordinate (Medium frequency range) ,  $Wp = 1.E+15$  rad/s ;  $\tau = 1.E-13^s$



Fig(41b) Magnetic field (Z-component) distribution of the excited wave near the metal surface with respect to Y - coordinate (Medium frequency range) ,  $Wp = 1.E+15$  rad/s ;  $\tau = 1.E-13^s$

$$K_{2y}' > 0 ; K_{2y}'' = 0$$

which means that all the incident energy is radiated out through the second medium, since  $K_{1y} < 0$  and  $K_{2y}' > 0$ .

In the case  $\epsilon_2'' \neq 0$ , but  $\epsilon_2'' < \epsilon_2'$ ,  $\epsilon_2'' < \epsilon_1 + \epsilon_2'$

From equation (1.24a)

$$K_x' = K_0 \sqrt{\frac{\epsilon_1 \epsilon_2'}{\epsilon_1 + \epsilon_2'}} > 0 \quad \text{-----} \quad (1.60)$$

$$K_x'' = K_0 \sqrt{\frac{\epsilon_1 \epsilon_2''}{\epsilon_1 + \epsilon_2'}} \cdot \frac{\epsilon_1 \epsilon_2''}{2\epsilon_2'(\epsilon_1 + \epsilon_2')} > 0 \quad \text{-----} \quad (1.61)$$

See figures (1.3a) and (1.4a)

From equation (1.15)

$$K_{1y}' = \sqrt{K_0^2 \epsilon_1^2 - K_x'^2} = -K_0 \frac{\epsilon_1}{\sqrt{\epsilon_1 + \epsilon_2'}} < 0 \quad \text{-----} \quad (1.62)$$

$$K_{1y}'' = -\frac{K_x' K_x''}{K_{1y}'} = +K_0 \frac{\epsilon_1 \epsilon_2'' \sqrt{\epsilon_1 + \epsilon_2'}}{2(\epsilon_1 + \epsilon_2')^2} > 0 \quad \text{-----} \quad (1.63)$$

From equation (2.2)

$$K_{2y}' = \sqrt{K_0^2 \epsilon_2'^2 - K_x'^2} = +K_0 \frac{\epsilon_2'}{\sqrt{\epsilon_1 + \epsilon_2'}} > 0 \quad \text{---} \quad (1.64)$$

$$K_y^{2''} = \frac{K_0 \epsilon_2'' - 2K_x' K_x''}{2K_{2y}'} = \frac{K_0 \epsilon_2'' [2\epsilon_1 + \epsilon_2'] \cdot \sqrt{\epsilon_1 + \epsilon_2'}}{2 \cdot (\epsilon_1 + \epsilon_2')^2} > 0 \quad \text{---} \quad (1.65)$$

See figures (1.5a) and (1.6a)

From equations (1.27) to (1.30) and using equations (1.60) to (1.65)

$$S_y^I = -\frac{1}{2W\epsilon_0} \cdot \frac{K_0}{\sqrt{\epsilon_1 + \epsilon_2'}} < 0 \quad (1.66)$$

$$S_y^{II} = -\frac{1}{2W\epsilon_0} \cdot \frac{K_0}{\sqrt{\epsilon_1 + \epsilon_2'}} < 0 \quad (1.67)$$

$$S_x^I = \frac{1}{2W\epsilon_0} \cdot \frac{K_0 \sqrt{\epsilon_1 \cdot \epsilon_2'}}{\epsilon_2' \sqrt{\epsilon_1 + \epsilon_2'}} > 0 \quad (1.68)$$

$$S_x^{II} = \frac{1}{2W\epsilon_0} \cdot \frac{K_0 \sqrt{\epsilon_1 \cdot \epsilon_2'}}{\epsilon_2' \sqrt{\epsilon_1 + \epsilon_2'}} > 0 \quad (1.69)$$

For this subrange  $S_x^I$ ,  $S_x^{II}$  and  $|S_y| = |S_y^I| = |S_y^{II}|$  have close order of magnitude. Thus

$$S_{tot} = \sqrt{(S_x^I + S_x^{II})^2 + S_y^2} = \frac{K_0}{2W\epsilon_0} \cdot \sqrt{\frac{(\epsilon_1 + \epsilon_2')^2 \epsilon_1 \epsilon_2'}{\epsilon_1 \cdot \epsilon_2' \cdot (\epsilon_1 + \epsilon_2')}} \quad (1.70)$$

The normalized power flows can be expressed as

$$S_{xn}^I = \frac{S_y^I}{S_{tot}} = \frac{\epsilon_2}{\sqrt{(\epsilon_1 + \epsilon_2')^2 + \epsilon_1 \cdot \epsilon_2'}} > 0 \quad (1.71)$$

$$S_{xn}^{II} = \frac{S_x^{II}}{S_{tot}} = \frac{\epsilon_1}{\sqrt{(\epsilon_1 + \epsilon_2')^2 + \epsilon_1 \cdot \epsilon_2'}} > 0 \quad (1.72)$$

$$S_{yn} = \frac{S_y^I}{S_{tot}} = \frac{S_y^{II}}{S_{tot}} = -\frac{\sqrt{\epsilon_1 \cdot \epsilon_2'}}{\sqrt{(\epsilon_1 + \epsilon_2')^2 + \epsilon_1 \cdot \epsilon_2'}}$$

In the limiting cases: with  $\epsilon_1 = 1$

$$W = W_p ; S_{xn}^I = 0 ; S_{xn}^{II} = 1 ; S_{yn} = 0$$

$$W = \infty ; S_{xn}^I = \frac{1}{\sqrt{5}} ; S_{xn}^{II} = \frac{1}{\sqrt{5}} ; S_{yn} = -\frac{1}{\sqrt{5}}$$

$$(S_{xn}^I + S_{xn}^{II}) + S_{yn}^2 = \left(\frac{1}{\sqrt{5}} + \frac{1}{\sqrt{5}}\right)^2 + \left(-\frac{1}{\sqrt{5}}\right)^2 = 1$$

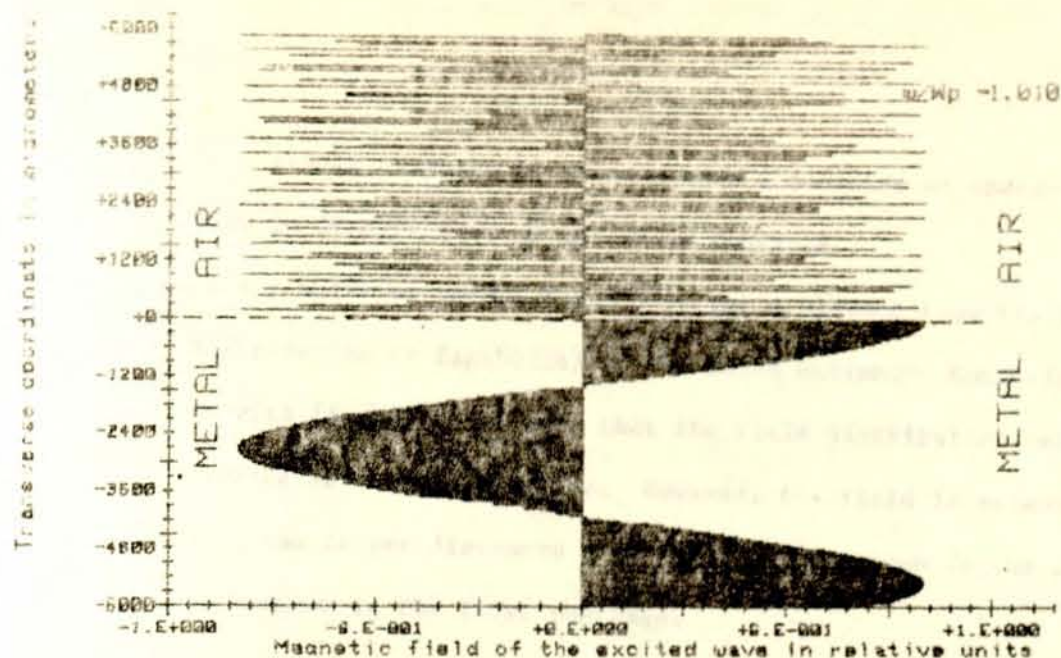
The same results follow from figures (10a), (10a), and (10\*3). The field distribution for the excitation in the third subrange is shown at fig. 12.

### 1.3 Dispersion Equation for Strong Absorption Case

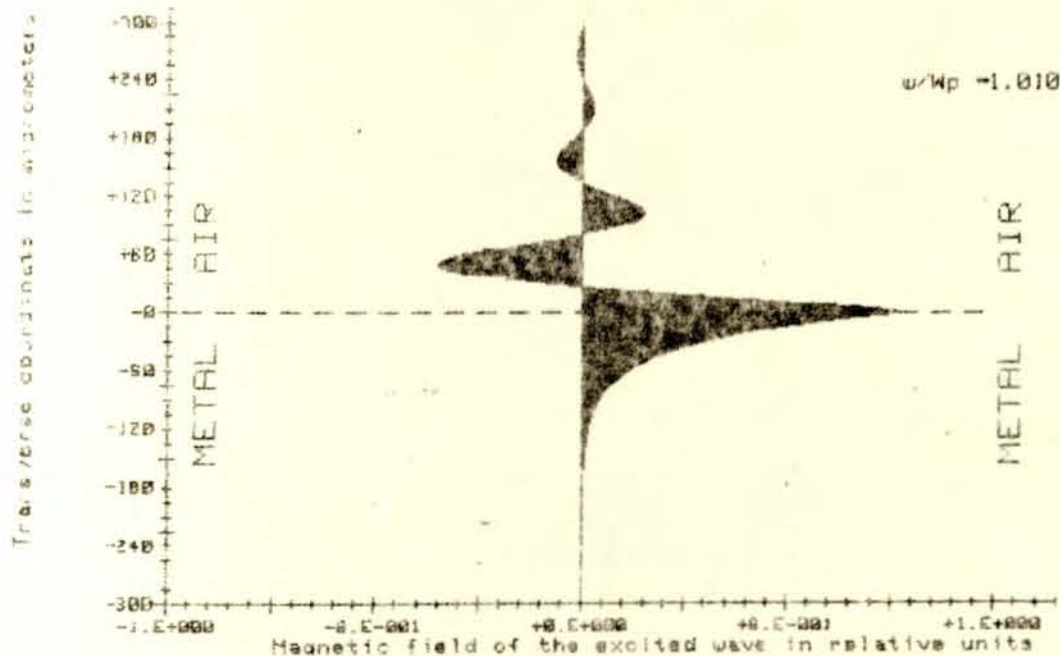
The results of calculations according to exact equations (1.24a), (1.15), (1.22) and equations (1.27) to (1.30), equations (1.3), and (1.4b) are represented at figures (13b) to (14b) (letter "b" refers to  $\tau = 10^{-13}$  sec)

Among the particularities of these results it is necessary to point out the following.

1. Growth of Real parts of  $K_y$  wave vector in the first subrange, see figure (15b).
2. As a result of point 1, we note the growth of energy flow in OY direction in the first subrange, see figure (16b).
3. However, it does not bring vital changes in the field distribution of plasmon in the first subrange (see fig. (10b)) in the sense that the plasmon type of field distribution remains. On it becomes clear that in strong absorption case it is not possible to compress the field so close to the interface beyond  $0.3\lambda_0$  at  $1/e$  level. Where  $\lambda_0$  is the wave length of the exciting light in vacuum.
4. Growth of imaginary parts of  $K_y$  wave vector in the third subrange see figure (16b).



Fig(12a) Magnetic field (Z-component) of the excited wave near the metal surface with respect to transverse Y - coordinate, (Big frequency range) .  $\omega_p = 1.E+15 \text{ rad/s}$  ;  $\tau = 1.E+12^* \text{ s}$



Fig(12b) Magnetic Field (Z-component) of the excited wave near the metal surface with respect to transverse Y - coordinate, (Big frequency range) .  $\omega_p = 1.E+15 \text{ rad/s}$  ;  $\tau = 1.E-13^* \text{ s}$

5. As a result of point 4, we note that a decrease of energy flow in OY direction in the third subrange.
6. As a results of points 4 and 5 we get a plasmon type field distribution at fig.(1.12(b) in the third subrange. Comparing it with fig.(1.12 a) we note that the field distribution became considerably less radiative. However, the field is extended at  $10^3$  time larger distances from the interface than in the case of plasmon in the first subrange.

2.1 Derivation of SP1P equation for dielectric medium 1 - metal film dielectric medium 3.

Consider a thin metallic film with  $\epsilon_2$  and thickness  $h$  boundarying with dielectric medium 1 with  $\epsilon_1$  and dielectric medium 3 with  $\epsilon_3$ .  
Suppose  $\epsilon_3 \geq \epsilon_1$

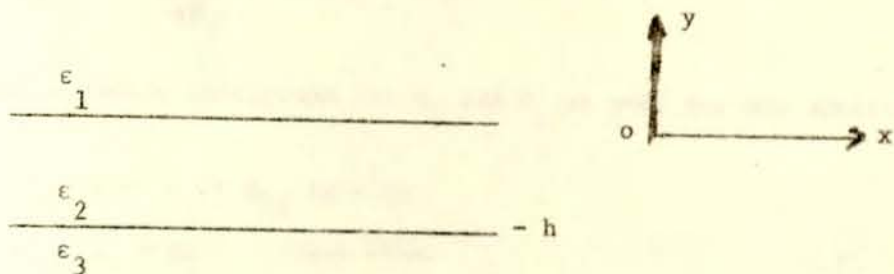


Fig. (2.1) Schematic diagram of thin metallic film ( $\epsilon_2$ ) boundarying dielectric medium 1 ( $\epsilon_1$ ), and dielectric medium 3 ( $\epsilon_3$ ).

Considering T.M polarization, the magnetic field  $H_z$  can be given respectively in the three media;

$$H_{z1} = A_1 e^{+iK_1 y} e^{i(K_x X - \omega t)}$$

$$H_{z2} = \left( A_2 e^{+iK_2 y} + B_2 e^{-iK_2 y} \right) e^{i(K_x X - \omega t)} \quad \text{----- (2.1)}$$

$$H_{z3} = A_3 e^{-iK_3 y} e^{i(K_x X - \omega t)}$$

The expression for  $H_{z2}$  contains two terms because there might be two waves travelling in the film due to reflections at  $\epsilon_1/\epsilon_2$  interface and at  $\epsilon_3/\epsilon_2$  interface. Their superposition describes a standing wave in  $OY$  direction with in the film.

From Maxwell's curl equation the corresponding  $E_x$  (tangential) components of the electric field in the three media respectively are;

$$E_{x1} = -A_1 \frac{K_{1y}}{W\epsilon_1} e^{+iK_{1y}Y} e^{i(K_x X - Wt)}$$

$$E_{x2} = \left[ -A_2 \frac{K_{2y}}{W\epsilon_2} e^{iK_{2y}Y} + B_2 \frac{K_{2y}}{W\epsilon_2} \right] e^{i(K_x X - Wt)} \quad (2.2)$$

$$E_{x3} = A_3 \frac{K_{3y}}{W\epsilon_3} e^{-iK_{3y}Y} e^{i(K_x X - Wt)}$$

Let's apply boundary conditions for  $H_z$  and  $E_x$  at  $y=0$ , for any arbitrary:

$$H_{z1}(y=0) = H_{z2}(y=0)$$

$$A_1 = A_2 + B_2 \quad (2.3)$$

$$E_{x1}(y=0) = E_{x2}(y=0)$$

$$-A_1 \frac{K_{1y}}{\epsilon_1} = -A_2 \frac{K_{2y}}{\epsilon_2} + B_2 \frac{K_{2y}}{\epsilon_2} \quad (2.4)$$

again applying boundary condition at  $y = -h$  for any arbitrary  $x$ :

$$H_{z2}(y=-h) = H_{z3}(y=-h)$$

$$A_2 e^{-iK_{2y}h} + B_2 e^{+iK_{2y}h} = A_3 e^{+iK_{3y}h} \quad (2.5)$$

$$E_{x2}(y=-h) = E_{x3}(y=-h)$$

$$-A_2 \frac{K_{2y}}{\epsilon_2} e^{-iK_{2y}h} + B_2 \frac{K_{2y}}{\epsilon_2} e^{+iK_{2y}h} = A_3 \frac{K_{3y}}{\epsilon_3} e^{+iK_{3y}h} \quad (2.6)$$

Suppose  $A_1$  is given, in this case equations (2.3) — (2.6) form a system of four equations with  $A_2, B_2, A_3$ , and  $K_x$  unknown noting that  $K_{1y}$ , and  $K_{2y}$  can be expressed through  $K_x$ , and the expression for  $K_{3y}$  can be derived from the wave equation for medium 3 similarly as it was done for medium. 1. Therefore;

$$K_{3y} = \sqrt{K_0^2 \epsilon_3 - K_2^2} \quad \text{-----} \quad (2.7)$$

In order to derive the dispersion equation ( $K_x = f(w)$ ) we shall exclude all amplitude factors from equations (2.4)  $\rightarrow$  (2.6)

From equations (2.3) and (2.4)

$$- (A_2 + B_2) \frac{K_{1y}}{\epsilon_1} = - (A_2 - B_2) \frac{K_{2y}}{\epsilon_2} \quad \text{-----} \quad (2.8)$$

or

$$- B_2 \left[ \frac{K_{1y}}{\epsilon_1} + \frac{K_{2y}}{\epsilon_2} \right] = A_2 \left[ \frac{K_{1y}}{\epsilon_1} - \frac{K_{2y}}{\epsilon_2} \right]$$

Multiplying equation (2.5) by a factor  $\frac{K_{3y}}{W\epsilon_3}$  and subtracting from the result equation (2.6)

$$(A_2 e^{-iK_{2y}h} + B_2 e^{+iK_{2y}h}) \frac{K_{3y}}{W\epsilon_3} - (-A_2 \frac{K_{2y}}{W\epsilon_2} e^{-iK_{2y}h} + B_2 \frac{K_{2y}}{W\epsilon_2} e^{+iK_{2y}h}) = 0$$

$$A_2 e^{-iK_{2y}h} \left[ \frac{K_{3y}}{\epsilon_3} + \frac{K_{2y}}{\epsilon_2} \right] + B_2 e^{+iK_{2y}h} \left[ \frac{K_{3y}}{\epsilon_3} - \frac{K_{2y}}{\epsilon_2} \right] = 0$$

$$A_2 + B_2 e^{2iK_{2y}h} \left[ \frac{K_{3y}}{\epsilon_3} - \frac{K_{2y}}{\epsilon_2} \right] = 0$$

$$\left[ \frac{K_{3y}}{\epsilon_3} + \frac{K_{2y}}{\epsilon_2} \right]$$

$$A_2 - B_2 r_{23} e^{2iK_{2y}h} = 0$$

$$A_2 = B_2 r_{23} e^{2iK_{2y}h} \quad \text{-----} \quad (2.9)$$

Substitution of equation (2.9) into equation (2.8) gives

$$B_2 = B_2 r_{12} \cdot r_{23} e^{2iK_{2y}h}$$

$$-1 = r_{12} r_{23} e^{2iK_{2y}h}$$

$$r_{21} r_{23} e^{2iK_{2y}h} = 1 \quad \text{-----} \quad (2.10)$$

where 
$$r_{21} = \frac{\frac{K_{2y}}{\epsilon_2} - \frac{K_{1y}}{\epsilon_1}}{\frac{K_{2y}}{\epsilon_2} + \frac{K_{1y}}{\epsilon_1}} \quad (2.11)$$

$$r_{23} = \frac{\frac{K_{2y}}{\epsilon_2} - \frac{K_{3y}}{\epsilon_3}}{\frac{K_{2y}}{\epsilon_2} + \frac{K_{3y}}{\epsilon_3}} \quad (2.12)$$

Equation (2.10) represents together with equations (2.11), (2.12), (1.15), (1.22), and (2.7) an exact dispersion equation for a thin metallic film [2].

### 2.2 Approximate solution for the dispersion equation.

Let's suppose that thickness  $h$  of the metallic film is big enough, so that the influence of medium 3 on the dispersion properties is small. In this case we can build an approximate solution using the solution expressed in equation (1.24a) for the semi-infinite case as the basis. Thus we'll express:

$$K_x = K_{x0} + K_{x1} \quad (2.13)$$

where  $K_{x0}$  is given by equation (1.24a)

$K_{x1}$  is a small quantity describing the influence of medium 3.

For this purpose let's denote the reciprocal of the left side of equation (2.10) as a function of  $K_x$

$$f(K_x) = (r_{21} r_{23} e^{2iK_{2y}h})^{-1} = \frac{1}{r_{21}} \cdot \frac{1}{r_{23}} e^{-2iK_{2y}h} \quad (2.14)$$

Let's expand  $f(K_x)$  in Taylor's series near the point  $K_x = K_{x0}$ , where  $K_{x0}$  is given by equation (1.24a) for the semi-infinite case

$$f(K_x) = f(K_{x0}) + \frac{\partial f}{\partial K_x} \Big|_{K_{x0}} K_{x1} + \dots \quad (2.15)$$

In appendix A it is shown that

$$f(K_{x0}) = 0 \quad (2.16)$$

$$\frac{\partial f}{\partial K_x} \Big|_{K_{x0}} = \frac{\epsilon_2 - \epsilon_1}{2K_0} \left( \frac{\epsilon_1 - \epsilon_2}{\epsilon_1 \epsilon_3} \right)^{3/2} \cdot \frac{1}{r_{23}^0} e^{-12K_{2y}^0 h} \quad (2.17)$$

$$r_{23}^0 = \frac{\epsilon_3 - \sqrt{\epsilon_1 \epsilon_3 + \epsilon_2 (\epsilon_3 - \epsilon_1)}}{\epsilon_3 + \sqrt{\epsilon_1 \epsilon_3 + \epsilon_2 (\epsilon_3 - \epsilon_1)}} \quad (2.18)$$

$$K_{2y}^0 = iK_0 \frac{(\epsilon_2 - \epsilon_1)}{\sqrt{-(\epsilon_1 + \epsilon_2)}} \quad (2.19)$$

Since  $f(K_x) = 1$  (see equations (2.10) and (2.14)) substitution of equation (2.16) to (2.19) into equation (2.15) gives

$$K_{x1} = K_0 \left( \frac{2}{\epsilon_2 - \epsilon_1} \right) \cdot \left( \frac{\epsilon_1 \epsilon_2}{\epsilon_1 + \epsilon_2} \right)^{3/2} \cdot r_{23}^0 e^{+2iK_{2y}^0 h} \quad (2.20)$$

Let's analyze equation (2.20) for the case when  $\epsilon_2'' = 0$ . First from equation (2.18) we get:

$$r_{23}^0 = \frac{\epsilon_3 - \sqrt{\epsilon_1 \epsilon_3 + \epsilon_2 (\epsilon_3 - \epsilon_1)}}{\epsilon_3 + \sqrt{\epsilon_1 \epsilon_3 + \epsilon_2 (\epsilon_3 - \epsilon_1)}} \quad (2.21)$$

The expression under the square root is negative in the range of frequencies  $0 \leq W \leq W^*$ . Where  $W^*$  is determined from the condition;

$$\epsilon_1 \epsilon_3 + \left(1 - \frac{W^2}{W_p^2}\right) (\epsilon_3 - \epsilon_1) = 0$$

$$W^* = W_p \cdot \sqrt{\frac{\epsilon_3 - \epsilon_1}{\epsilon_1 \epsilon_3 + \epsilon_3 - \epsilon_1}} \quad (2.22)$$

The frequency  $W^*$  corresponds also to the intersection point of graphs  $K_{xu}^{\prime}(W)$  and  $K_3(W)$ .

$$K_0 \sqrt{\frac{\epsilon_1 \epsilon_2' (W^*)}{\epsilon_1 + \epsilon_2' (W^*)}} = K_0 \sqrt{\epsilon_3} \quad (2.23)$$

It means  $W^*$  is the maximum frequency for a SPLP to be excited by the light incident from medium 3 on the  $\epsilon_1/\epsilon_2$  interface.

To avoid imaginarity under the square root let's rewrite equation (2.21) as

$$r_{23}^o = \frac{\epsilon_3 - i \sqrt{[\epsilon_1 \epsilon_3 + \epsilon_2' (\epsilon_3 - \epsilon_1)]}}{\epsilon_3 + i \sqrt{[\epsilon_1 \epsilon_3 + \epsilon_2' (\epsilon_3 - \epsilon_1)]}}$$

$$= \frac{\epsilon_3^2 + [\epsilon_1 \epsilon_3 + \epsilon_2' (\epsilon_3 - \epsilon_1)] + i 2\epsilon_3 \sqrt{[\epsilon_1 \epsilon_3 + \epsilon_2' (\epsilon_3 - \epsilon_1)]}}{\epsilon_3^2 - [\epsilon_1 \epsilon_3 + \epsilon_2' (\epsilon_3 - \epsilon_1)]} \quad (2.24)$$

Finally the real and imaginary components of  $K_x$  can be written as (it follows from equations (2.13), (2.20), (2.24);

$$K_x^{\prime} = K_0 \sqrt{\frac{\epsilon_1 \epsilon_2'}{\epsilon_1 + \epsilon_2'}} + K_0 \frac{2}{\epsilon_2 - \epsilon_1} \left( \frac{\epsilon_1 \epsilon_2'}{\epsilon_1 + \epsilon_2'} \right)^{3/2} \frac{\epsilon_3 + [\epsilon_1 \epsilon_3 + \epsilon_2' (\epsilon_3 - \epsilon_1)]}{3 - [\epsilon_1 \epsilon_3 + 2(\epsilon_3 - \epsilon_1)]} \cdot \text{EXP} \left[ 2K_{oh} + \frac{\epsilon_2'}{\sqrt{-(\epsilon_1 + \epsilon_2')}} \right] \quad (2.25)$$

$$K_x^{\prime\prime} = -K_0 \frac{2}{\epsilon_2' \epsilon_1} \left( \frac{\epsilon_1 \epsilon_2'}{\epsilon_1 + \epsilon_2'} \right)^{3/2} \frac{2\epsilon_3 \sqrt{[\epsilon_1 \epsilon_3 + \epsilon_2' (\epsilon_3 - \epsilon_1)]}}{\epsilon_3^2 - [\epsilon_1 \epsilon_3 + \epsilon_2' (\epsilon_3 - \epsilon_1)]} \text{EXP} \left[ 2K_{oh} - \frac{\epsilon_2'}{\epsilon_1 + \epsilon_2'} \right] \quad (2.26)$$

For the frequency range  $W^* < W \leq \frac{W_p}{\sqrt{\epsilon_1 + \epsilon_2'}}$ ,  $r_{23}^o$  becomes a purely real

quantity, making  $K_x^{\prime\prime} = 0$ . Thus, in this range of frequency, the real part of  $K_x$  can be expressed as;

$$K'_x = K_0 \sqrt{\frac{\epsilon_1 \cdot \epsilon_2'}{\epsilon_1 + \epsilon_2'}} + K_0 \frac{2}{\epsilon_2' - \epsilon_1} \cdot \left( \frac{\epsilon_1 \epsilon_2'}{\epsilon_1 + \epsilon_2'} \right)^{3/2} \left\{ \frac{\epsilon_3 - \sqrt{\epsilon_1 \epsilon_3 + \epsilon_2' (\epsilon_3 - \epsilon_1)}}{\epsilon_3 + \sqrt{\epsilon_1 \epsilon_3 + \epsilon_2' (\epsilon_3 - \epsilon_1)}} \right\} \times$$

$$\times E_{xp} \left[ \frac{2K_0 h}{\sqrt{-(\epsilon_1 + \epsilon_2')}}} \right] \quad (2.27)$$

The graph for  $K'_x$  as a function of  $W$  for different value of thickness  $h$  of the metallic film is shown at figures (2.2a) and (2.2b) by a continuous (solid) line. The broken line at these figures represent the dispersion graph for  $K'_{x0}$  (semi infinite case). The comparison of the two types of lines at each figure shows that the approximation introduced by equations (2.13) and (2.20) is valid in the whole range of frequencies  $0 < \frac{W}{p} < \frac{1}{\sqrt{\epsilon_1 + 1}}$  only if the thickness of the film is greater than the order of 0.3 - 0.4  $\mu\text{m}$ .

On the other hand for a narrow frequency range  $0 < W < W^{**}$  the coincidence of the two types of lines is good for metallic films, of infinite small thickness.

The value of  $W^{**}$  is determined from the condition  $R_e(r_{23}^0(W^{**})) = 0$ . Which means from equation (2.24).

$$\epsilon_3^2 + \epsilon_1 \epsilon_3 + \epsilon_2' (\epsilon_3 - \epsilon_1) = 0$$

$$\frac{\epsilon_2'}{2} = - \frac{(\epsilon_3^2 + \epsilon_1 \epsilon_3)}{(\epsilon_3 - \epsilon_1)}$$

$$1 - \frac{W^2}{W^{**2}} = - \frac{(\epsilon_3^2 + \epsilon_1 \epsilon_3)}{(\epsilon_3 - \epsilon_1)}$$

$$1 + \frac{\epsilon_3^2 + \epsilon_1 \epsilon_3}{\epsilon_3 - \epsilon_1} = \frac{W^2}{W^{**2}}$$

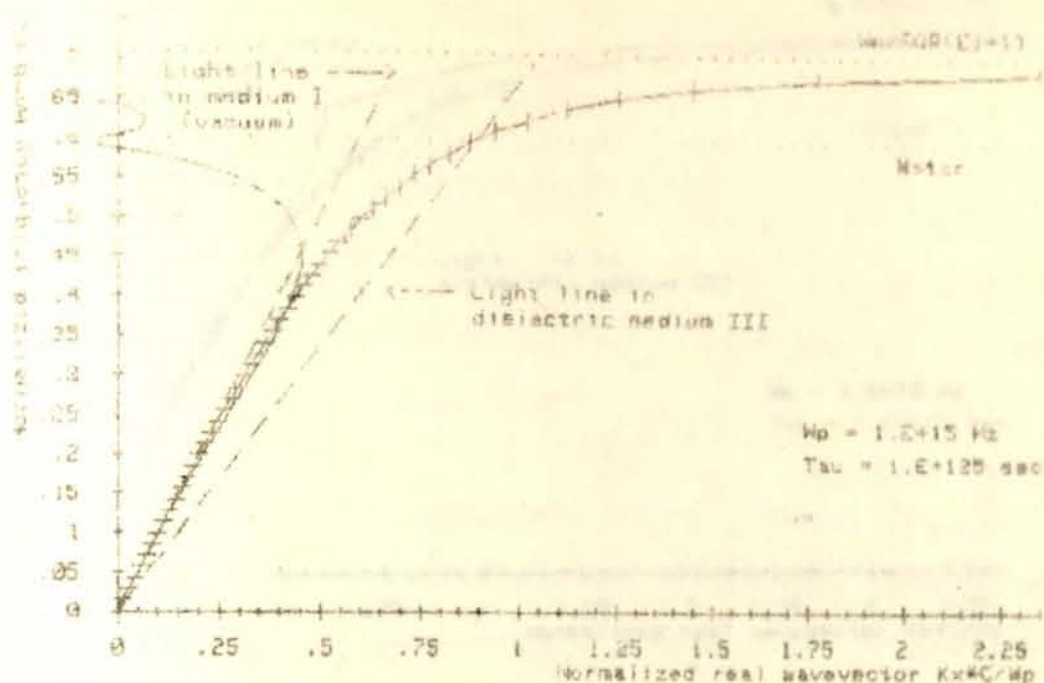


Fig. (2.2a) SPiP dispersion curve of REAL  $K_x$  as a function of frequency  $\omega$  (a) - for thin metallic film of thickness  $H$  bounding dielectric media (EI and E3) - continuous line, (b) - for infinite media METAL/DIELECTRIC interface (broken line).  $H = .04$  micrometers

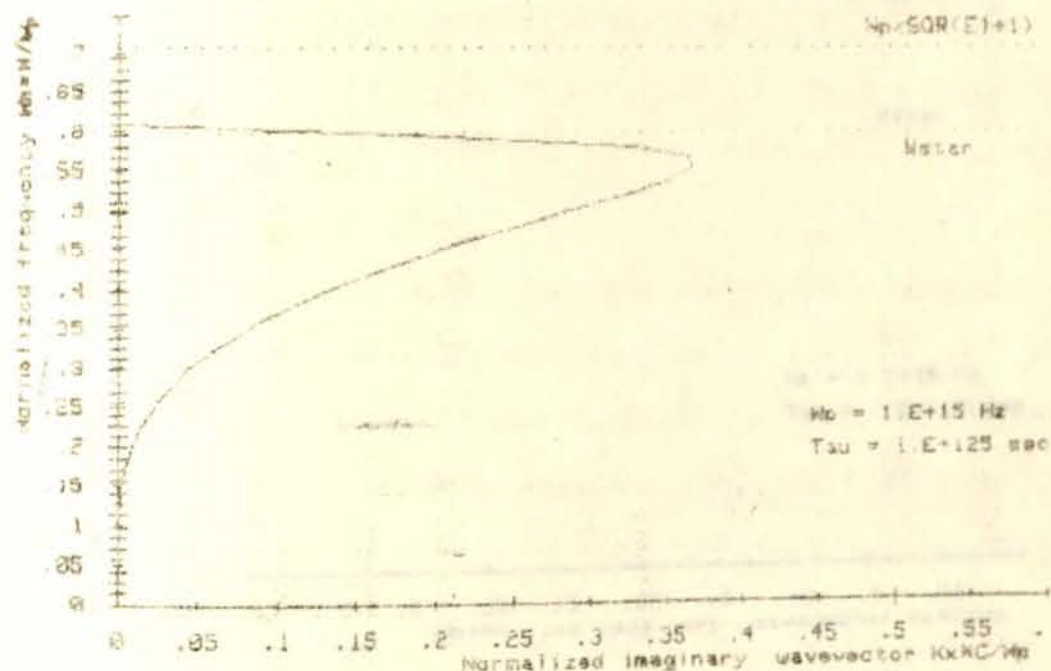


Fig. (2.2a) SPiP dispersion graph of IMAGINARY  $K_x$  as a function of frequency: (a) - for thin metallic film of thickness  $H$  bounding dielectric media (EI and E3) - continuous line (b) - for infinite media METAL/AIR interface (broken line).  $H = .04$  micrometers

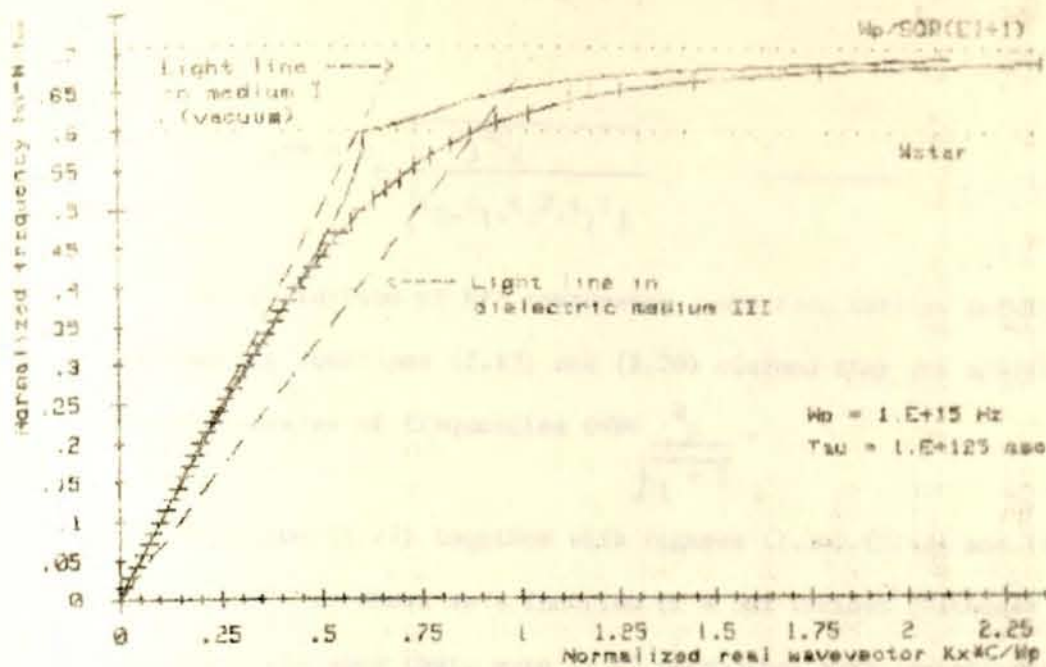


Fig. (2.2b) SPIP dispersion curve of REAL  $k_x$  as a function of frequency : (a) - for thin metallic film of thickness  $H$  bounding dielectric media ( $\epsilon_1$  and  $\epsilon_3$ ) - continuous line, (b) - for infinite media METAL/DIELECTRIC interface (broken line).  $H = .2$  micrometers.

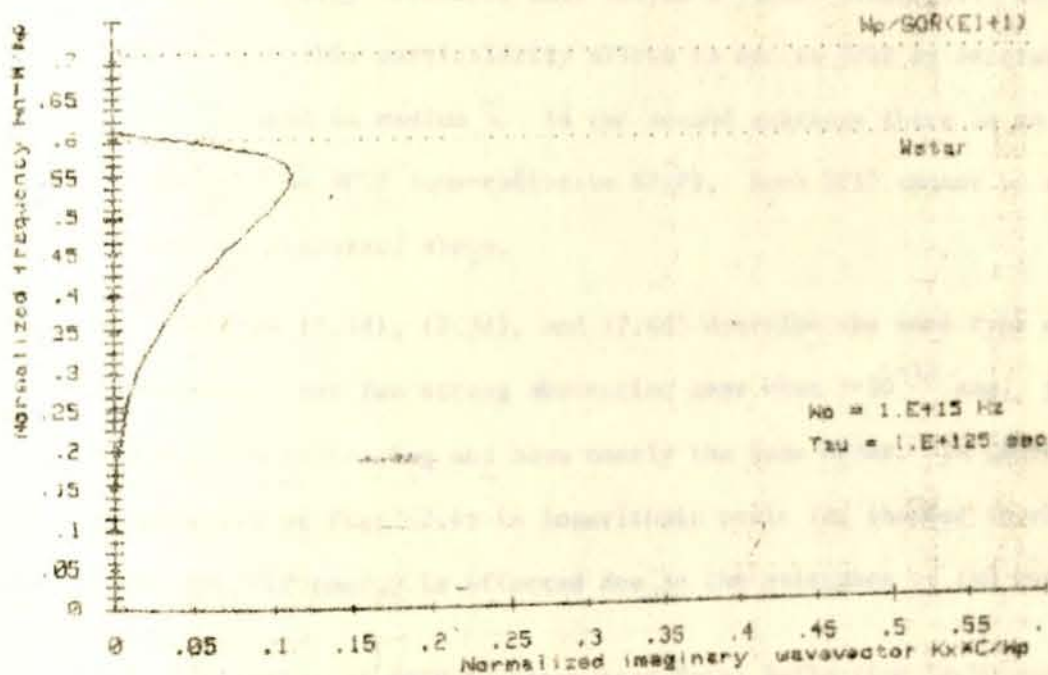


Fig. (2.3b) SPIP dispersion graph of IMAGINARY  $k_x$  as a function of frequency : (a) - for thin metallic film of thickness  $H$  bounding dielectric media ( $\epsilon_1$  and  $\epsilon_3$ ) - continuous line ; (b) - for infinite media METAL/AIR interface (broken line).  $H = .2$  micrometers.

$$W^{**} = W_p \frac{\epsilon_3 - \epsilon_1}{\sqrt{\epsilon_3 - \epsilon_1 + \epsilon_3^2 + \epsilon_1 \epsilon_3}} \quad (2.28)$$

The definition of  $W^{**}$  represents a new fact. Earlier Authors [3,4] introducing equations (2.13) and (2.20) claimed they are applicable in the whole range of frequencies  $0 < W < \frac{W_p}{\sqrt{\epsilon_1 + 1}}$ .

Equation (2.27) together with figures (2.3a) (2.4a) and (2.4c) at which  $K_x''$  is shown as a function of  $W$  for various thickness of metallic film show that, even if  $\epsilon_2''$  approaches zero (according  $\tau = 10^{125}$  sec) the value of  $K_x''$  does not tend to zero for  $0 < W < W^*$ , and it tends to zero for  $W^* < W < \frac{W_p}{\sqrt{\epsilon_1 + 1}}$ . This means that in the first subrange we have naturally a leakage of energy from SPIP into medium 3 (leaky plasmons), On the other hand exactly this particularity allows to excite SPIP by external light source located in medium 3. In the second subrange there is no leakage of energy from SPIP (non-radiative SPIP), Such SPIP cannot be excited in the way discussed above.

Figures (2.2d), (2.3d), and (2.4d) describe the same type of dependences, but for strong absorption case when  $\tau = 10^{-13}$  sec. Both  $K_{x0}$  and  $K_{x1}$  are increasing and have nearly the same order. In general the graph drawn at Fig. (2.4) in logarithmic scale is, in order to show how much the SPIP energy is affected due to the existence of the metallic film

### 2.3 Excitation of SPIP by Attenuated Total Reflection Technique

Several techniques are available in the experimental study of SPIP, and their use is dictated by the frequency and the wave number range in which the excitation is being examined. For example at short wave lengths

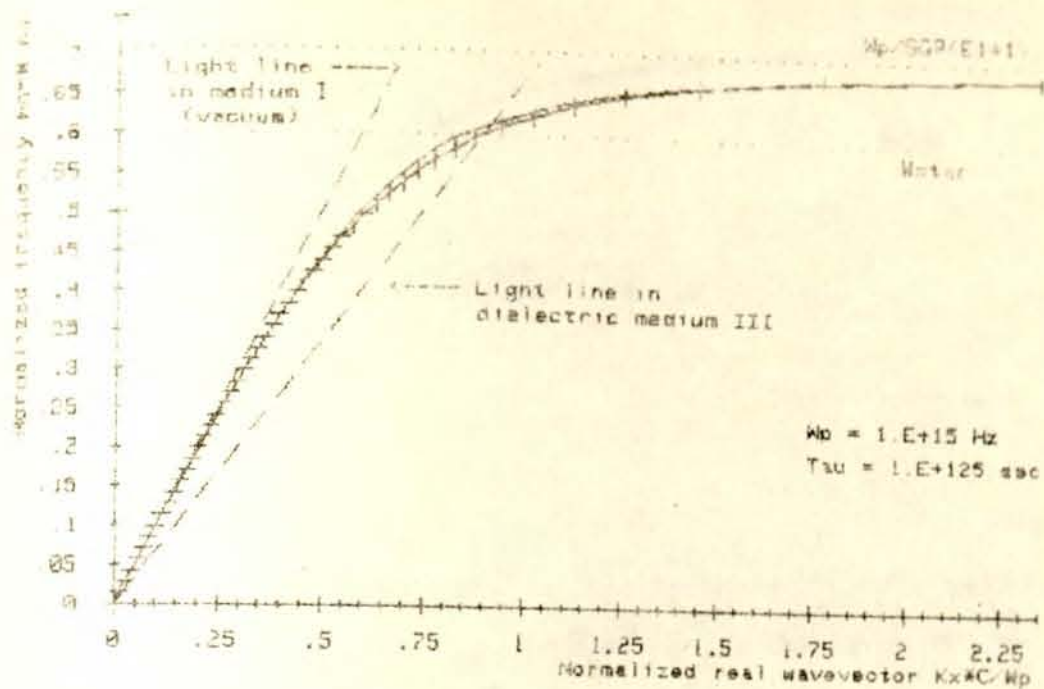


Fig. (2.2C) SPIP dispersion curve of REAL  $k_x$  as a function of frequency: (a) - for thin metallic film of thickness  $H$  bounding dielectric media ( $E1$  and  $E3$ ) - continuous line, (b) - for infinite media METAL/DIELECTRIC interface (broken line).  $H = .4$  micrometers

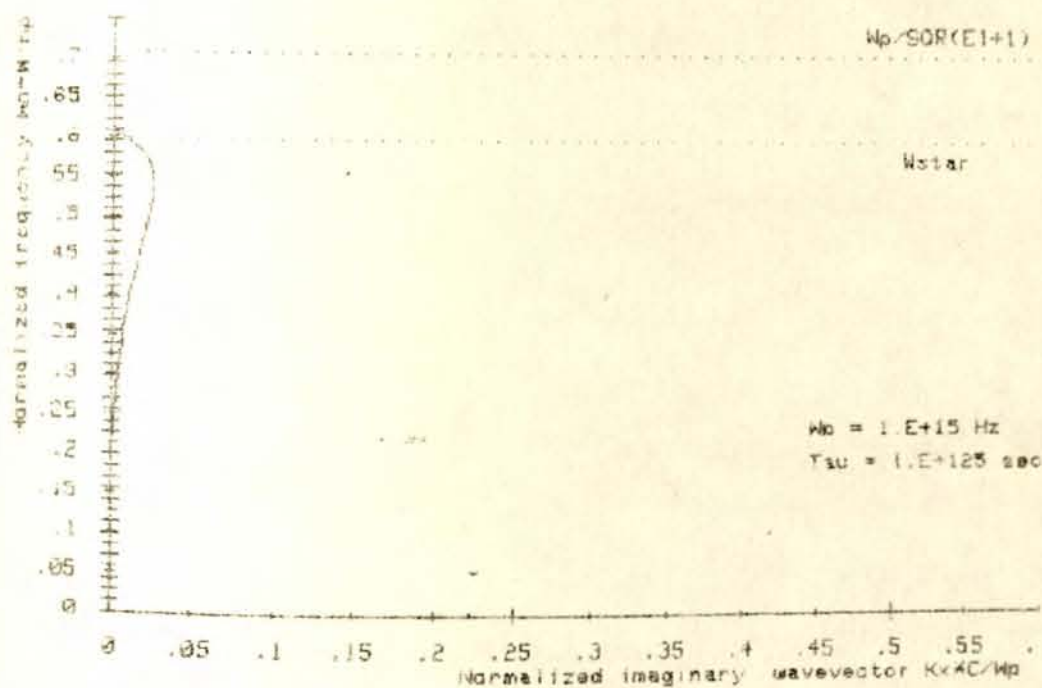


Fig. (2.3C) SPIP dispersion graph of IMAGINARY  $k_x$  as a function of frequency: (a) - for thin metallic film of thickness  $H$  bounding dielectric media ( $E1$  and  $E3$ ) - continuous line; (b) - for infinite media METAL/AIR interface (broken line).  $H = .4$  micrometers

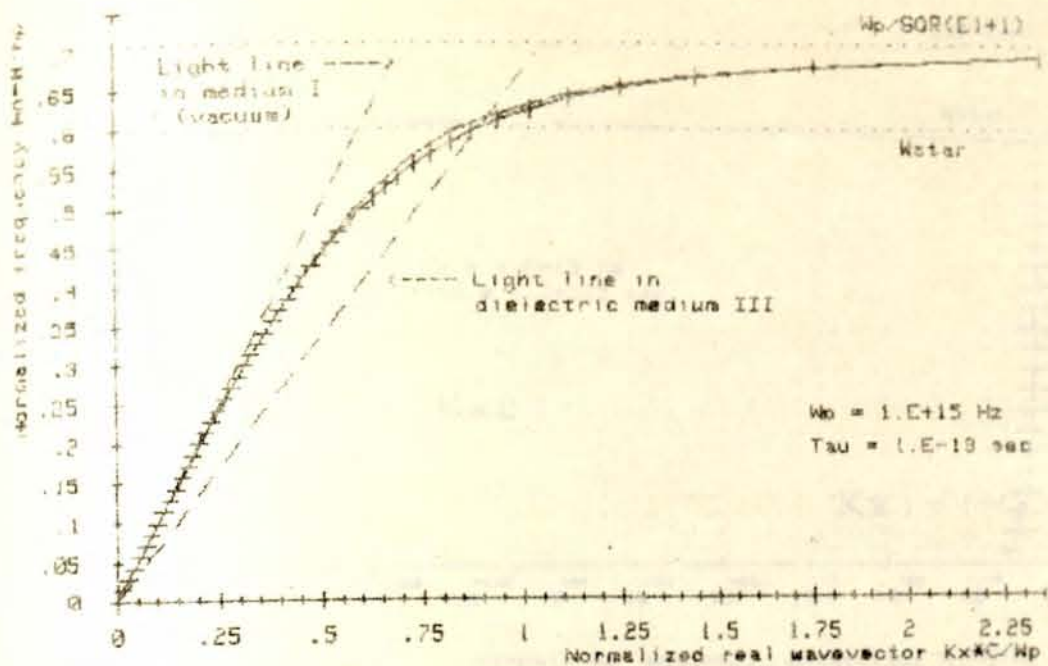


Fig. 2.2d) SPIP dispersion curve of REAL  $k_x$  as a function of frequency  $\omega$  (a) - for thin metallic film of thickness  $H$  bounding dielectric media ( $\epsilon_1$  and  $\epsilon_3$ ) - continuous line, (b) - for infinite media METAL/DIELECTRIC interface (broken line),  $H = .4 \text{ micrometers}$

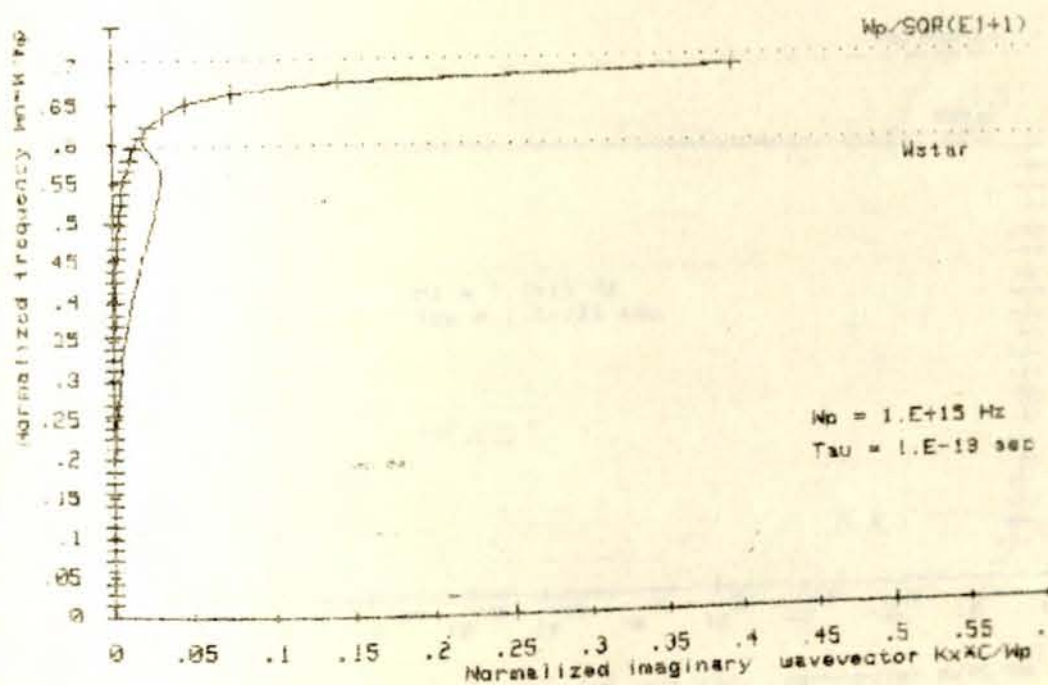


Fig. 2.3d) SPIP dispersion graph of IMAGINARY  $k_x$  as a function of frequency; (a) - for thin metallic film of thickness  $H$  bounding dielectric media ( $\epsilon_1$  and  $\epsilon_3$ ) - continuous line, (b) - for infinite media METAL/AIR interface (broken line),  $H = .4 \text{ micrometers}$

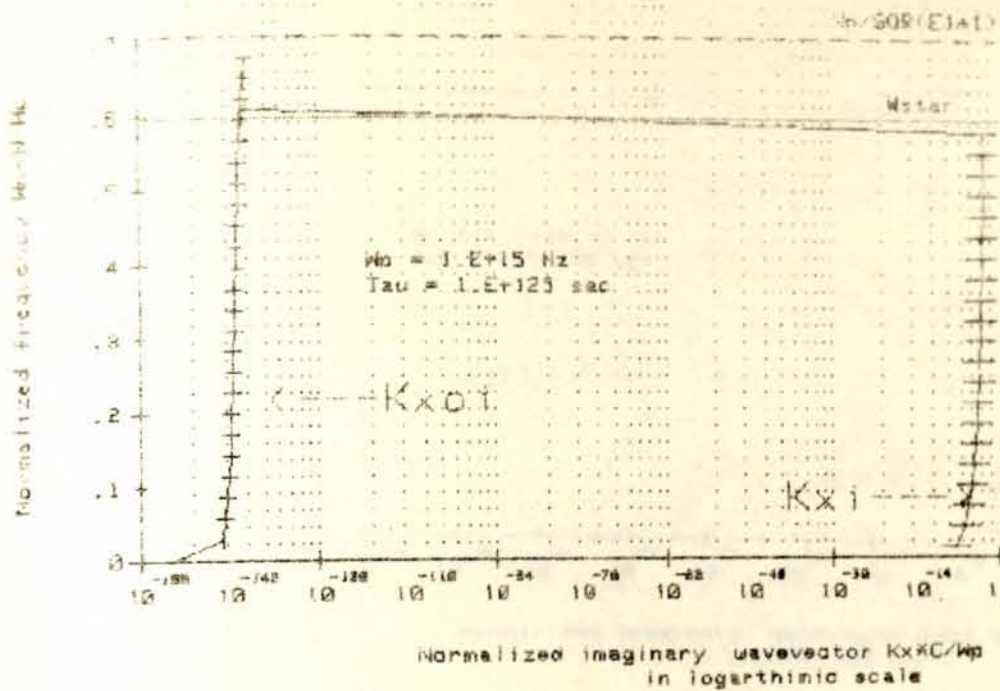


Fig. (2.40) SPIP dispersion graph of imaginary  $K_x$  as a function of frequency: (a)- for thin metallic film of thickness  $H$  bounding dielectric media ( $E_1$  and  $E_3$ ) (---|---|--- line); (b)- for infinite media METAL/AIR interface (I-I-I-I line).  $H = .04$  micrometers

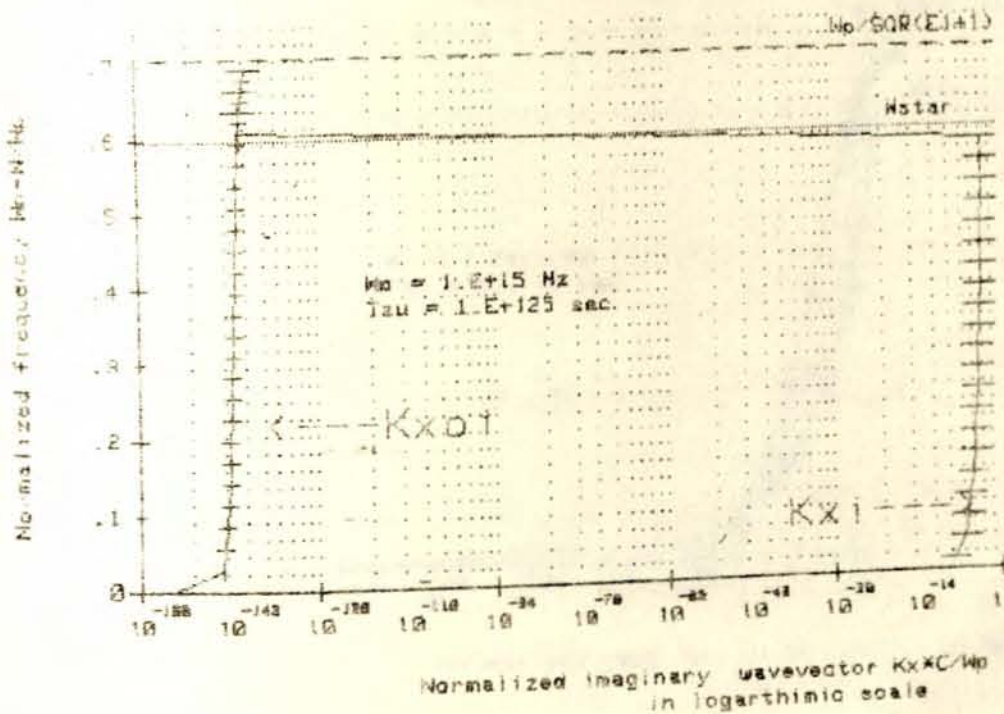


Fig. (2.41) SPIP dispersion graph of imaginary  $K_x$  as a function of frequency: (a)- for thin metallic film of thickness  $H$  bounding dielectric media ( $E_1$  and  $E_3$ ) (---|---|--- line); (b)- for infinite media METAL/AIR interface (I-I-I-I line).  $H = .2$  micrometers

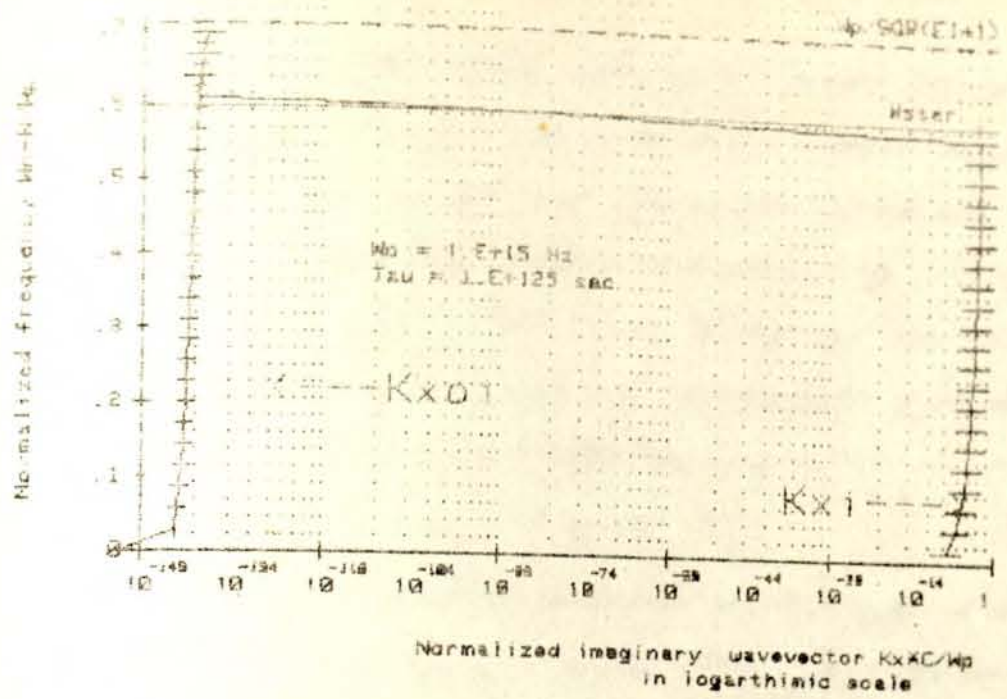


Fig. (2.40) SPIP dispersion graph of imaginary  $K_x$  as a function of frequency: (a)- for thin metallic film of thickness  $H$  bounding dielectric media ( $E_1$  and  $E_3$ ) |---| line; (b)- for infinite media METAL/AIR interface (I-I-I-I line).  $H = .4$  micrometers

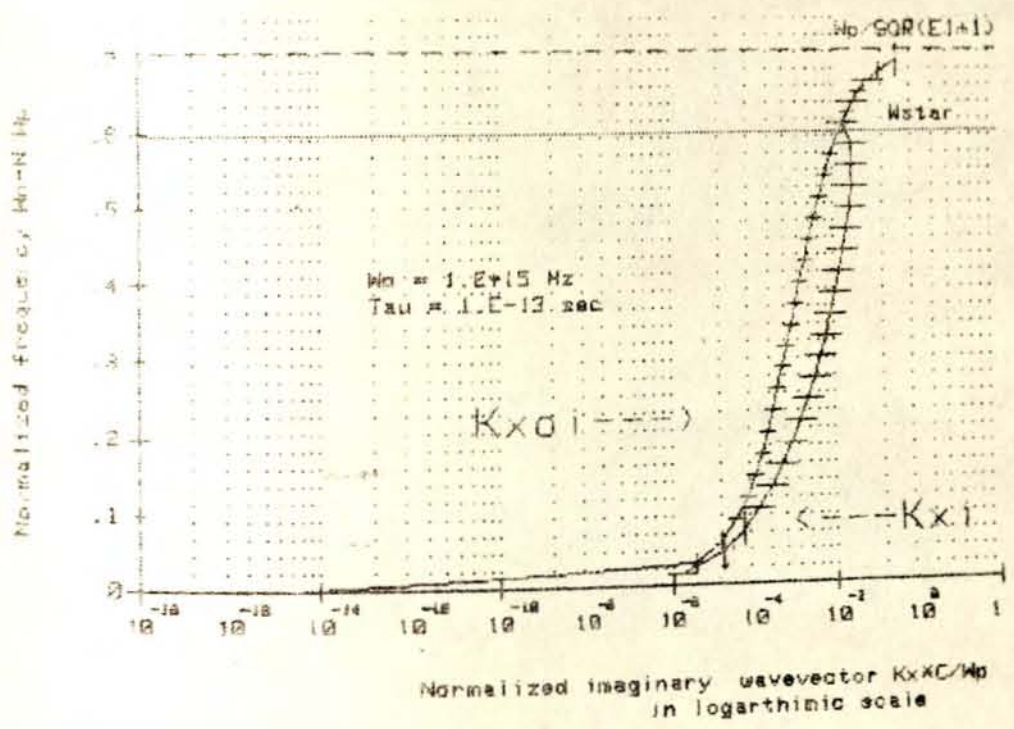


Fig. (2.40) SPIP dispersion graph of imaginary  $K_x$  as a function of frequency: (a)- for thin metallic film of thickness  $H$  bounding dielectric media ( $E_1$  and  $E_3$ ) |---| line; (b)- for infinite media METAL/AIR interface (I-I-I-I line).  $H = .4$  micrometers

(that is large wave number values) where the SP1P is most "Plasmon like" (see fig. 2.2) the most suitable probe of the dispersion equation is an experiment involving electrons, such as thin film electron diffraction [5]. Conversely, at larger wave lengths (that is small wave number values) where the SP1P is most "photon-like" (see fig. 2.2) the most suitable probe is an experiment involving light of the appropriate frequency, and it is one such technique that is discussed here, which is known as attenuated total reflection (ATR) [1].

ATR involves the use of the evanescent wave that is set up at a conducting medium/air interface when light in a high refractive index dielectric medium such as glass, suffers total internal reflection [6]. It is the reduction of the reflected wave due to absorption that is called ATR. If the weakening occurs by some other means it is usually called frustrated total internal reflection (FTIR). It is remarkable that FTIR can be traced back to Newton [7] and the knowledge and use of ATR has been wide spread only since the early 1960s due to pioneering work by Fahrenfort and Harrik [8,9]. In spite of all this work, however, the fundamental idea of using ATR to generate SP1P was first published by Otto [10] as late as 1968.

An inspection of the dispersion curves (see fig. 1.3) reveals that in the photon like region, where it might be thought that SP1P could be stimulated by incident electromagnetic waves, the dispersion curve, in the first subrange  $0 < k < \frac{\omega}{\sqrt{\epsilon_1 + 1}}$  lies below the light line. Unfortunately, for a plane electromagnetic wave incident on the interface between  $\epsilon_1 = 1$  and  $\epsilon_2$  at some angle  $\theta_1$ , the relationship between the component of wave

number parallel to the surface and  $\theta_1$  is given by:

$$K_x^i = \frac{W}{C} \theta_1 \sin \theta_1 \quad \text{-----} \quad (2.29)$$

This corresponds to a line steeper than the light line on Fig. (2.2) and hence, to the region above the light line, therefore SPP can't be generated. This awkward difficulty can be overcome in an ATR system as first proposed by Otto [10] and subsequently by Kretschmann [11], fig. (2.5).

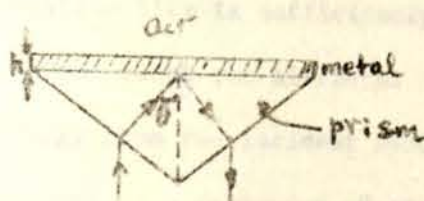


Fig. (2.5) Kretschmann Prism-metal-Air ATR Configuration with an active film of thickness  $h$  deposited on the base of the prism.

In this thesis we'll stick to Kretschmann's Scheme, which proved to be more convenient for practical use. Light incident, through the prism on to the prism-metal film interface at angles greater than the critical angle  $\theta_{3crit}$  is normally totally reflected back out through the prism:

$$\theta_{3crit} = \text{arc sin } \frac{n_2'}{n_3} \quad \text{-----} \quad (2.30)$$

However, under total internal reflection conditions there will always be an exponentially decaying evanescent field extending into the metallic film. The totally reflected wave has a component of wave number parallel to the surface now is given by equation:

$$K_x^r = \frac{W}{C} \sqrt{\epsilon_3} \sin \theta_3 \quad \text{-----} \quad (2.31)$$

The corresponding dispersion curve (see fig. 2.2) in the small  $K$  region lies only below the light line. The evanescent wave, created by

total reflection in the prism, actually exists in the range  $\theta_{3crit} < \theta_3 \leq 90^\circ$ . Hence the range of SPLP real wave number (in OX direction) associated with the evanescent wave is

$$\frac{\omega}{c} < K_x < \frac{\omega}{c} \sqrt{\epsilon_3} \quad \text{-----} \quad (2.32)$$

and corresponds to a region above the prism light line, but below the air or vacuum light line (see fig. 1.3).

From a practical point of view it is evident that, provided the thickness of the metallic film is sufficiently small, then the evanescent field from the prism can reach the air/metal film interface and SPLP can be excited. Energy from the incident wave is then used to stimulate a surface wave resulting in a weakening of the reflected intensity returned by the prism.

#### 2.4 ATR Modal

Let us consider a T-M polarization incident from dielectric medium 3 (prism) at an angle  $\theta_3$  to the normal of the medium 3/metal film interface (see fig. 2.6). The magnetic field in each medium may be expressed in the form

$$\begin{aligned} H_{z1} &= A_1 e^{+iK_{2y} Y} e^{i(K_x X - \omega t)} \\ H_{z2} &= (A_2 e^{+iK_{2y} Y} + B_2 e^{-iK_{2y} Y}) e^{i(K_x X - \omega t)} \quad \text{-----} \quad (2.33) \\ H_{z3} &= (A_3 e^{+iK_{3y} Y} + B_3 e^{-iK_{3y} Y}) e^{i(K_x X - \omega t)} \end{aligned}$$

Using the Maxwell's Curl equation with  $J = 0$ , that is  $\nabla \times \vec{H} = \epsilon \frac{\partial \vec{E}}{\partial t}$  the corresponding tangential component electric field distributions are given respectively for the three media by

$$E_{x1} = \frac{A_1 K_{1y}}{\omega \epsilon_1} e^{i k_{1y} Y} e^{i(K_x X - \omega t)}$$

$$E_{x2} = -\frac{A_2 K_{2y}}{\omega \epsilon_2} e^{i K_{2y} Y} + \frac{B_2 K_{2y}}{\omega \epsilon_2} e^{i K_{2y} Y} e^{i(K_x X - \omega t)} \quad (2.34)$$

$$E_{x3} = -\frac{A_3 K_{3y}}{\omega \epsilon_3} e^{i K_{3y} Y} + \frac{B_3 K_{3y}}{\omega \epsilon_3} e^{-i K_{3y} Y} e^{i(K_x X - \omega t)}$$

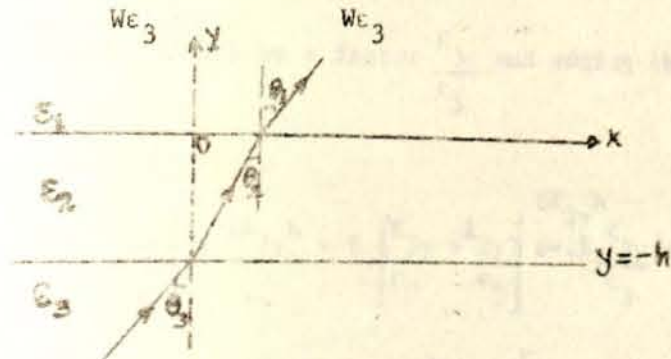


Fig. (2.3) illustration of the two interface model for an ATR system for Prism-Metal-Air (PMA) configuration.

Applying boundary conditions at  $Y = 0$  and  $Y = -h$ ;

$$A_1 = A_2 + B_2 \quad (2.35)$$

$$-\frac{A_1 K_{1y}}{\epsilon_1} = -\frac{A_2 K_{2y}}{\epsilon_2} + \frac{B_2 K_{2y}}{\epsilon_2} \quad (2.36)$$

$$A_2 e^{-i K_{2y} h} + B_2 e^{i K_{2y} h} = A_3 e^{-K_{3y} h} + B_3 e^{+i K_{3y} h} \quad (2.37)$$

$$-\frac{A_2 K_{2y}}{\epsilon_2} e^{-i K_{2y} h} + \frac{B_2 K_{2y}}{\epsilon_2} = -\frac{A_3 K_{3y}}{\epsilon_3} e^{-i K_{3y} h} + \frac{B_3 K_{3y}}{\epsilon_3} \quad (2.38)$$

From equation (2.35) and (2.36)

$$-(A_2 + B_2) \frac{K_{1y}}{\epsilon_1} = -\frac{A_2 K_{2y}}{\epsilon_2} + \frac{B_2 K_{2y}}{\epsilon_2}$$

$$A_2 \left( \frac{K_{2y}}{\epsilon_2} - \frac{K_{1y}}{\epsilon_1} \right) = B_2 \left( \frac{K_{2y}}{\epsilon_2} + \frac{K_{1y}}{\epsilon_1} \right)$$

$$\frac{B_2}{A_2} = \frac{\left[ \frac{K_{2y}}{\epsilon_2} - \frac{K_{1y}}{\epsilon_1} \right]}{\left[ \frac{K_{2y}}{\epsilon_2} + \frac{K_{1y}}{\epsilon_1} \right]} = r_{21} \quad (2.39)$$

$r_{21}$  is reflection coefficient at the interface of medium 2/medium 1.

Multiplying equation (2.37) by a factor  $\frac{K_{3y}}{\epsilon_3}$  and adding the result with

equation (2.38) we get

$$A_2 \left[ \frac{K_{3y}}{\epsilon_3} - \frac{K_{2y}}{\epsilon_2} \right] e^{-iK_{2y}h} + B_2 \left[ \frac{K_{3y}}{\epsilon_3} + \frac{K_{2y}}{\epsilon_2} \right] e^{iK_{2y}h} = 2B_3 \frac{K_{3y}}{\epsilon_3} e^{iK_{3y}h} \quad (2.40)$$

Again multiplying equation (2.37) by a factor  $\frac{K_{3y}}{\epsilon_3}$  and from the result subtracting equation (2.38) we get

$$A_2 \left[ \frac{K_{3y}}{\epsilon_3} + \frac{K_{2y}}{\epsilon_2} \right] e^{-iK_{2y}h} + B_2 \left[ \frac{K_{3y}}{\epsilon_3} - \frac{K_{2y}}{\epsilon_2} \right] e^{iK_{2y}h} = 2A_3 \frac{K_{3y}}{\epsilon_3} e^{-iK_{3y}h} \quad (2.41)$$

Dividing equation (2.40) by equation (2.41) results;

$$\frac{A_2 \left[ \frac{K_{3y}}{\epsilon_3} - \frac{K_{2y}}{\epsilon_2} \right] e^{-iK_{2y}h} + B_2 \left[ \frac{K_{3y}}{\epsilon_3} + \frac{K_{2y}}{\epsilon_2} \right] e^{iK_{2y}h}}{A_2 \left[ \frac{K_{3y}}{\epsilon_3} + \frac{K_{2y}}{\epsilon_2} \right] e^{-iK_{2y}h} + B_2 \left[ \frac{K_{3y}}{\epsilon_3} - \frac{K_{2y}}{\epsilon_2} \right] e^{iK_{2y}h}} = \frac{B_3}{A_3} e^{2iK_{3y}h} \quad (2.42)$$

Using equation (2.39), equation (2.42) can be arranged to give

$$A_2 r_{32} + A_2 r_{21} e^{2iK_{2y}h} = \frac{B_3}{A_3} e^{2iK_{3y}h} \quad (2.43)$$

$$A_2 + A_2 r_{32} r_{21} e^{2iK_{2y}h}$$

or

$$\frac{r_{32} + r_{21} e^{2iK_{2y}h}}{1 + r_{32} r_{21} e^{2iK_{2y}h}} = \frac{B_3}{A_3} e^{2iK_{3y}h} = r \quad (2.44)$$

$$\text{where } r_{32} = \frac{\left[ \frac{K_{3y}}{\epsilon_3} - \frac{K_{2y}}{\epsilon_2} \right]}{\left[ \frac{K_{3y}}{\epsilon_3} + \frac{K_{2y}}{\epsilon_2} \right]} \quad \text{-----} \quad (2.45)$$

is the coefficient of reflection at the interface of medium 3/medium 2.

$r$  is coefficient of reflection for medium 3.

Quantities  $r_{21}$ ,  $r_{32}$  and  $r$  can be expressed in terms of incident angle  $\theta_3$ .

Using Snell's Law

$$\begin{aligned} K_{1y} &= K_1 \cos\theta_1 = K_0 \sqrt{\epsilon_1} \cos\theta_1 \\ K_{2y} &= K_2 \cos\theta_2 = K_0 \sqrt{\epsilon_2} \cos\theta_2 \quad \text{-----} \quad (2.46) \\ K_{3y} &= K_3 \cos\theta_3 = K_0 \sqrt{\epsilon_3} \cos\theta_3 \end{aligned}$$

From Snell's law,

$$\begin{aligned} \sqrt{\epsilon_3} \sin\theta_3 &= \sqrt{\epsilon_2} \sin\theta_2 \\ \sqrt{\epsilon_2} \sin\theta_2 &= \sqrt{\epsilon_1} \sin\theta_1 \\ \cos\theta_1 &= \sqrt{1 - \frac{\epsilon_3 \sin^2\theta_3}{\epsilon_1}} \quad \text{-----} \quad (2.47) \\ \cos\theta_2 &= \sqrt{1 - \frac{\epsilon_3 \sin^2\theta_3}{\epsilon_2}} \end{aligned}$$

Using equations (2.46) and (2.47)

$$\begin{aligned} r_{21} &= \frac{\sqrt{\epsilon_1} \sqrt{1 - \frac{\epsilon_3 \sin^2\theta_3}{\epsilon_2}} - \sqrt{\epsilon_2} \sqrt{1 - \frac{\epsilon_3 \sin^2\theta_3}{\epsilon_1}}}{\sqrt{\epsilon_1} \sqrt{1 - \frac{\epsilon_3 \sin^2\theta_3}{\epsilon_2}} + \sqrt{\epsilon_2} \sqrt{1 - \frac{\epsilon_3 \sin^2\theta_3}{\epsilon_1}}} \quad \text{-----} \quad (2.48) \end{aligned}$$

$$r_3^2 = \frac{\sqrt{\epsilon_2 \cos \theta_3 - \sqrt{\epsilon_3} \sqrt{1 - \frac{\epsilon_3}{\epsilon_2} \sin^2 \theta_3}}}{\sqrt{\epsilon_2 \cos \theta_3 + \sqrt{\epsilon_3} \sqrt{1 - \frac{\epsilon_3}{\epsilon_2} \sin^2 \theta_3}}} \quad (2.49)$$

$$r = \frac{r_{32} + r_{21} e^{(2iK_0 \cdot \sqrt{\epsilon_2 - \epsilon_3} \sin^2 \theta_3)}}{1 + r_{32} r_{21} e^{(2iK_0 \cdot \sqrt{\epsilon_2 - \epsilon_3} \sin^2 \theta_3)}} \quad (2.50)$$

Note that  $r_{21}$ ,  $r_{32}$  and  $r$  are complex quantities, and in experiment it is the reflectance  $R = |r|^2$  which is determined.

### 2.5 Typical Results

As an example of the use of the ATR technique for the SPIP excitation data for sodium (a good free electron metal, which has a complex refractive index  $n_2 = 0.044 + 12.42i$ ) was used. The computer simulated experiment was run for a fixed angle scan and a fixed frequency scan. Table 1 contains a truncated copy of the data file showing the interesting parts of a fixed angle scan for Prism-Metal film-Air structure using a free electron model with data appropriate to sodium. The graph obtained with this data is shown in Fig. 2.7. This scan at  $60^\circ$  shows a deep minimum in the reflected intensity at a frequency  $w/w_p \sim 0.57$ . This corresponds to a "pole" in  $R_{21}$  that is at a slightly lower frequency (see third column in the table 1). The difference is due to the perturbation by the prism of the metal/air interface.

As a second example, a truncated set of results is displayed in table 2 for a fixed frequency scan. The graphs obtained from this data is shown at figure 2.8.

It can be seen that the reflected intensity in the fourth column of table 2 exhibits a sharp peak at  $\sim 42^\circ$  which is the critical angle for a prism air interface. This feature is typical of the PMA configuration and is due to the fact that the final medium in the system is Air with  $n_1 = 1$ . An examination of the third column containing  $R_{21} = |r_{21}|^2$  reveals a very large peak near  $47^\circ$  corresponding to the launching of a surface wave associated with the metal/air interface. Note that the reflected intensity shows a minimum very near to this angle, the shift being due again to the fact that perturbation occurs because we really have a coupled system. The degree to which this perturbation occurs is a function of the film thickness. It is possible to determine the optimum value of  $h$  and corresponding  $w/w_p$  for which  $R \rightarrow 0$ .

As an example of such opportunity we prepared figures (2.9) and (2.10) in which the frequency curve becomes very sharp and the  $R \min \sim 0$

TABLE 1. Fixed angle calculation. Reflectivity of PRISM-METAL FILM-AIR struct as a function of the normalized incident frequency.  $R_{32}$  - is the reflectivity of the PRISM/METAL film interface;  $R_{21}$  - is the reflectivity of METAL/AIR interface. The angle of the ATR scan  $\theta = 60$  degrees  
 Relative dielectric permittivities: PRISM -  $\epsilon_3 = 2.25$ , METAL film -  $\epsilon_2(\omega)$ ,  $\epsilon_1(\omega)$ , AIR -  $\epsilon_1 = 1$ .  
 Thickness of the film  $H = .04$  micrometers, plasma frequency  $\omega_p = 8.38197252587E+15$  Hz, relaxation time  $\tau = 1.00593208114E-14$  sec.

$\omega/\omega_p$	$R_{32}$	$R_{21}$	Total reflectance	
1.E-6	.999076341509	1.00037159662	.880473950791	1
.090001	.934010552955	1.55521045039	.869103716413	7
.180001	.940474202187	2.51882248753	.878710779317	13
.270001	.948764893815	4.51441171474	.895891395757	19
.360001	.956985811829	10.0539888904	.908153856989	25
*	*	*	*	*
.435001	.963123778141	29.1701862487	.903651770634	30
.450001	.964254614904	39.8566971917	.898830846811	31
.465001	.965352327785	57.122416416	.891380952001	32
.480001	.966417016022	89.5088067708	.879988161923	33
.495001	.967448947899	160.299144058	.862398996631	34
.510001	.968448530528	365.928884118	.834603369888	35
.525001	.969416283523	1457.05359428	.789382132437	36
.540001	.970352816224	7521.79345258	.714912895797	37
.555001	.971258808138	901.24544344	.602150260562	38
.570001	.972134992231	273.526575918	.495479634049	39
.585001	.972982140764	127.966080293	.52592711851	40
.600001	.973801053353	73.3643921814	.668102897844	41
.615001	.974592546973	47.2773954259	.78701960122	42
.630001	.975357447648	32.8641032323	.858129511243	43
.645001	.976096583589	24.0888097073	.898967450695	44
*	*	*	*	*
.660001	.976810779581	18.3617548936	.92338623537	45
.810001	.982753222042	3.33142988724	.976643432098	55
.960001	.986988381919	1.23591977197	.985164027118	65
1.110001	.990039023208	.598545378843	.989344787862	75
1.260001	.99226452126	.334117933587	.991979549061	85
1.410001	.993909765483	.204019366569	.993791698303	95

TABLE 2. Fixed normalized frequency calculation. Reflectivity of PRISM-METAL FILM-AIR structure as a function of the incident angle.  $R_{32}$  - is the reflectivity of the PRISM/METAL film interface;  $R_{21}$  - is the reflectivity of the METAL/AIR interface. The freq. of the ATR scan  $\omega/\omega_0 = .382$  rad/sec  
 Relative dielectric permittivities: PRISM -  $\epsilon_3 = 2.25$ , METAL film -  $\epsilon_2(\omega) = -5.8462817042$ ,  $\epsilon_2(\omega) = .212578670128$ , AIR -  $\epsilon_1 = 1$ .  
 Thickness of the film  $H = .04$  micrometers plasma frequency  $\omega_0 = 8.38197252587E+15$  Hz.  $\tau = 100583208114E-14$  sec

Teta (deg)	R32	R21	Total reflectance	
4	.967858965634	.974499371602	.677776988447	1
20	.965457243788	.970399395708	.659782534977	5
36	.960997189305	.960297853665	.625991039039	9
*	*	*	*	*
36.05	.950982735032	.960277751031	.626044302114	10
37.15	.960667418691	.960036946689	.628775064618	32
38.25	.960358328985	.960422612618	.636157131225	54
39.35	.960057159185	.962099997981	.652866945083	76
40.45	.959765703781	.966805029838	.691682855938	98
41.55	.959485863685	.982309968519	.816592150038	120
42.65	.959219651436	5.54559165123	.978017995094	142
43.75	.958969196284	17.2892818316	.964375983017	164
44.85	.958736749076	55.9680051784	.914137010827	186
45.95	.95852468882	285.972833139	.800017778117	208
47.05	.958335516777	3778.26024784	.691960572604	230
48.15	.958171379830	465.025457783	.694936453403	252
49.25	.958036553675	142.019214892	.744603867245	274
50.35	.95793245339	74.2787967453	.798761332324	296
51.45	.957862632866	48.35861158	.820765319316	318
*	*	*	*	*
52	.95784156941	40.9121947329	.833142742612	329
56	.961850632179	9.34117225286	.930999930053	336
80	.979321035409	6.79104970606	.970477089832	343

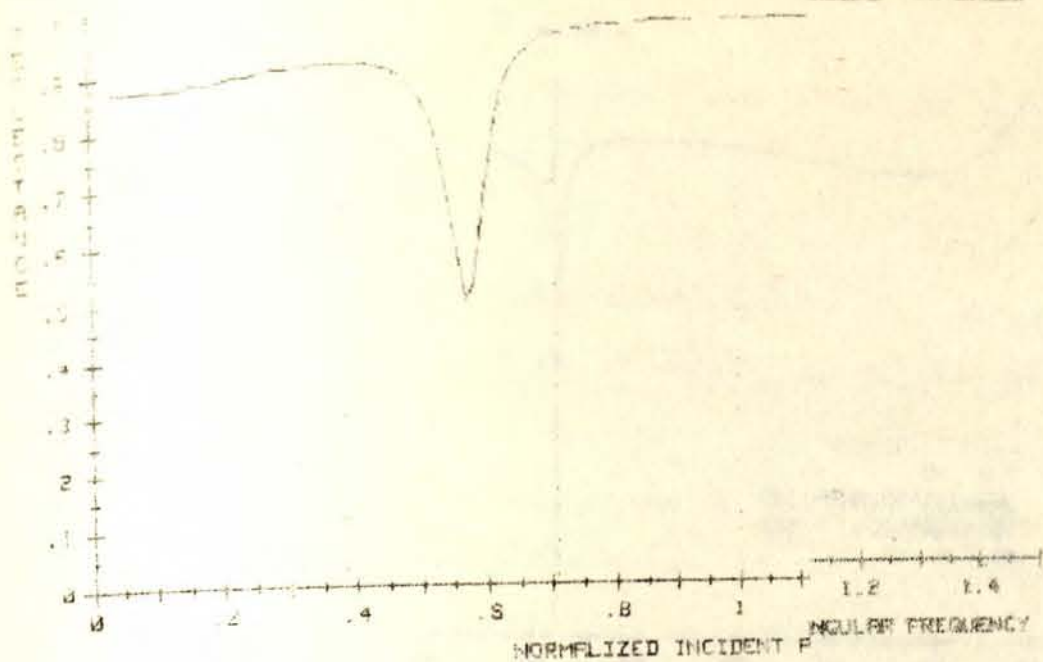


Fig. 2.7 Graph of reflectivity  $R$  as a function of incident angular frequency  $\omega$  for PMR configuration at  $\theta = 50^\circ$  micrometers. Thickness of the metal film  $H = 0.38E+15$  rad/second;  $\tau = 1.01E-14$  sec.

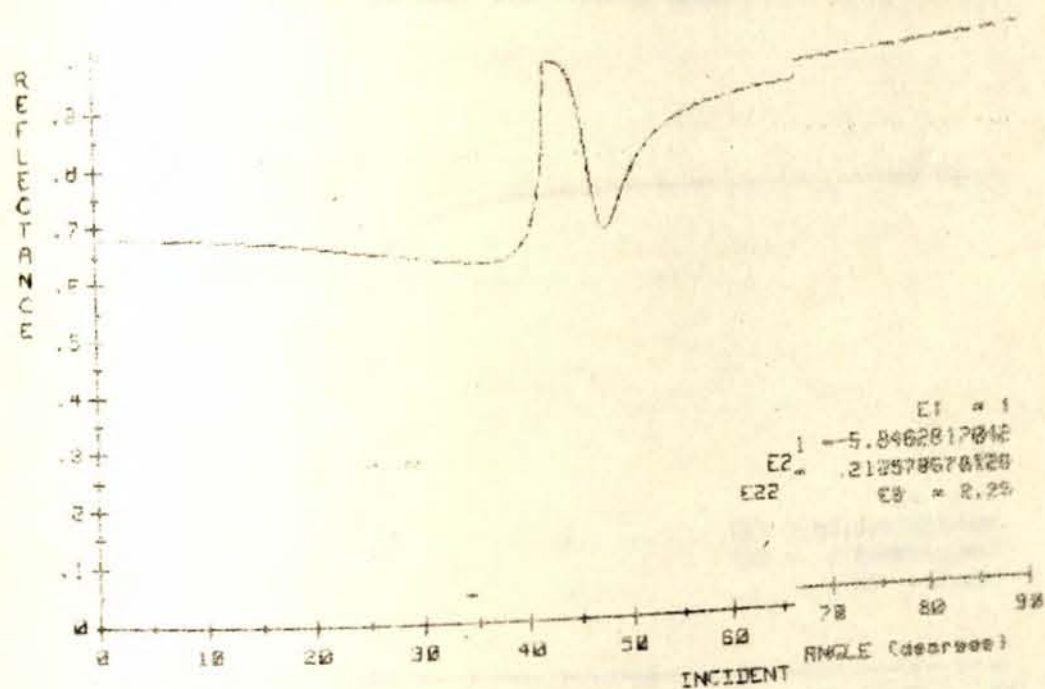


Fig. 2.8 Graph of reflectivity  $R$  as a function of incident angle  $\theta$  for PMR configuration at normalized frequency of  $\omega = 0.382$  micrometers. Thickness of the metal film  $H = 0.38E+15$  rad/second;  $\tau = 1.01E-14$  sec.

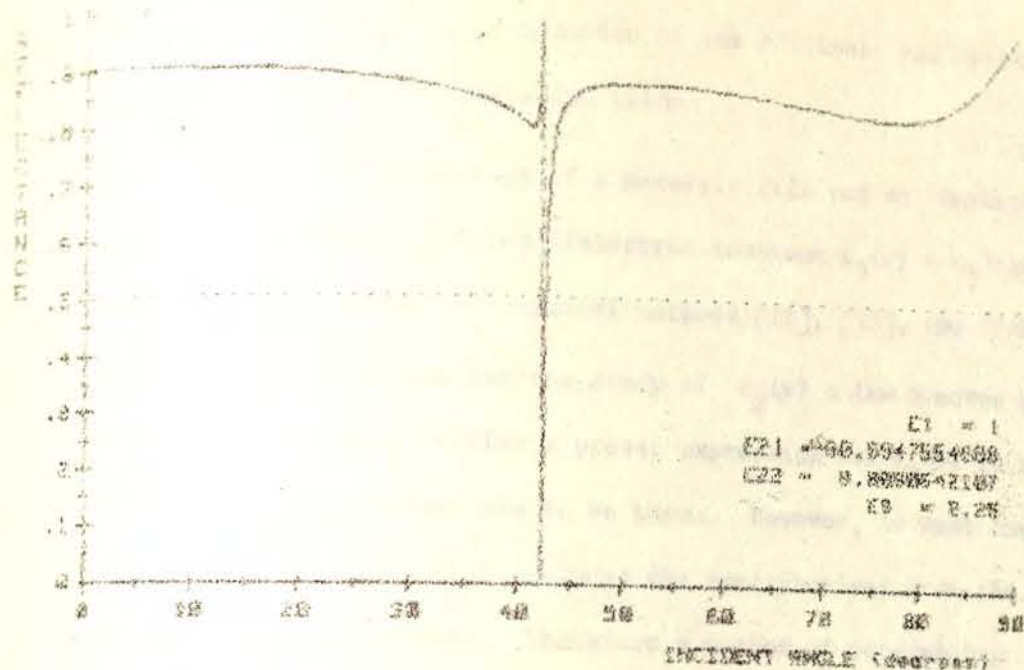


Fig. 2.9 Graph of reflectivity  $R$  as a function of incident angle  
 Tota for PPR configuration at normalized frequency of sound  
 $\omega/\omega_p = .118$ . Thickness of the metal film  $H = .64$  microns.  
 $\omega_p = 8.38E+12$  rad/sec;  $\gamma = 1.81E-14$  sec.

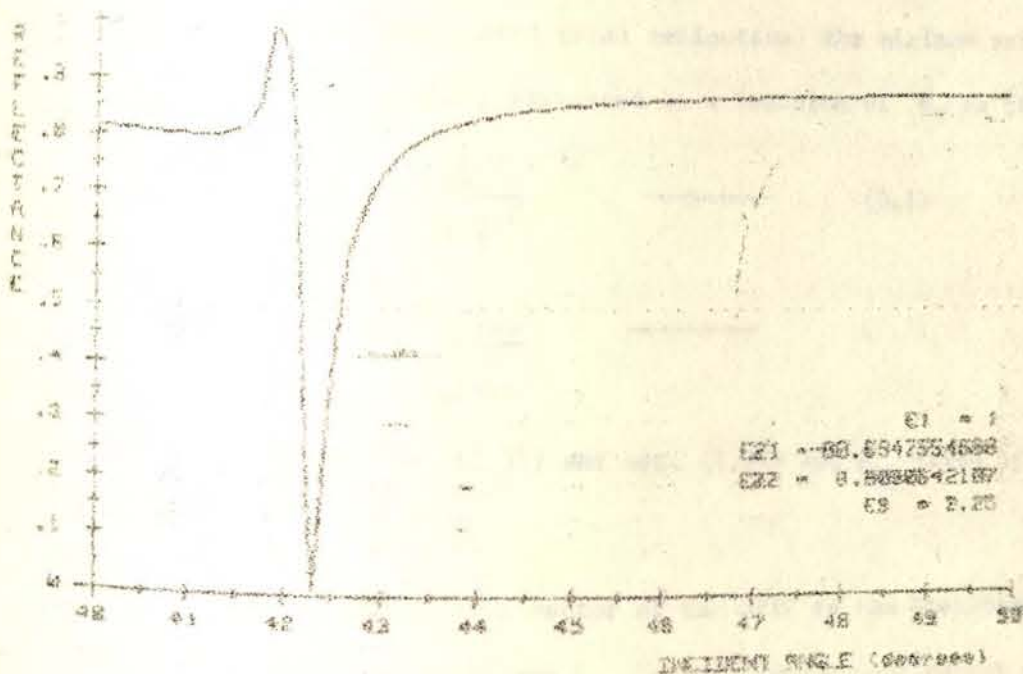


Fig. 2.10 Graph of reflectivity  $R$  as a function of incident angle  
 Tota for PPR configuration at normalized frequency of sound  
 $\omega/\omega_p = .118$ . Thickness of the metal film  $H = .64$  microns.  
 $\omega_p = 8.38E+12$  rad/sec;  $\gamma = 1.81E-14$  sec.

### 3.1 Use of SPIP for determination of the thickness and optical constants of thin metallic films

The optical properties of a metallic film can be characterized by a frequency dependent complex dielectric constant  $\epsilon_2(\omega) = \epsilon_2' + i\epsilon_2''$  (see eqn. (1.24b)). Among many optical methods [12], [13], the SPIP technique is particularly suited for the study of  $\epsilon_2(\omega)$  a few hundred angstroms in thickness. In many studies a preset expression for  $\epsilon_2(\omega)$  is required. That is  $w_p$  and  $\tau$  values are to be known. However, in most cases a preset expression for  $\epsilon_2(\omega)$  that includes the contributions from the inter band transition is impossible. Therefore a method of determining  $\epsilon_2(\omega)$  and  $h$  at any given frequency without a preset  $\epsilon_2(\omega)$  expression is needed. Such method is described in the article [3]. The basic formulas and the concept are as follows, the geometry of the method is shown on fig. (2.5), with the angle of incidence of the external monochromatic plane wave  $\theta$  close to  $\theta_{ATR}$  (of attenuated total reflection) the minimum reflectance  $R_{min}$  can be approximately expressed as a function of  $\theta$ , as [4]

$$R_{min} = 1 - \frac{4\eta}{(1+\eta)^2} \quad \text{-----} \quad (3.1)$$

$$\text{where } \eta = \frac{I_m(K_{x0})}{I_m(K_{x1})} \quad \text{-----} \quad (3.2)$$

With  $K_{x0}$  given by eqn. (1.31) and eqn. (1.32) and  $K_{x1}$  given by eqn. (2.20) and  $K_x = K_{x0} + K_{x1}$ .

Here  $K_x$  is the complex wave vector of the SPIP in the Kretschmann configuration (see fig. (2.5) and  $K_{x0}$  is the complex wave vector of the SPIP at the metal - vacuum interface in the absence of the prism (semi infinite case, described in chapter 1).  $K_{x1}$  is the perturbation to  $K_{x0}$

In the presence of the prism,  $\frac{I_R}{I_{R_0}}$  describes intrinsic damping in the absence of the prism, represents the pole-loss,  $\frac{I_R}{I_{R_0}}$  describes the radiative damping in the presence of the prism, represents the leakage loss of SPR back into the prism.

The reflectance has a Lorentz dip at  $\theta = \theta_{ATR}$  with a half width  $W_G$  (when  $\frac{I_R}{I_{R_0}}(K_x) \ll \frac{I_R}{I_{R_0}}(K_x)$ )

$$W_G = 2 \Gamma_m(K_x) \cos(\theta_{ATR}) \frac{c}{\sqrt{\epsilon_2} W} \quad (3.3)$$

with

$$\theta_{ATR} = \arcsin \left( \frac{K_x}{\epsilon_2} \cdot \frac{c}{\sqrt{\epsilon_2} W} \right) \quad (3.4)$$

with eqns. (3.1) to (3.4) and eqns. (2.20), (1.31), and (1.32) one can determine  $\epsilon_2(W)$  and  $h$  of a metal film from the measured  $R$  versus  $W$  curve, by best fitting of the data with  $R$  given by eqn. (3.1)

A detailed description of the necessary steps is given in section 3.2 where we first suggest a more convenient modification of this method.

### 3.2 A suggested modification of the method for the determination of $\epsilon_2(W)$ and $h$ .

The measured quantities are  $\theta_{ATR}$ ,  $W_G$ , and  $R_{min}$  under the assumption that

$$\frac{R(K_x)}{I_{R_0}} \approx \frac{R(K_x)}{I_{R_0}} = \frac{W}{C} \cdot \sqrt{\frac{\epsilon_1 \epsilon_2}{\epsilon_1 + \epsilon_2}} \quad \text{see eqn. (1.24b) and using eqn. (3.4),}$$

one can arrive to a formula;

$$\epsilon_2^r = \frac{\epsilon_1 \epsilon_3 \sin^2 \theta_{ATR}}{\epsilon_3 \sin^2 \theta_{ATR}} \quad (3.5)$$

Next eqn. (3.3) can be written as

$$I_{m \times}^K = \frac{W\theta}{2} \frac{1}{\cos\theta_{ATR}} \frac{W}{C} \sqrt{\epsilon_3} = I_{m \times o}^K + I_{m \times l}^K \quad (3.6)$$

with

$$I_{m \times o}^K = \frac{W}{C} \sqrt{\frac{\epsilon_1 + \epsilon_2}{\epsilon_1 + \epsilon_2'}} \frac{\epsilon_1 + \epsilon_2''}{2 \epsilon_2' (\epsilon_1 + \epsilon_2')} \quad (3.7)$$

on the other hand, from eqn. (3.1)

$$\eta = \frac{(1 + R_{\min}) + 2\sqrt{R_{\min}}}{1 - R_{\min}} = \frac{1 + \sqrt{R_{\min}}}{1 + \sqrt{R_{\min}}} \quad (3.8)$$

The choice of algebraic signs in eqn. (3.8) should be based upon the physical sense of which is clear from eqn. (3.2). In the limiting case  $h \rightarrow \infty$   $I_{m \times l}^K$  should vanish, giving  $\eta \rightarrow \infty$ . This result can be achieved from eqn. (3.8) if the upper signs (both in the numerator and the denominator) are used with  $R_{\min} \rightarrow 1$ . This case would be denoted as  $\eta_+$ . In the other limiting case  $h \rightarrow 0$ , the perturbation  $I_{m \times l}^K$  prevails over  $I_{m \times o}^K$ , therefore  $\eta \rightarrow 0$ . This result follows from eqn. (3.8) if the lower signs are used, with  $R_{\min} \rightarrow 1$ . This case would be denoted as  $\eta_-$ .

This consideration of the limiting cases suggest that there must be a switch from the upper case to the lower case as  $h$  change from  $\infty$  to 0. This abrupt change occurs at  $h = h_{opt}$ , when  $R_{\min} \rightarrow 0$ . The qualitative graph for  $\eta = \eta(h)$  is shown at fig. (3.1a).

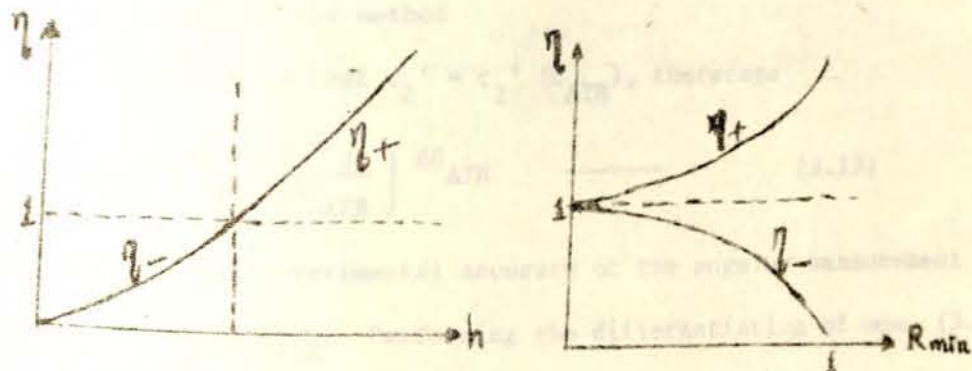


Fig. (3.1a) Illustration to the switch of sign operation.

with the help from eqn. (3.8), (3.2), (3.7), (3.6) and (3.5)

$$\begin{aligned} I_{m \ x1}^K &= \frac{I_{m \ x0}^K}{R} ; \\ I_{m \ x1}^K &= \frac{W_\theta}{2} \frac{1}{\cos\theta_{ATR}} \frac{W}{C} \sqrt{\epsilon_3} - I_{m \ x0}^K \quad (3.9) \end{aligned}$$

$$I_{m \ x0}^K \cdot (1+\eta) = \frac{W_\theta}{2} \frac{1}{\cos\theta_{ATR}} \frac{W}{C} \sqrt{\epsilon_3}$$

with

$$\epsilon_2'' = \frac{W_\theta}{2} \left( 1 + \sqrt{R_{min}} \right) \frac{\epsilon_1^2 \epsilon_3 \tan\theta}{(\epsilon_1 - \epsilon_3 \sin^2\theta)^2} \quad (3.10)$$

where the upper sin (+) is for  $h > h_{opt}$ , and the lower sign (-) for  $h < h_{opt}$

$$\text{At } h = h_{opt} \quad R_{min} = 0.$$

Now using eqns. (3.10), (3.7) and (3.9) we can derive a formula, which is useful for the final step for determination of  $h$ .

$$I_{m \ x1}^K = \frac{W}{C} \frac{W_\theta \sqrt{\epsilon_3}}{4 \cos\theta_{ATR}} \left( 1 + \sqrt{R_{min}} \right) \quad (3.11)$$

where the convention of algebraic signs is the same as above.

Eqn. (3.11) gives the experimentally measured values of  $(I_{m \ x1}^K)_{xp}$ .

The theoretical value of  $(I_{m \ x1}^K)_{theor.}$  as a function of  $h$  is given by eqn. (2.20). The numerical solution of the equation:

$$(I_{m \ x1}^K)_{(h)}_{theor.} = (I_{m \ x1}^K)_{xp} \quad (3.12)$$

gives the experimentally determined thickness  $h$  of the metallic film.

### 3.3 The accuracy of the method

Eqn. (3.5) shows that  $\epsilon_2' = \epsilon_2'(\theta_{ATR})$ , therefore

$$|\Delta\epsilon_2'| = \left| \frac{\partial\epsilon_2'}{\partial\theta_{ATR}} \right| \Delta\theta_{ATR} \quad (3.13)$$

Where  $\Delta\theta_{ATR}$  is the experimental accuracy of the angular measurement of the resonant angle  $\theta_{ATR}$ . Performing the differentiation of eqn. (3.5)

the relative accuracy of  $\epsilon_2'$  determination can be expressed

$$\frac{|\Delta \epsilon_2'|}{|\epsilon_2'|} = \frac{2\epsilon_1 \Delta \theta \text{ATR}}{(\epsilon_1 - \epsilon_3 \sin^2 \theta) \tan \theta} \quad (3.14)$$

Similarly, eqn. (3.1) indicates  $\epsilon_2'' = \epsilon_2''(\theta_{\text{ATR}}, W_\theta, R_{\text{min}})$ , therefore:

$$|\Delta \epsilon_2''| = \left| \frac{\partial \epsilon_2''}{\partial \theta_{\text{ATR}}} |\Delta \theta_{\text{ATR}}| + \frac{\partial \epsilon_2''}{\partial W_\theta} |\Delta W_\theta| + \frac{\partial \epsilon_2''}{\partial R_{\text{min}}} |\Delta R_{\text{min}}| \right. \quad (3.15)$$

where  $\Delta W_\theta$ ,  $\Delta R_{\text{min}}$  are experimental accuracies of measurements for half-width of the resonant curve and minimum of reflectance respectively.

performing partial differentiation of eqn. (3.10) gives

$$\frac{\partial \epsilon_2''}{\partial \theta} = \frac{W_\theta}{2} (1 + \sqrt{R_{\text{min}}}) \epsilon_1^2 \epsilon_3 \left[ \frac{\sec^2 \theta (\epsilon_1 - \epsilon_3 \sin^2 \theta) + 4\epsilon_3 \sin^2 \theta}{(\epsilon_1 - \epsilon_3 \sin^2 \theta)^2} \right] \quad (3.16)$$

$$\frac{\partial \epsilon_2''}{\partial W_\theta} = \frac{1}{2} (1 + \sqrt{R_{\text{min}}}) \frac{\epsilon_1^2 \epsilon_3 \tan \theta}{(\epsilon_1 - \epsilon_3 \sin^2 \theta)^2} \quad (3.17)$$

$$\frac{\partial \epsilon_2''}{\partial R_{\text{min}}} = \pm \frac{W_\theta}{4} \frac{\epsilon_1^2 \epsilon_3 \tan \theta}{(\epsilon_1 - \epsilon_3 \sin^2 \theta)^2} \cdot \frac{1}{\sqrt{R_{\text{min}}}} \quad (3.18)$$

where the convention of the algebraic signs is the same as above.

Let's normalize eqns (3.16) to (3.18) with respect to  $\epsilon_2''$

$$\frac{\partial \epsilon_2''}{\epsilon_2'' \partial \theta} = \frac{\epsilon_1 - \epsilon_3 \sin^2 \theta + 4\epsilon_3 \sin^2 \theta \cos^2 \theta}{\sin \theta \cos \theta (\epsilon_1 - \epsilon_3 \sin^2 \theta)} \quad (3.19)$$

$$\frac{\partial \epsilon_2''}{\epsilon_2'' \partial W_\theta} = \frac{1}{W_\theta} \quad (3.20)$$

$$\frac{\partial \epsilon_2''}{\epsilon_2'' \partial R_{\min}} = \frac{1}{2 \sqrt{R_{\min}} (1 + \sqrt{R_{\min}})} \quad (3.21)$$

Hence, substituting eqns. (3.19) to (3.21) into eqn. (3.15) the relative accuracy of  $\epsilon_2''$  determination can be expressed as;

$$\left| \frac{\Delta \epsilon_2''}{\epsilon_2''} \right| = \left| \frac{\epsilon_1 - \epsilon_3 \sin^2 \theta + 4 \epsilon_3 \sin^2 \theta \cos^2 \theta}{\sin \theta \cos \theta (\epsilon_1 - \epsilon_3 \sin^2 \theta)} \right| \left( \frac{\Delta \theta}{\theta} + \frac{\Delta W \theta}{W \theta} + \frac{1}{2 \sqrt{R_{\min}} (1 + \sqrt{R_{\min}})} \Delta R_{\min} \right) \quad (3.22)$$

The relative accuracy of  $h$  determination was determined by numerical procedure as the described in the next paragraph.

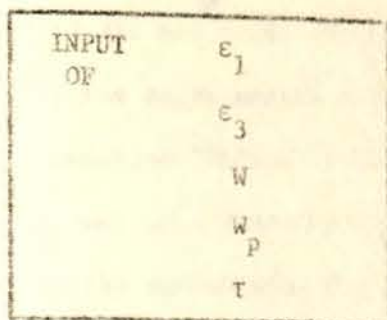
### 3.4 The Computer Program

The basic idea of the computer program is represented on Fig. (3.1b) and (3.1c). The program first simulates the values of  $\theta_{ATR}$ ,  $W_\theta$  and  $R_{\min}$  as if they were measured in an ideal experiment with out any instrumental error ( $\Delta \theta = \Delta W_\theta = \Delta R = 0$ ). These values of  $\theta_{ATR}$ ,  $W_\theta$  and  $R_{\min}$  are named as "expected experimental values".

With an expected experimental value of  $\theta_{ATR}$  from eqn. (3.4) it is possible to find the value of  $\epsilon_2'_{\text{exp}}$  from eqn. (3.5). Note that, since instrumental error  $\Delta \theta$  is neglected, the result might be affected only by the approximation made in the theory. The calculations and comparison with the exact value of  $\epsilon_2'_{\text{theor}}$  given by eqn. (1.24b) show that  $\Delta \epsilon_2' = \epsilon_2'_{\text{theor}} - \epsilon_2'_{\text{exp}}$  really depends upon the frequency used. The following results were obtained.

$$\left( \frac{\Delta \epsilon_2'}{\epsilon_2'} \right)_{\text{theor}} \left( \frac{W}{W_p} = 0.05 \right) = 5.7\% \quad \left( \frac{\Delta \epsilon_2'}{\epsilon_2'} \right)_{\text{theor P}} \left( \frac{W}{W} = 0.3 \right) = 0.2\%$$

$$\left( \frac{\Delta \epsilon_2'}{\epsilon_2'} \right)_{\text{theor}} \left( \frac{W}{W_p} = 0.1 \right) = 1.4\%$$



Determination of the exact theoretical values of  $\epsilon_2'$  and  $\epsilon_2''$  with eqn. 1.24b

For a given value of  $h$   
 $I_{m \times 0} K'$  and  $I_{m \times 1} K'$  are determined with a subroutine "Filmdisp" (eqn. 1.32, 2.20)

The expected experimental values of  $\theta_{ATR}$ ,  $W_\theta$  and  $R_{min}$  are found through eqns. (3.1), (3.2), (3.3) and (3.4)

For the found expected experimental value of  $\theta_{ATR}(h)$  and given  $W$ , the value of  $h_{opt}$  is found with a subroutine " $\theta_{pt} - h$ " (eqn. for  $R$ )

$\left| \frac{\Delta \epsilon_2'}{\epsilon_2'} \right|$  is found with a subroutine " $E_{21}$  accuracy"



NO  $\left| \frac{\epsilon_2''}{\epsilon_2''} \right|$  is found with a subroutine " $E_{22}$  accuracy"

yes  $\frac{\Delta \epsilon_2''}{\epsilon_2''}$  is found with a subroutine " $E_{22}$  accuracy"

Using eqn. (3.1), (3.3), and (3.4) and the expected experimental values of  $\theta_{ATR}$ ,  $W_0$ ,  $R_{min}$ , the experimental value of  $h$  is found. The procedure involves a subroutine "Bisect" from the numerical analysis library which finds the root of a function  $(I_{m \times l}^K)_{exp} - (I_{m \times l}^K)_{theor}$ , see eqn. (2.20), (3.11), the subfunction FNF (H), a subroutine "Film disp 2", in which  $\epsilon_2'$  and  $\epsilon_2''$  are calculated as experimentally determined (see eqn. (3.5), (3.10))

$\frac{h_{exp}}{h_{exp}}$  as a function of  $\Delta\theta_{ATR}$ ,  $\Delta W_0$ ,  $\Delta R_{min}$  is numerically calculated and stored in arrays  $Dh_0(*)$ ,  $Dh_1(*)$  and  $Dh_2(*)$ . The total error is stored in an array  $D_{ht}(*)$

Next h

PRINTING The graphs of  $\frac{\Delta\epsilon_2'}{\epsilon_2'}$ ,  $\frac{\Delta\epsilon_2''}{\epsilon_2''}$ ,  $\frac{\Delta h_{exp}}{h_{exp}}$  versus h

(The list of the program is found in Appendix B.)

Fig. (3.1c) Block diagram of the computer program.

This frequency dependence becomes clear if we recall that eqn. (2.2) is valid only for  $\frac{\epsilon_2''}{|\epsilon_2'|} \ll 1$ . If we check this ratio at the specified

frequencies, we get,  $\frac{\epsilon_2''}{|\epsilon_2'|} \left(\frac{W}{W_p} = 0.05\right) = 0.24$ ;  $\frac{\epsilon_2''}{|\epsilon_2'|} \left(\frac{W}{W_p} = 0.1\right) = 0.12$ ;

$\frac{\epsilon_2''}{|\epsilon_2'|} \left(\frac{W}{W_p} = 0.3\right) = 0.04$

Since the value of  $\epsilon'_{2\text{exp}}$  is used in the subsequent evaluations of  $\epsilon''_{2\text{exp}}$  and  $h_{\text{exp}}$  the first conclusion can be made.

### Conclusion 1

The accuracy of the method has a tendency to improve as the frequency grow from 0 upto  $W^{**}$  (see eqn. (2.28)). For frequencies greater than  $W^{**}$  the accuracy again starts to deteriorate because the perturbation term in eqn. (2.13) becomes comparable to the basic term, making the solution (see eqn. (2.20)) invalid.

The first try of the program without any instrumental error allow to estimate the accuracy of the mathematical software used in the method. The errors made due to a finite accuracy of the software we'll call "software errors". It is clear that the 'software errors' in determination of  $\epsilon'_2$ ,  $\epsilon''_2$ ,  $h$  should be always less than the errors which originate from finite instrumental accuracy. These latter errors we'll call experimental errors. For a practical use the instrumental error can be taken as  $\Delta\theta = \Delta W = 5''$ ,  $\Delta R = 0.01$ . These values are used in the second, third, fourth and fifth tries of the program, when all partial experimental and a total experimental errors are calculated. It is necessary to underline that the 'software error' is always incorporated in the calculation of the experimental errors, and for this reason it must be always checked first.

### 3.5 Analysis of the Methods Accuracy

As an example of the kind of results obtained from this program, data for sodium

( $\omega_p = 8.38197252597 \times 10^{15}$  Hz,  $\tau = 1.00583208114 \times 10^{-14}$  sec) was used. The refractive index of the prism was taken as,  $n_3 = 1.5$ . The surrounding medium was air with  $n_1 = 1$ . Typical results are shown at fig. (3.2) (3.3a), (3.3b), (3.3c), (3.4a), (3.4b), and (3.4c).

Fig. (3.2) shows that  $\frac{\Delta \epsilon_2'}{|\epsilon_2'|_{\text{exp}}}$  is independent from  $h$  which

is understandable since  $R_{e, X_0}$  used in eqn. (3.4) does not depend upon  $h$ . On the other hand the comparison of the curves at fig. (3.2) with the values of  $\frac{\Delta \epsilon_2'}{|\epsilon_2'|_{\text{theor}}}$  shows that; the theoretical error is roughly

3 times bigger than the experimental error due to  $\Delta \theta \neq 0$ .

## Conclusion 2

It is reasonable to perform the measurements for the determination of  $\epsilon_2'$  only for normalized frequencies not less than  $\frac{\omega}{\omega_p} = 0.1$ . For less frequencies the software error rapidly grows bringing the total experimental error to  $\sim 8\%$  at  $\frac{\omega}{\omega_p} = 0.05$ .

The most striking result comes from Figs. (3.3a), (3.3b), and (3.3c) at which  $\frac{\Delta \epsilon_2''}{\epsilon_2''_{\text{exp}}}$  as a function of  $h$  is shown for different normalized frequencies.

The figures show that a decisive contribution to the total experimental error comes from a partial experimental error due to an instrumental error in measuring  $R_{\min}$ . In particular at  $h$  in the vicinity of  $h_{\text{opt}}$ , when the value of  $R_{\min} \neq 0$ , this partial experimental error exhibits an unlimited growth. This result is

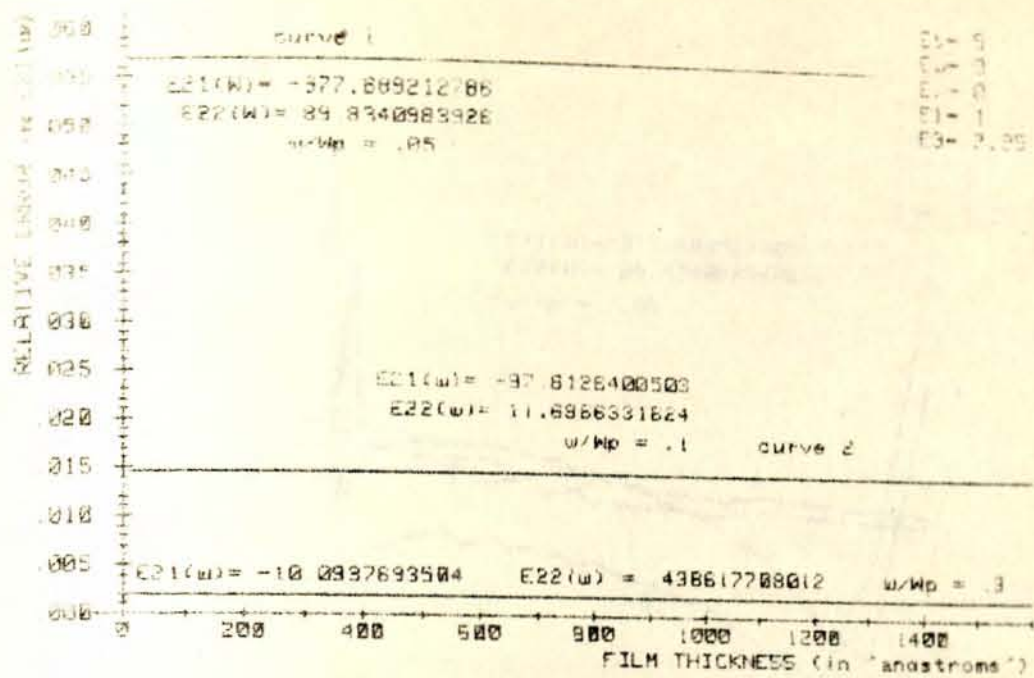


Fig. 3.2 Dependence of relative error in determination of  $E_{21}(w)$  on the thickness of metallic film. Absolute errors of measurement:  $E_t$  - for the resonant angle,  $E_w$  - for the half-width of the resonant curve,  $E_r$  - for the minimum reflectivity at resonance.

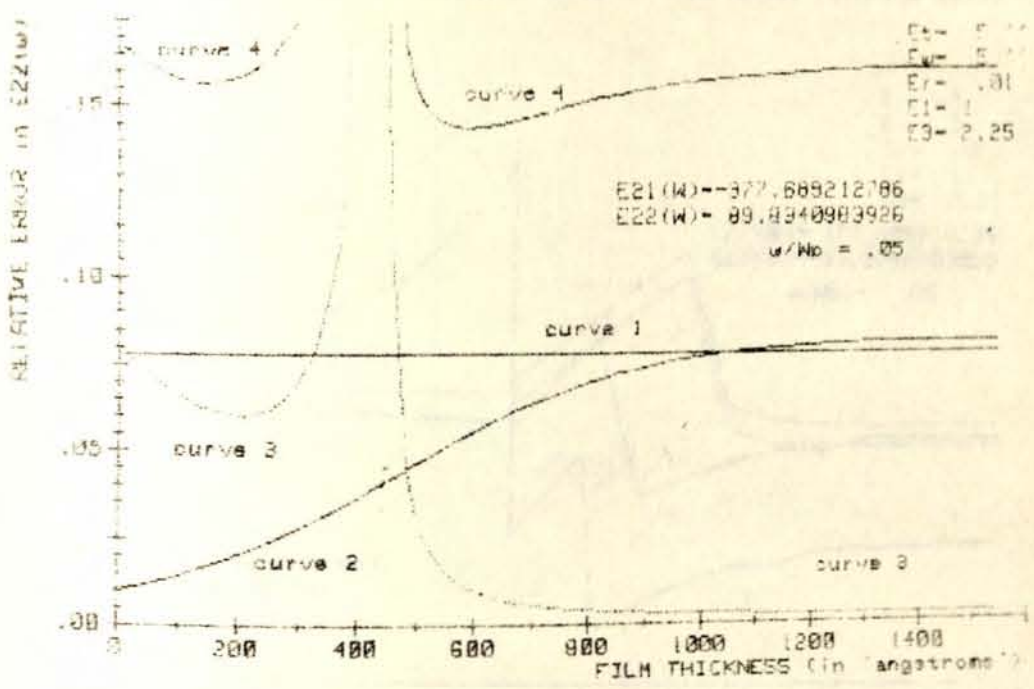


Fig. 3.30 Dependence of relative error in determination of  $E_{22}(w)$  versus thickness of metal film. Curve 1 gives a partial relative error due to finite accuracy in measuring the resonant angle, curve 2 - in halfwidth, curve 3 - in  $R_{min}$ , curve 4 - the total relative error.

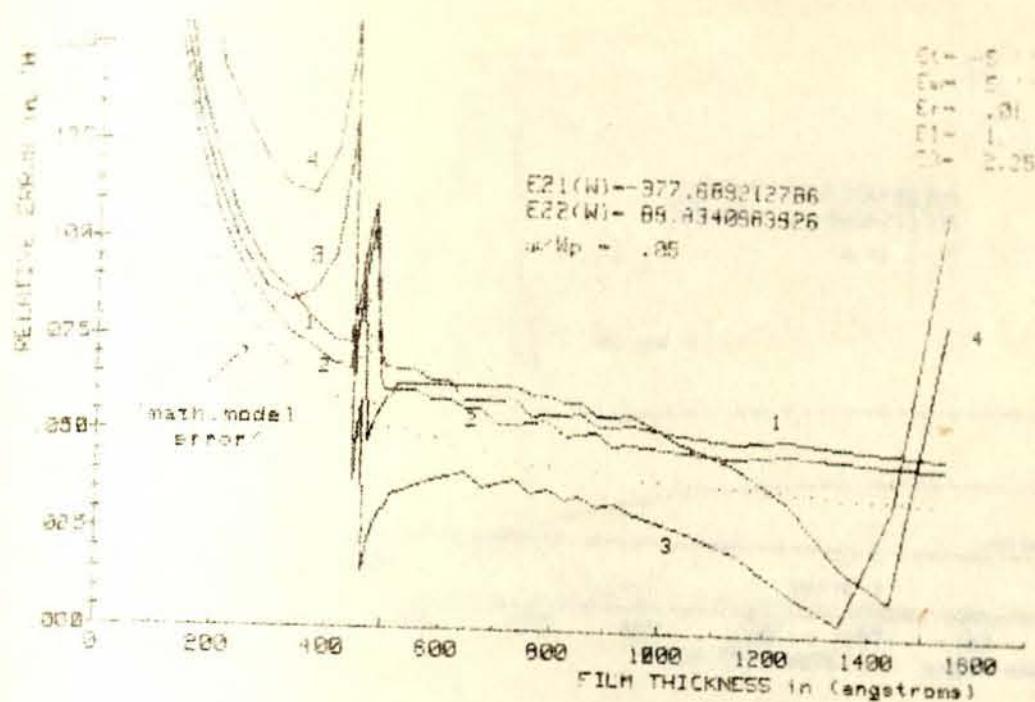


Fig. 3.40 Dependence of relative error in thickness on thickness of the metallic film. Curve 1 gives a partial relative error due to finite accuracy in measuring the resonant angle, curve 2 - in half-width, curve 3 - in  $R_{in}$ , curve 4 - the total relative error

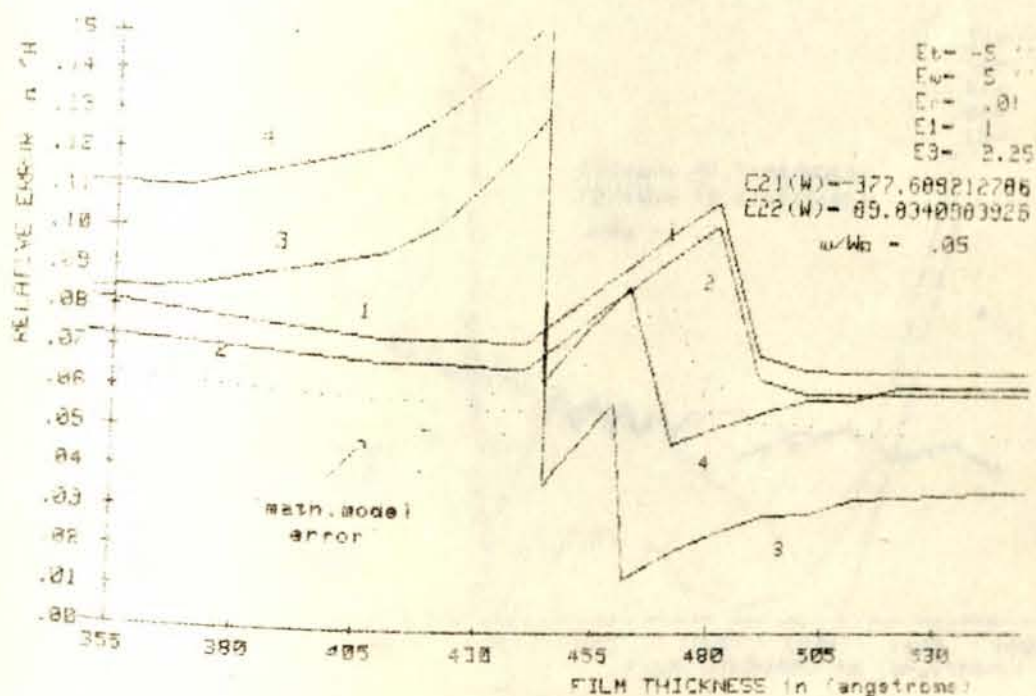


Fig. 3.40 (expanded scale) Dependence of relative error in thickness on the thickness of the metallic film.

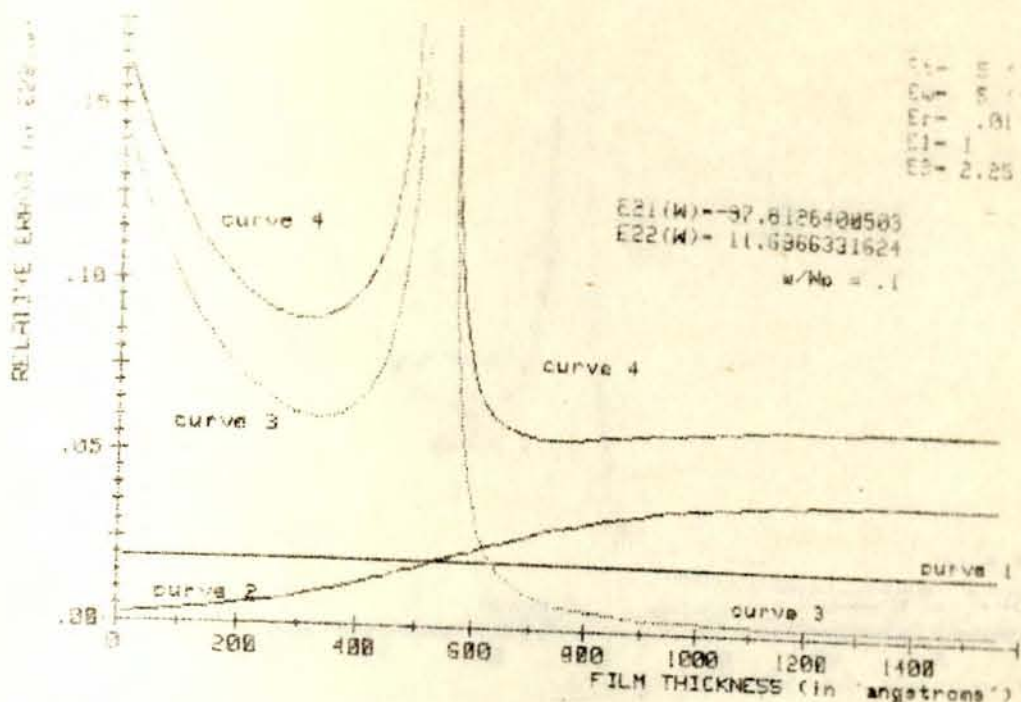


Fig. 3.3b) Dependence of relative error in determination of  $E_{22}(w)$  versus thickness of metal film. Curve 1 gives a partial relative error due to finite accuracy in measuring the resonant angle, curve 2 - in half-width, curve 3 - in  $R_{min}$ , curve 4 - the total relative error

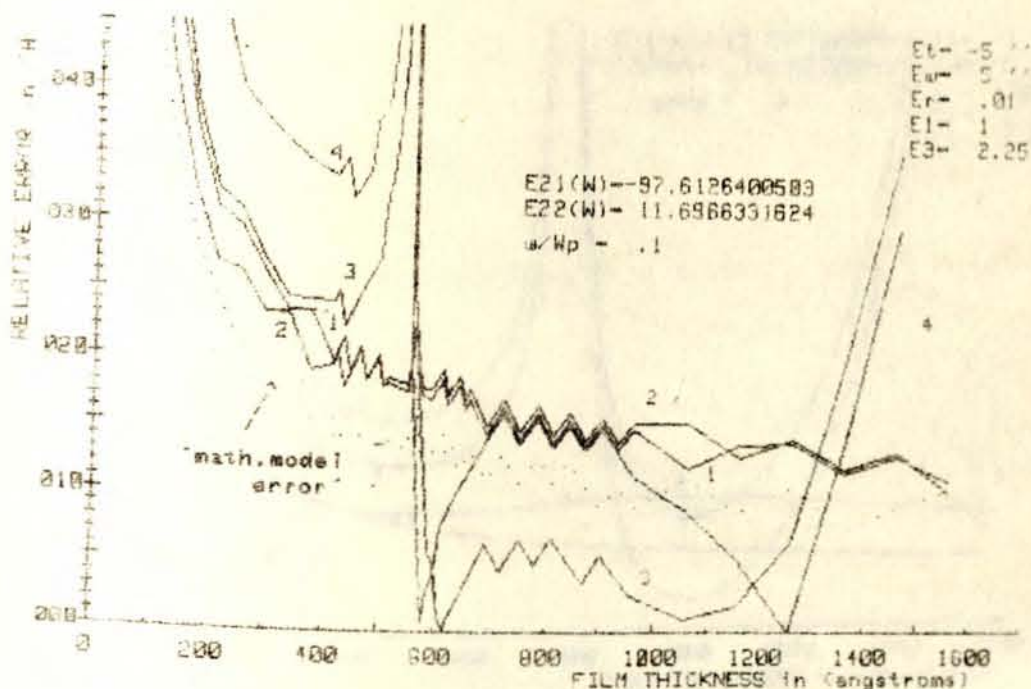


Fig. 3.4b) dependence of relative error in thickness on thickness of the metallic film. Curve 1 gives a partial relative error due to finite accuracy in measuring the resonant angle, curve 2 - in half-width, curve 3 - in  $R_{min}$ , curve 4 - the total relative error

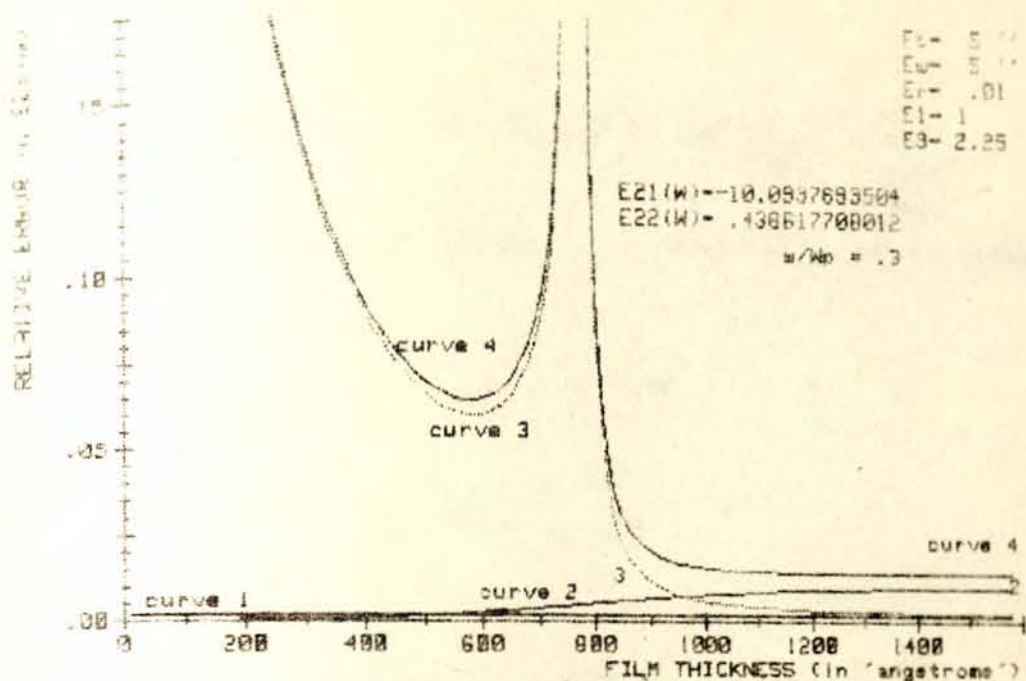


Fig. 3.3C Dependence of relative error in determination of  $E_{22}(w)$  versus thickness of metal film. Curve 1 gives a partial relative error due to finite accuracy in measuring the resonant angle, curve 2 - in half-width, curve 3 - in  $R_{min}$ , curve 4 - the total relative error

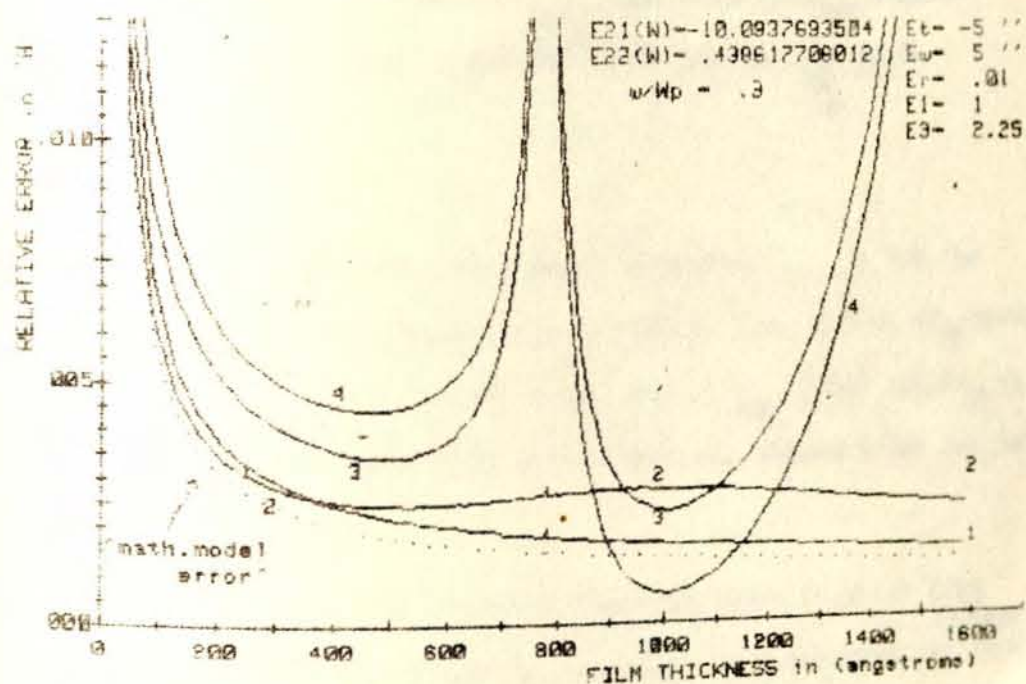


Fig. 3.3C Dependence of relative error in thickness on thickness of the metallic film. Curve 1 gives a partial relative error due to finite accuracy in measuring the resonant angle, curve 2 - in half-width, curve 3 - in  $R_{min}$ , curve 4 - the total relative error

also supported by eqn. (3.18) which shows that  $\left| \frac{\partial \epsilon_2''}{\partial R_{\min}} \right| \sim \frac{1}{\sqrt{R_{\min}}}$ .

The 'software error' for the used frequencies has the following values

$$\frac{\Delta \epsilon_2''}{\epsilon_2'' \text{ theor.}} \left( \frac{W}{W_p} = 0.05 \right) = 5.7\%$$

$$\frac{\Delta \epsilon_2''}{\epsilon_2'' \text{ theor.}} \left( \frac{W}{W_p} = 0.1 \right) = 1.5\%$$

$$\frac{\Delta \epsilon_2''}{\epsilon_2'' \text{ theor.}} \left( \frac{W}{W_p} = 0.3 \right) = 0.2\%$$

### Conclusion 3

It is meaning less to perform the measurement for metal films with thickness values close to  $h_{\text{opt}}$ . The value of  $h_{\text{opt}}$  depends mostly upon  $\frac{W}{W_p}$  and ranges from  $400\text{\AA}^{\circ}$ - $750\text{\AA}^{\circ}$  for  $0.05 < \frac{W}{W_p} < 0.3$ .

### Conclusion 4

For metal films with thicknesses other than  $h_{\text{opt}} \pm 100$  the relative error of determination of  $\epsilon_2''$  ranges from 17% at  $W/W_p = 0.05$  to ~2% at  $W/W_p = 0.3$  and  $h > 1000\text{\AA}^{\circ}$  only. For  $h < h_{\text{opt}} - 100\text{\AA}^{\circ}$  and  $W/W_p = 0.3$  the error has a minimum of ~7% at  $h \sim 600\text{\AA}^{\circ}$  and rapidly grows for less thicknesses.

At figs. (3.4a), (3.4b), and (3.4c) the relative error  $\left( \frac{\Delta h}{h} \right)_{\text{exp}}$  as a function of  $h$  with normalized frequency as a parameter is shown.

Since  $h_{\text{exp}}$  is determined using  $\epsilon_2'_{\text{exp}}$  and  $\epsilon_2''_{\text{exp}}$ , it is the most affected because the errors made at all preceding steps are accumulated

now. In particular  $(\Delta \epsilon_2'')_{\text{exp}} \rightarrow \infty$  as  $h \rightarrow h_{\text{opt}}$  cases.  $\Delta h \rightarrow \infty$  as  $h \rightarrow h_{\text{opt}}$

Besides this we have a 'software error' (showing by a dotted line) growing to infinity as  $h \rightarrow 0$ . It happens because the assumption

$|K_{x0}| \ll |K_{x1}|$  in the perturbation approach (see eqn. (2.13)) fails as  $h \rightarrow \infty$ . For thicknesses greater than  $1500 \text{ \AA}$ ,  $\frac{\Delta h}{h_{\text{exp}}}$  also grows due to

the growth of the partial error in measuring  $R_{\text{min}}$ . At these big thicknesses  $R_{\text{min}} \rightarrow 1$ , which requires an accurate distinction from the unity.

#### Conclusion 5

The measurement of the thickness of the metal film is reasonable to perform if  $100 \text{ \AA} < h < 600 \text{ \AA}$ ,  $850 \text{ \AA} < h < 1200 \text{ \AA}$  at  $W/W_p = 0.3$  with the relative error  $\sim 0.5$ ,

if  $250 \text{ \AA} < h < 500 \text{ \AA}$  with relative error  $\sim 2.5\%$ , and

$600 \text{ \AA} < h < 1250 \text{ \AA}$  with relative error  $\sim 0.8\%$  at  $W/W_p = 0.1$

$480 \text{ \AA} < h < 1400 \text{ \AA}$  with relative error  $\sim 3.5\%$  at  $W/W_p = 0.05$ .

Summary

1. It is shown that radiative SPLP can exist at normalized frequencies higher than  $\frac{W}{W_p}$  for strong absorbing media. Practically useful range of  $\frac{W}{W_p}$  might be  $100 < \frac{W}{W_p} < 5$ .
2. The energy transportation performed by SPLP consists of two flows: one in the dielectric medium, the other in metal. It is shown that for  $0 < w < \frac{W_p}{\sqrt{\epsilon_1 + 1}}$  the two flows have opposite directions with the net flow in the direction of the flow in the dielectric medium. For  $w > \frac{W_p}{\sqrt{\epsilon_1 + 1}}$ , both flows have the same direction.
3. A dispersion equation for SPLP in thin metal films was derived. An approximate solution of this equation was suggested and tested.
4. The method of determination of complex  $\epsilon(w)$  and  $h$  of metal or semiconductor film without a preset expression for  $\epsilon(w)$  was modified.
5. A frequency range  $0.1 < \frac{W}{W_p} < \frac{W^{**}}{W_p}$  in which the method is practically applicable is established.
6. It is found that the method diverges for  $\epsilon_2''$  and  $h$  determination in the vicinity of  $h_{opt}$ . For determination of  $h$  the method also diverges as  $h \rightarrow 0$ .
7. It is found that within the specified frequency range  $0.1 < \frac{W}{W_p} < \frac{W^{**}}{W_p}$  the accuracy of determination  $\epsilon_2'$  is not less than 2%. The accuracy of determination  $\epsilon_2''$  and  $h$  depends upon the thickness of the film and can range from 0.5% to 2.5%. Thickness less than  $100A^0$ , greater than  $1400A^0$ , and  $h_{opt} \pm 100A^0$  should be excluded reliable measurements.

8. Computer program capable of;

- analysing dispersion properties of SP1P (semi-infinite case)
- analysing power flows in SP1P (semi-infinite case)
- simulating ATR model
- finding an approximate solution of the dispersion equation of SP1P in a thin film
- determining the values of  $\epsilon_2'$ ,  $\epsilon_2''$ , and  $h$  from experimentally measured  $\theta_{ATR}$ ,  $W_\theta$  and  $R_{min}$
- assessing the accuracy of the method

was designed.

References

- [1] G.C. Aers and A.D. Boardman physics programs ed. by A.D. Boardman John Wiley and sons, 1980.
- [2] Principles of optics M. Born, E. Wolf Pergamon Press, 1959.
- [3] W.F. Chen, J.M. Chen "Use of surface plasma waves for determination of the thickness and optical constants of thin metallic film", J. Opt. Soc. Am/vol. 71, No.2 (189-191) February 1981.
- [4] I. Pockrand "surface plasma oscillations at silver surfaces with thin transparent and absorbing coatings", Surf. Sci. 72, 577-588 (1978).
- [5] C. Kunz, Z. Phys. V. 196, 311 (1966).
- [6] G.R. Fowles, Introduction to modern optics.
- [7] I Newton Optiks II, Book 8, 97 (1817).
- [8] J. Fahrenfort, Spectrochim Acta, V.17, 698 (1961).
- [9] N.J. Harrick, Phy.Rev., V.125, 1165, (1962),
- [10] A Otto Z.Phys. V.216, 398 (1968).
- [11] E. Kretschmann. Z.Phys. V.241, 313 (1971)
- [12] F. Abels, ed. Optical properties and electronic structure of metals and alloys, (North Holland, Amsterdam, 1965).
- [13] T. Lopez - Rios, G. Vuye "Use of surface plasmon excitation for determination of the thickness and optical constants of very thin surface layers," Surf. Sci. 81, 529-538 (1978).

Appendix A. Calculation of terms in the Taylor's series expansion of the dispersion eqn. (2.10)

From eqn. (2.14) it is clear that

$$f(K_{x0}) = \frac{1}{r_{21}^0} \cdot \frac{1}{r_{23}^0} e^{-2iK_{2y}^0 h} \quad (A.1)$$

where

$$\frac{1}{r_{21}^0} = \frac{\epsilon_1 K_{2y}^0 + \epsilon_2 K_{1y}^0}{\epsilon_1 K_{1y}^0 - \epsilon_2 K_{2y}^0} = \frac{i\epsilon_1 K_0 (-\epsilon_2)}{\sqrt{-(\epsilon_1 + \epsilon_2)}} + \frac{i\epsilon_2 K_0 \epsilon_1}{\sqrt{-(\epsilon_1 + \epsilon_2)}} = 0 \quad (A.2)$$

$$\frac{i\epsilon_1 K_0 (-\epsilon_2)}{\sqrt{-(\epsilon_1 + \epsilon_2)}} - iK_0 \epsilon_2 \frac{\epsilon_1}{\sqrt{-(\epsilon_1 + \epsilon_2)}}$$

$$\frac{1}{r_{23}^0} = \frac{\epsilon_3 K_{2y}^0 + \epsilon_2 K_{3y}^0}{\epsilon_3 K_{2y}^0 - \epsilon_2 K_{3y}^0} = \frac{\epsilon_3 + \sqrt{\epsilon_1 \epsilon_3 + \epsilon_2' (\epsilon_3 - \epsilon_1)}}{\epsilon_3 - \sqrt{\epsilon_1 \epsilon_3 + \epsilon_2' (\epsilon_3 - \epsilon_1)}} \quad (A.3)$$

$$K_{1y}^0 = iK_0 \frac{\epsilon_1}{\sqrt{-(\epsilon_1 + \epsilon_2)}} \quad \text{-----} \quad (A.4)$$

$$K_{2y}^0 = iK_0 \frac{-\epsilon_2}{\sqrt{-(\epsilon_1 + \epsilon_2)}} \quad \text{-----} \quad (A.5)$$

$$K_{3y}^0 = \sqrt{K_0^2 \epsilon_3 - K_{x0}^2} = K_0 \frac{\sqrt{-(\epsilon_1 \epsilon_3 + \epsilon_2' (\epsilon_3 - \epsilon_1))}}{\sqrt{-(\epsilon_1 + \epsilon_2')}} \quad \text{-----} \quad (A.6)$$

Note that  $K_{3y}^0$  is real for  $0 < W < W^*$  and is imaginary for  $W^* < W < \frac{W}{P}$

Eqn. (A.2) shows that  $f(K_{x0}) = 0$ .

From eqn. (2.14) we have

$$\begin{aligned} \left. \frac{\partial f}{\partial K_x} \right|_{K_{x0}} &= \left. \frac{\partial}{\partial K_x} \left( \frac{1}{r_{21}} \cdot \frac{1}{r_{23}} e^{-2iK_{2y}h} \right) \right|_{K_{x0}} \\ &= \left. \frac{\partial}{\partial K_x} \left( \frac{1}{r_{21}} \right) \right|_{K_{x0}} \cdot \frac{1}{r_{23}} e^{-2iK_{2y}^0 h} + \frac{1}{r_{21}^0} \left. \frac{\partial}{\partial K_x} \left( \frac{1}{r_{23}} \right) \right|_{K_{x0}} \cdot e^{-2iK_{2y}^0 h} \\ &\quad + \frac{1}{r_{21}^0} \cdot \frac{1}{r_{23}^0} \left. \frac{\partial}{\partial K_x} \left( e^{-2iK_{2y}h} \right) \right|_{K_{x0}} \quad \text{-----} \quad \text{(A.7)} \end{aligned}$$

but from (A.2),  $\frac{1}{r_{21}^0} = 0$  which results the second and the third terms of

the right expression in (A.7) to be zero.

$$\left. \frac{\partial f}{\partial K_x} \right|_{K_{x0}} = \left. \frac{\partial}{\partial K_x} \left( \frac{1}{r_{21}} \right) \right|_{K_{x0}} \frac{1}{r_{23}^0} e^{-2iK_{2y}^0 h} \quad \text{-----} \quad \text{(A.8)}$$

where

$$\left. \frac{\partial}{\partial K_x} \left( \frac{1}{r_{21}} \right) \right|_{K_{x0}} = \left. \frac{\partial}{\partial K_x} \left( \frac{U}{V} \right) \right|_{K_{x0}} = \frac{\frac{\partial U}{\partial K_x} V - U \frac{\partial V}{\partial K_x}}{V^2} \quad \text{-----} \quad \text{(A.9)}$$

$$\text{with } U = -\epsilon_1 \sqrt{K_0^2 \epsilon_2 - K_x^2} + \epsilon_2 \sqrt{K_0^2 \epsilon_1 - K_x^2}$$

$$V = -\epsilon_1 \sqrt{K_0^2 \epsilon_2 - K_x^2} - \epsilon_2 \sqrt{K_0^2 \epsilon_1 - K_x^2}$$

$$\begin{aligned} \left. \frac{\partial U}{\partial K_x} \right|_{K_{x0}} &= K_{x0} \left[ \frac{-\epsilon_1}{\sqrt{K_0^2 \epsilon_2 - K_0^2} \frac{\epsilon_1 \epsilon_2}{\epsilon_1 + \epsilon_2}} - \frac{\epsilon_2}{\sqrt{K_0^2 \epsilon_1 - K_0^2} \frac{\epsilon_1 \epsilon_2}{\epsilon_1 + \epsilon_2}} \right] \\ &= \frac{K_{x0}}{K_0} (\epsilon_1^2 - \epsilon_2^2) \sqrt{\frac{\epsilon_1 + \epsilon_2}{\epsilon_1 \cdot \epsilon_2}} \end{aligned}$$

$$V \Big|_{K_{x0}} = -K_0 \frac{\epsilon_1 \epsilon_2}{\sqrt{\epsilon_1 + \epsilon_2}} - K_0 \frac{\epsilon_1 \epsilon_2}{\sqrt{\epsilon_1 + \epsilon_2}} = -2K_0 \frac{\epsilon_1 \epsilon_2}{\sqrt{\epsilon_1 + \epsilon_2}}$$

The term  $\frac{\partial V}{\partial K_x} \Big|_{K_{x0}}$  vanishes

thus

$$\frac{U}{\partial K_x} \Big|_{K_{x0}} \cdot \frac{1}{V} \Big|_{K_{x0}} = \frac{(\epsilon_1^{2-\epsilon_2} \epsilon_1^{+\epsilon_2})}{2K_0 \epsilon_1 \cdot \epsilon_2 \epsilon_1 \cdot \epsilon_2}$$

$$\left( \frac{\partial V}{\partial K_x} \cdot \frac{1}{V} \right) \Big|_{K_{x0}} = \frac{\epsilon_2^{-\epsilon_1}}{2K_0} \left( \frac{\epsilon_1 + \epsilon_2}{\epsilon_1 \cdot \epsilon_2} \right)^{3/2} \text{-----} \quad (\text{A.10})$$

equation (A.8), (A.10), (2.10) and (2.4) imply that

$$\frac{\partial f}{\partial K_x} \Big|_{K_{x0}} = \frac{(\epsilon_2^{-\epsilon_1})}{2K_0} \left( \frac{\epsilon_1 + \epsilon_2}{\epsilon_1 \cdot \epsilon_2} \right)^{3/2} \frac{1}{r_{23}^0} e^{-2iK_{2y}^0 h} \text{----} \quad (\text{A.11})$$

which results in

$$K_{x1} = \frac{2K_0}{(\epsilon_2^{-\epsilon_1})} \left( \frac{\epsilon_1 \cdot \epsilon_2}{\epsilon_1 + \epsilon_2} \right)^{3/2} r_{23}^0 e^{-2iK_{2y}^0 h} \text{-----} \quad (\text{A.12})$$

APPENDIX -8-

```

1  PROGRAM which determines the accuracy of the SPIP method
2  | This particular version is designed for normalized frequency w/Wp=.05
3  DIM Det22(300),DewZZ(300),Der22(300),De22(300),Hh(300),Di(300),Dr(300)
4  DIM Root(2),F_(2),Err(2),Dh(300),Dho(300),Dh1(300),Dh2(300),Dht(300)
5  DIM Ho(300),Hi(300),H2(300),Ht(300)
6  INTEGER Screen(1:1024,1:36,1:3),Screen1(1:1024,1:32,1:3)
7  COM E3,E21,E22,E1
8  COM /Exp/ E21e,E22e
9  COM /H/ Teta,Wt,Rm
10 COM /Err/ Tetae,Wte,Rme
11 COM /H_opt/ Hopimt          ! Common Optimal thickness in 'meters'
12 COM /Wp/ Wp
13 COM /Tau/ Tau
14 COM /W/ W
15 COM /K/ Kx1iexp
16 C=2.998E+8          ! Speed of light in m/s
17 Pi=3.14159265358979
18 |
19 Et=5/3600*Pi/180          ! Exp. error in measuring Teta (in rad)
20 Ew=Et          ! Exp. error in measuring half-width Wt (in rad)
21 Er=.01          ! exp. error in measuring Minimum Reflectivity
22 |
23 E1=1
24 E3=2.25          ! Dielectric permittivity of the GLASS PRISM
25 Wp=8.38197252587E+15          ! Plasma Frequency for SODIUM
26 Tau=1.00583208114E-14          ! Relaxation Time for SODIUM
27 GO TO 3160 | 1800 | 13160 | 2850 | 1800
28 | LOADSUB E22accuracy FROM "E22acci"
29 | LOADSUB Filndisp FROM "F1"
30 | LOADSUB E21accuracy FROM "E21acci"
31 | LOADSUB E22accu FROM "E22acc2"
32 | LOADSUB Ref1 FROM "RPMA3"
33 | LOADSUB Fr12 FROM "RPMA3"
34 | LOADSUB Fr23 FROM "RPMA3"
35 | LOADSUB Fex FROM "RPMA3"
36 | LOADSUB Opt_h FROM "Opt_h"
37 | LOADSUB Bisect FROM "Bisect"
38 | LOADSUB FNMax FROM "Max"
39 |
40 M=1          ! Counts the number of attempt
41 | INPUT "Normalized frequency Wn =",Wn
42 Wn=.3
43 INPUT "No,N1,N2",No,N1,N2
44 PRINT No,N1,N2,"Attempt number = ",M
45 W=Wn*Wp
46 E21=1-Wp^2/(W^2+1/Tau^2)          ! E21 is needed for Filndisp
47 E22=1/(W*Tau)*Wp^2/(W^2+1/Tau^2)
48 |
49 J=1          ! Counts the array index

```

```

490 H_step=40
500 H=-30
510 H_exp=5
520 H=H+H_step
530 Hmt=H*t.E-10
540 CALL Filndisp(W,Wp,Tau,Hmt,E1,E3,Kxr,Kxi,Kxor,Kxoi,Kxir,Kxii)
550 ! For the given Hmt,E1,E2,W,Wp,Tau
560 ! Kxor - REAL part for semiinfinite case
570 ! Kxoi - IMAG. part for semiinfinite case
580 ! Kxir - first order correction to Kxor for a metal film of finite thick-
590 ! Kxii - first order correction to Kxoi for a film of given 'H'
600 ! Kxr - REAL part of OX - wavevector for a metal film of thickness 'H'
610 ! Kxi - IMAG. part of OX - wavevector for a metal film of thickness 'H'
620 ! NOTE ! ALL WAVEVECTORS ARE IN NORMALIZED FORM !!!
630 Eta=Kxoi/Kxii
640 Rm=1-4*Eta/(1+Eta)^2
650 Kxi=Kxi*Wp/C
660 Teta=ASN(Kxor/Wn/SQR(E3))
670 Wt=2*Kxi*COS(Teta)*C/W/SQR(E3)
680 ! In the preceding part of the program the expected experimental values
690 ! of Teta,Wt,Rm were calculated. The following part of the program
700 ! is based exclusively on these experimentally determined values
710 ! NOTE, THAT THESE ARE EXACT EXPERIMENTAL VALUES
720 ! *****
730 ! *****
740 !
750 IF N0=0 THEN Tetae=Teta
760 IF N1=0 THEN Wte=Wt
770 IF N2=0 THEN Rme=Rm
780 IF N0=+1 THEN Tetae=Teta+Et
790 IF N1=+1 THEN Wte=Wt+Ew
800 IF N2=+1 THEN Rme=Rm+Er
810 IF N0=-1 THEN Tetae=Teta-Et
820 IF N1=-1 THEN Wte=Wt-Ew
830 IF N2=-1 THEN Rme=Rm-Er
840 !
850 IF Rme<0 THEN Rme=1.E-8
860 S2=SIN(Tetae)*SIN(Tetae)
870 E21e=E1*E3*S2/(E1-E3*S2)
880 K=-1
890 E22e=Wte*(1+K*SQR(Rme))*E1^2*E3*TAN(Tetae)/(2*(E1-E3*S2)^2)
900 E22o=Wte*E1^2*E3*TAN(Tetae)/(2*(E1-E3*S2)^2)
910 D1(J)=E22o-E22e
920 !
930 Dr(J)=D1(J)-D1(J-1)
940 IF Dr(J)>0 AND J>1 THEN K=+1
950 IF Dr(J)<0 THEN K=-1
960 IF J=1 THEN K=-1
970 Prod=Dr(J)*Dr(J-1)
980 !
990 IF Prod<0 AND J>2 THEN Hopt1=H
1000 !
1010 !
1020 IF K=-1 THEN Hoptmt=1.E-6
1030 IF K=+1 THEN Hoptmt=Hopt1*1.E-10
1040 !
1050 E22e=Wte*(1+K*SQR(Rme))*E1^2*E3*TAN(Tetae)/(2*(E1-E3*S2)^2)
1060 !
1070 PRINT "E21-E21e =",E21-E21e,"E22-E22e =",E22-E22e,"Prod =",Prod

```



```

1630 MOVE 4,0
1640 LABEL "in half-width, curve 3 - in R min, curve 4 - the total relative err
1650 MOVE 112,88
1660 LABEL "E1=";E1
1670 MOVE 112,85
1680 LABEL "E3=";E3
1690 I
1700 MOVE 112,87
1710 PEN 2
1720 LABEL "Et=" ;Et*3600*180/Pi;"'"
1730 MOVE 112,94
1740 PEN 3
1750 LABEL "Ew=" ;Ew*3600*180/Pi;"'"
1760 MOVE 112,91
1770 PEN 4
1780 LABEL "Er=" ;Er
1790 MOVE 115,37
1800 PEN 7
1810 LABEL "curve 4"
1811 MOVE 46,60
1812 LABEL "curve 4"
1820 MOVE 16,30
1830 PEN 2
1840 LABEL "curve 1"
1850 PEN 3
1860 MOVE 56,31
1870 LABEL "curve 2"
1871 MOVE 126,32
1872 LABEL "2"
1880 MOVE 50,50
1890 PEN 4
1900 LABEL "curve 3"
1901 MOVE 73,33
1902 LABEL "3"
1910 PEN 5
1920 VIEWPORT 10,128,25,100
1930 WINDOW -50,1600,-.01,.175
1940 AXES 100,.005,0,0,2,5,2
1950 PEN -1
1960 VIEWPORT 9,12,28,32
1970 AXES 10,1,0,0,1,1,5
1980 VIEWPORT 12,15,24,28
1990 AXES 1000,.005,0,0,1,1,5
2000 VIEWPORT 10,128,25,100
2010 PEN 5
2020 CLIP OFF
2030 LOG 8
2040 FOR I=0 TO 1450 STEP 200
2050 MOVE I,-.003
2060 LABEL USING "#,K";I
2070 NEXT I
2080 LOG 8
2090 FOR I=0 TO .5 STEP .05
2100 MOVE -25,I
2110 LABEL USING "#,.DD";I
2120 NEXT I
2130 MOVE 1400,.125
2140 LABEL "E21(0)=";E21
2150 MOVE

```

! Horizontal deleting  
! Vertical deleting



```

2750 MOVE 112,97
2760 LABEL "E1=" ;(Tetae-feta)*3600*180/Pi;""
2770 PEN 3
2780 MOVE 112,94
2790 LABEL "Ew=" ;(Wte-Wt)*3600*180/Pi;""
2800 PEN 4
2810 MOVE 112,91
2820 LABEL "Er=" ;Rme-Rm
2830 PEN 5
2840 MOVE 70,97
2850 LABEL "E21(W)=" ;E21
2860 MOVE 70,94
2870 LABEL "E22(W)=" ;E22
2880 MOVE 75,90
2890 LABEL "w/Wp =" ;Wm
2900 MOVE 38,55
2910 PEN 7
2920 LABEL "4"
2930 MOVE 104,64
2940 LABEL "4"
2950 MOVE 40,46
2960 PEN 4
2970 LABEL "3"
2980 MOVE 78,40
2990 LABEL "3"
3000 MOVE 30,42
3010 PEN 3
3020 LABEL "2"
3030 MOVE 78,45
3040 LABEL "2"
3041 MOVE 120,45
3042 LABEL "2"
3050 MOVE 27,46
3060 PEN 2
3070 LABEL "1"
3080 MOVE 120,37
3090 LABEL "1"
3100 PEN 1
3110 MOVE 11,37
3120 LABEL "math.model"
3130 MOVE 20,34
3140 LABEL "error"
3150 MOVE 20,40
3160 DEG
3170 LDIR 60
3180 LABEL "---->"
3190 LDIR 0
3200 PEN 5
3210 VIEWPORT 10,128,29,100
3220 WINDOW -10,1700,-.0001,.0125
3230 AXES 100,.0005,0,0,5,5,2
3240 CLIP OFF
3250 LORG 6
3260 FOR I=0 TO 1600 STEP 200
3270 MOVE I,-.00025
3280 LABEL USING "#,K,";I
3290 NEXT I
3300 LORG 8
3310 FOR I=0 TO .05 STEP .005

```



```

3900 MOVE 112,85
3910 LABEL "E3=" ;E3
3920 PEN 2
3930 MOVE 112,87
3940 LABEL "E3=" ;(Tetae-Teta)*3500*180/P1;""
3950 PEN 3
3960 MOVE 112,84
3970 LABEL "E4=" ;(Wta-Wt)*3500*180/P1;""
3980 PEN 4
3990 MOVE 112,81
4000 LABEL "E4=" ;Rna-Rm
4010 PEN 5
4020 MOVE 90,81
4030 LABEL "E21(W)=" ;E21
4040 MOVE 90,78
4050 LABEL "E22(W)=" ;E22
4060 MOVE 100,74
4070 LABEL "w/Wp =" ;Wn
4080 PEN 7
4090 MOVE 30,85
4100 LABEL "4"
4110 MOVE 85,48
4120 LABEL "4"
4130 PEN 4
4140 MOVE 32,73
4150 LABEL "3"
4160 MOVE 95,38
4170 LABEL "3"
4180 PEN 3
4190 MOVE 25,60
4200 LABEL "2"
4210 MOVE 85,69
4220 LABEL "2"
4230 PEN 2
4240 MOVE 42,66
4250 LABEL "1"
4260 MOVE 80,75
4270 LABEL "1"
4280 PEN 1
4290 MOVE 30,42
4300 LABEL "math.model"
4310 MOVE 35,35
4320 LABEL "error"
4330 MOVE 40,46
4340 DEG
4350 LDIR 45
4360 LABEL "---->"
4370 LDIR 0
4380 PEN 5
4390 VIEWPORT 10,128,28,100
4400 WINDOW 350,550,-.001,.152
4410 AXES 25,.01,355,0.5,5,2
4420 CLIP OFF
4430 LORG 6
4440 FOR X=355 TO 550 STEP 25
4450 MOVE X,-.002
4460 LABEL USING "#,K," ;X
4470 NEXT X
4480

```

```

4490 LORG R
4500 FOR Y=0 TO .15 STEP .01
4510 MOVE 350,Y
4520 LABEL USING "#,DD",Y
4530 NEXT Y
4540 CLR ON
4550
4560 PEN 2
4570 FOR J=2 TO 80
4580
4590 IF H0(J)>0 THEN PLOT H0(J),ABS(Dh0(J)) ! Partial error in teta
4600 NEXT J
4610 PENUP
4620 PEN 3
4630 FOR J=2 TO 80
4640 IF H1(J)>0 THEN PLOT H1(J),ABS(Dh1(J)) ! Partial error in Wt
4650 NEXT J
4660 PENUP
4670 PEN 4
4680 FOR J=2 TO 80
4690 IF ABS(Dh2(J))>1 THEN 4710 ! Partial error in R min
4700 IF H2(J)>0 THEN PLOT H2(J),ABS(Dh2(J))
4710 NEXT J
4720 PENUP
4730 PEN 7
4740 FOR J=2 TO 80
4750 IF ABS(Dh3(J))>1 THEN 4770
4760 IF H3(J)>0 THEN PLOT H3(J),ABS(Dh3(J))
4770 NEXT J
4780 PENUP
4790 PEN 1
4800 LINE TYPE 3
4810 FOR J=2 TO 80
4820 IF ABS(Dh(J))>1 THEN 4840
4830 IF Hh(J)>0 THEN PLOT Hh(J),ABS(Dh(J)) ! Indicates only the computational
4840 NEXT J ! error of the computer program
4850 PENUP
4860 END
4870
4880 SUB E22accuracy(Teta,Wt,Rm,Et,Ew,Er,E1,E21,E22,E3,H,Det22,Dew22,Der22,De22)
4890 ! This subprogram should be used for 'H' greater than 'Hopt'
4900 ! Et - experimental accuracy of "Teta" determination
4910 ! Ew - of "Wt" determination
4920 ! Er - of "Ref" determination
4930 Ssq=SIN(Teta)*SIN(Teta)
4940 Rsq=SQR(Rm)
4950 Br=E1-E3*Ssq
4960 A=1+Rm+2*Rsq
4970 B=1+Rsq
4980 Dent=(Br+4*E3*Ssq)/Br/TAN(Teta)/(COS(Teta)^2) ! Normalized Dent
4990 Derw=1/Wt ! Normalized Derw
5000 Derr=(B^2-.5*A)/Rsq/A/B ! Normalized Derr
5010 Det22=ABS(Dent)*Et
5020 Dew22=ABS(Derw)*Ew
5030 Der22=ABS(Derr)*Er
5040 De22=Det22+Dew22+Der22
5050 SUBEND
5060

```

```

3080 X1=ABS(X)
3090 Y1=ABS(Y)
3100 IF X1<=0 THEN 5130
3110 Cabs=Y1
3120 SUBEXIT
3130 IF X1<0 THEN 5160
3140 Cabs=X1
3150 SUBEXIT
3160 IF X1>Y1 THEN Cabs=X1+SQR(1+(Y1/X1)^2)
3170 IF X1<Y1 THEN Cabs=Y1+SQR(1+(X1/Y1)^2)
3180 SUBEND I

```

```

5190 SUB Csqrt(A,B,R,I)
5200 IF (A<0) OR (B<0) THEN 5240
5210 R=0
5220 I=0
5230 SUBEXIT
5240 CALL Cabs(A,B,Cabs)
5250 R=SQR(ABS(A)+Cabs)*.5)
5260 IF A<0 THEN 5280
5270 I=B/(R+R)
5280 SUBEXIT
5280 IF B<0 THEN I=-R
5300 IF B/=0 THEN I=R
5310 R=B/(I+I)
5320 SUBEND I

```

```

5330 SUB Cdivid(A1,B1,A2,B2,R,I)
5340 C=A2+A2+B2+B2
5350 IF C<0 THEN 5390
5360 PRINT FNLine(2);"ERROR IN SUBPROGRAM Cdivid."
5370 PRINT "DIVISOR IS ZERO.",FNLine(2)
5380 PAUSE
5390 R=(A2+A1+B2+B1)/C
5400 I=(A2+B1-B2+A1)/C
5410 SUBEND I

```

```

5420 SUB Cexp(A,B,R,I)
5430 RAD
5440 R=EXP(A)*COS(B)
5450 I=EXP(A)*SIN(B)
5460 SUBEND I

```

```

5470 SUB Cmult(A1,B1,A2,B2,R,I)
5480 R=A1*A2-B2+B1
5490 I=A1*B2+B1*A2
5500 SUBEND I

```

```

5510 I
5520 SUB Filmdisp(W,Wp,Tau,H,E1,E3,Kxr,Kxi,Kxor,Kxoi,Kxin,Kxii)
5530 I This subprogram calculates the OX - wavevector of a plasmon propagating
5540 I The other interface of the metal film is with dielectric medium III,
5550 I E1 - relative dielectric permittivity of the medium I (air)
5560 I W - is the frequency of the source of light in Hz
5570 I H - is the thickness of the metal film in 'meters'
5580 I Wp - is the plasma frequency in Hz
5590 I Tau - is the relaxation time in seconds
5600 I Kxr - REAL part of OX - wavevector of plasmon in metal film
5610 I Kxi - IMAG. part of OX - wavevector of plasmon in metal film
5620 I C - speed of light in vacuum in m/s

```

5630 K0=WT  
 5640 E21=1-WP\*\*2/(W\*\*2+1/TAU\*\*2) ; wavevector of light in vacuum in 1/μ  
 5650 E22=WP\*\*2/(W\*\*2+1/TAU\*\*2)/W/TAU ; REAL E2(w) of the metal film  
 5660 Gnm=(E1+E21)\*\*2+E22\*\*2 ; IMAG E2(w) of the metal film

5670 A0=(E1+E21\*(E1+E21)+E1+E22\*\*2)/Dnm  
 5680 B0=E22\*E1\*\*2/Dnm  
 5690 A4=E1+E3+E21\*(E3-E1)  
 5700 B4=E22\*(E3-E1)  
 5710 A7=2\*E1\*E21  
 5720 B7=2\*E1\*E22  
 5730 A8=E1\*\*2-E22\*\*2-E1\*\*2  
 5740 B8=2\*E21\*E22

5750 LOADSUB Cabs FROM "Complex"  
 5760 LOADSUB Csqrt FROM "Complex"  
 5770 CALL Csqrt(E1+E21,E22,A1,B1)  
 5780 CALL Csqrt(A0,B0,K1,K2)  
 5790 U=C/WP ; Normalizing factor

5800 KX0R=K0\*K1\*U  
 5810 KX0I=K0\*K2\*U  
 5820 LOADSUB Cdivid FROM "Complex"  
 5830 CALL Cdivid(-2\*K0\*H\*E22,+2\*K0\*H\*E21,A1,B1,A2,B2) ; Sign changed  
 5840 LOADSUB Cexp FROM "Complex"

5850 CALL Cexp(A2,B2,A3,B3)  
 5860 CALL Csqrt(A4,B4,A5,B5)  
 5870 CALL Cdivid(E3-A5,-B5,E3+A5,+B5,A6,B6) ; A6,B6 - Real & Imag. parts of  
 5880 ; ; i/r32  
 5890 CALL Cdivid(A7,B7,A8,B8,A9,B9)  
 5900 LOADSUB Cmult FROM "Complex"

5910 CALL Cmult(A3,B3,+A6,+B6,A10,B10)  
 5920 CALL Cmult(A10,B10,A9,B9,A11,B11)  
 5930 CALL Cmult(KX0R,KX0I,1+A11,B11,KXR,KXI)  
 5940 ;  
 5950 KX1I=KXI-KX0I  
 5960 SUBEND

5970 ;  
 5980 SUB E21accuracy(Teta,Et,E1,E21,E22,E3,H,Det21,De21)  
 5990 ;  
 6000 ;  
 6010 ; Et=experimental accuracy of "Teta" determination  
 6020 Ssq=SIN(Teta)\*SIN(Teta)  
 6030 Br=E1-E3\*Ssq  
 6040 Dert=2\*E1/Br/TAN(Teta)  
 6050 Det21=ABS(Dert)\*Et  
 6060 De21=Det21  
 6070 SUBEND  
 6080 ;

6090 SUB E22accu(Teta,Wt,Rm,Et,Ew,Er,E1,E21,E22,E3,H,Det22,Der22,De22)  
 6100 ; This subprogram should be used for thicknesses "H" less than the  
 6110 ; optimal thickness  
 6120 ; Et - experimental accuracy of "Teta" determination  
 6130 ; Ew - of "Wt" determination  
 6140 ; Er - of "Ref" determination

6150 Ssq=SIN(Teta)\*SIN(Teta)  
 6160 Rsq=SQR(Rm)  
 6170 Br=E1-E3\*Ssq  
 6180 A=1+Rm-2\*Rsq  
 6190 B=1-Rsq  
 6200 Dert=(Br+4\*E3\*Ssq)/Br/TAN(Teta)/(COS(Teta)\*\*2) ; normalized Dert  
 6210 Derw=1/Wt ; normalized Derw  
 6220 ; ; normalized Derr

```

6230 DeL2=nb5*(Der1)*Et
6240 DeL2=nb5*(Derw)*Ew
6250 Der22=ARB*(Derr)*Er
6260 DeL2=De 22+Dew22+Der22
6270 SUBEND
6280 |
6290 SUB Refl(Teta,W,Rr,Imr,Ref,R12,R23,D,E1,E3,E21e,E22e)
6300 | Rr - is real part of the reflection coefficient of a single film
6310 | Imr - is the imaginary part of the reflection coefficient
6320 | Ref - is the reflectivity of a single film
6330 | Note, E1 - stands for the prism
6340 |       E3 - stands for the air
6350 E21=E21e
6360 E22=E22e
6370 P1=3.14159285358979
6380 CALL Fr12(Teta,W,Rr12,Imr12,E1,E3,E21e,E22e)
6390 CALL Fr23(Teta,W,Rr23,Imr23,E1,E3,E21e,E22e)
6400 CALL Fex(Teta,W,D,R5,I5,E1,E3,E21e,E22e)
6410 R12=Rr12^2+Imr12^2
6420 R23=Rr23^2+Imr23^2
6430 R1=Rr12
6440 I1=Imr12
6450 R2=Rr23
6460 I2=Imr23
6470 R=R2+R5-I2*I5
6480 I=I2+R5+R2*I5
6490 A6=R1+R
6500 B6=I1+I
6510 A7=1+R1*R-I1*I
6520 B7=I1+R+R1*I
6530 GOTO 6560
6540 A6=Rr12+Rr23+R5-Imr23*I5
6550 B6=Imr12+R5*Imr23+I5*Rr23
6560 A7=1+Rr12*(Rr23+R5-Imr23*I5)-Imr12*(R5*Imr23+I5*Rr23)
6570 B7=+Imr12*(Rr23+R5-Imr23*I5)+Rr12*(R5*Imr23+I5*Rr23)
6580 PRINT Rr12,Imr12,Rr23,Imr23,R5,I5
6590 PRINT A6,B6,A7,B7
6600 CALL Cdivid(A6,B6,A7,B7,Rr,Imr)
6610 Ref=Rr^2+Imr^2
6620 SUBEND
6630 |
6640 SUB Opt_h(Tetae,W,Hintl,Hfni,Hopt,Rmin,E3,E1,E21e,E22e)
6650 | A subprogram for finding the optimal thickness of the metal film at
6660 | which the coupling is maximum (REFLECTIVITY - minimum)
6670 | Teta - resonant angle in 'rad'
6680 | W - frequency of the source in 'Hz'
6690 | Hintl - initial thickness for the search in 'angstroms'
6700 | Hfni - final thickness for the search in 'angstroms'
6710 | Hopt - determined by this subprogram the value of the optimal thick-
6720 | ness in 'angstroms'
6730 | Rmin - the value of Reflectivity when H = Hopt
6740 | E3 - is for the prism
6750 Rmin=1
6760 H_step=50
6770 IF Hintl>580 AND Hintl<640 THEN H_step=1
6780 FOR Ha=Hintl TO Hfni STEP H_step
6790 Hmt=Ha+1.E-10
6800 CALL Refl(Tetae,W,Rr,Imr,Ref,R12,R23,Hmt,E3,E1,E21e,E22e)
6810 IF Ref<Rmin THEN Hopt=Ha
6820

```

```

6850 NEXT Ha
6860 SUBEND
6870
6880 SUB Fr12(Teta,w,Rr12,Imr12,E1,E3,E21e,E22e)
6890      ! Teta - is the angle of incidence
6900      ! W    - is the frequency of the light source
6910      ! Rr12 - is the real part of the reflection coefficient r12
6920      ! Imr12- is the imaginary part of the reflection coefficient r12
6930 E21=E21e
6940 E22=E22e
6950 A1=E21
6960 B1=E22
6970 Q=E21^2+E22^2
6980 S=SIN(Teta)*SIN(Teta)
6990 A2=1-E1+E21*S/Q
7000 B2=E1+E22*S/Q
7010 LOADSUB Csqrt FROM "Complex"
7020 LOADSUB Cabs FROM "Complex"
7030 CALL Csqrt(A1,B1,R1,I1)
7040 CALL Csqrt(A2,B2,R2,I2)
7050 R1=R1+COS(Teta)
7060 I1=I1+COS(Teta)
7070 R2=R2+SQR(E1)
7080 I2=I2+SQR(E1)
7090 R12=R1-R2
7100 Im12=I1-I2
7110 Rd12=R1+R2
7120 Imd12=I1+I2
7130 LOADSUB Cdivid FROM "Complex"
7140 CALL Cdivid(R12,Im12,Rd12,Imd12,Rr12,Imr12)
7150 SUBEND
7160
7170 SUB Fr23(Teta,w,Rr23,Imr23,E1,E3,E21e,E22e)
7180 E21=E21e
7190 E22=E22e
7200 S=SIN(Teta)*SIN(Teta)
7210 F=E3-E1*S
7220 A3=E21*E3^2-E1*S*E3^2
7230 B3=E22*E3^2
7240 IF F<0 THEN GOTO 7250
7250 R4=E21+SQR(F)
7260 I4=E22+SQR(F)
7270 R4=-E22+SQR(-F)
7280 I4=+E21+SQR(-F)
7290 CALL Csqrt(A3,B3,R3,I3)
7300 R34=R3-R4
7310 Im34=I3-I4
7320 Rd34=R3+R4
7330 Imd34=I3+I4
7340 CALL Cdivid(R34,Im34,Rd34,Imd34,Rr23,Imr23)
7350 SUBEND
7360
7370 SUB Fox(Teta,w,D,R5,I5,E1,E3,E21e,E22e)
7380 E21=E21e
7390 E22=E22e
7400 RAD

```

!real part of numerator  
 !imaginary part of numerator  
 !real part of denominator  
 !imaginary part of denominator

... magnitude in rad/m<sup>2</sup>

```

7430 Q=E21**2+E22**2
7440 S=SIN(Teta)*SIN(Teta)
7450 CALL Csqrt(E21,E22,Rn,In)
7460 G=1-E1*E21*S/Q
7470 H=E1*E22*S/Q
7480 CALL Csqrt(G,H,A2,B2)
7490 A5=-2*Ko*D*(In*A2+Rn*B2)
7500 B5=2*Ko*D*(Rn*A2-In*B2)
7510 GOTO 7570
7520 A1=+(-E1*S-E21)
7530 B1=-E22
7540 CALL Csqrt(A1,B1,A5,B5)
7550 A5=A5*2*Ko*D
7560 B5=B5*2*Ko*D
7570 CALL Cexp(A5,B5,R5,I5)
7580 SUBEND
7590 I
7600 DEF FNF(H)
7610 I Input thickness is in 'angstroms'
7620 COM E3,E21,E22,E1
7630 COM /Wp/ Wp
7640 COM /W/ W
7650 COM /K/ Kxliexp
7660 COM /Err/ Tetae,Wte,Rme
7670 COM /H_opt/ Hoptmt
7680 I
7690 Hmt=H*1.E-10 I thickness in meters
7700 CALL Filmdisp2(W,Wp,Tetae,Wte,Rme,Hoptmt,Hmt,E1,E3,Kxr,Kxi,Kxr,Kxi,Kxo1,Kxi1,K
7710 I NOTE I ALL WAVEVECTORS ARE IN NORMALIZED FORM !!!
7720 F=Kx11-Kxliexp
7730 I PRINT "H=";H,"Kx11=";Kx11,"Kxliexp=";Kxliexp,"(line 5070)"
7740 RETURN F
7750 FNEND
7760 I
7770 SUB Bisect(A,B,Maxbi,Tol,Deltax,Root(*),F_(*),Err(*),Nroots)
7780 OPTION BASE 1
7790 Baddta=(A)=B) OR (Maxbi<=0) OR (Tol<=0) OR (Deltax<=0) OR (Nroots<=0)
7800 IF Baddta=0 THEN 7860
7810 PRINT FNlin$(2);"ERROR IN SUBPROGRAM Bisect."
7820 PRINT "A=";A; " B=";B; " Maxbi=";Maxbi
7830 PRINT "Tol=";Tol; " Deltax=";Deltax; " Nroots=";Nroots;FNlin$(2)
7840 PAUSE
7850 GOTO 7730
7860 N=0
7870 Noroot=Nroots
7880 FOR I=1 TO Nroots
7890 Root(I)=9.999999E+99
7900 F_(I)=9.999999E+99
7910 Err(I)=9.999999E+99
7920 NEXT I
7930 X=A
7940 IF N=Noroot THEN SUBEXIT
7950 N=N+1
7960 Y=FNF(X)
7970 F=Y
7980 A=A+Deltax
7990 IF A>B THEN SUBEXIT
8000 X=A

```

```

8030 IF Prod>0 THEN 7970
8040 IF Prod<0 THEN 8140
8050 IF F<0 THEN 8080
8060 X=A-DeltaX
8070 Y=F
8080 Root(N)=X
8090 F_(N)=Y
8100 A=A+DeltaX
8110 Size=1.E-12
8120 Err(N)=Size
8130 GOTO 7930
8140 Left=A-DeltaX
8150 Right=A
8160 C=0
8170 X=(Left+Right)/2
8180 Y=FN(X)
8190 C=C+1
8200 IF C>Maxb1 THEN 8340
8210 IF ABS(Y)<Tol*FNMax(1,X) THEN 8290
8220 Prod=F*Y
8230 IF Prod<=0 THEN 8260
8240 Left=X
8250 GOTO 8170
8260 IF Prod=0 THEN 8290
8270 Right=X
8280 GOTO 8170
8290 Root(N)=X
8300 F_(N)=Y
8310 Size=Right-Left
8320 Err(N)=Size
8330 GOTO 7930
8340 PRINT FNLine(2); "MAX # OF BISECTIONS REACHED ON ROOT #";N
8350 PRINT "X BETWEEN ";Left; " AND ";Right
8360 PRINT "F(X)=";Y
8370 Size=Right-Left
8380 PRINT "ACCURACY TO ";Size
8390 PRINT "AVERAGE VALUE STORED IN Root(*) AS APPROXIMATE X";FNLine(2)
8400 Root(N)=(Left+Right)/2
8410 F_(N)=Y
8420 Err(N)=Size
8430 GOTO 7930
8440 SUBEND ;

```

```

8450 DEF FNMax(A0,A1,OPTIONAL A2,A3,A4,A5,A6,A7,A8,A9)
8460 Max=A0
8470 IF A1>Max THEN Max=A1
8480 IF NPAR=2 THEN RETURN Max
8490 IF A2>Max THEN Max=A2
8500 IF NPAR=3 THEN RETURN Max
8510 IF A3>Max THEN Max=A3
8520 IF NPAR=4 THEN RETURN Max
8530 IF A4>Max THEN Max=A4
8540 IF NPAR=5 THEN RETURN Max
8550 IF A5>Max THEN Max=A5
8560 IF NPAR=6 THEN RETURN Max
8570 IF A6>Max THEN Max=A6
8580 IF NPAR=7 THEN RETURN Max
8590 IF A7>Max THEN Max=A7

```

```

76 8610 IF A9>Max THEN Max=A9
8620 IF NPAR=9 THEN RETURN Max
8630 IF A9>Max THEN Max=A9
8640 RETURN Max
8650 FNEND I

```

```

8660 I
8670 SUB Filmdisp2(W,Wp,Tetae,Wte,Rme,Hopt,H,E1,E3,Kxr,Kx1,Kxor,Kxoi,Kxin,K
8680 I This subprogram calculates the  $OX$  - wavevector of a plasmon propaga
8690 I for EXPERIMENTALLY MEASURED resonant angle Tetae, half-width Wte,
8700 I minimum of reflectivity Rmin
8710 I The other interface of the metal film is with dielectric medium III
8720 I E1 - relative dielectric permittivity of the medium I (air)
8730 I W - is the frequency of the source of light in Hz
8740 I H - is the thickness of the metal film in 'meters'
8750 I Kxr - REAL part of  $OX$  - wavevector of plasmon in metal film
8760 I Kx1 - IMAG. part of  $OX$  - wavevector of plasmon in metal film
8770 C=2.998E+8
8780 Ko=W/C
8790 S2=SIN(Tetae)*SIN(Tetae)
8800 E21=E1+E3+S2/(E1-E3+S2)
8810 IF H<Hopt THEN K=-i
8820 IF H=Hopt THEN K=0
8830 IF H>Hopt THEN K=+i
8840 E22=Wte*(1+K*SQR(Rme))*E1^2+E3*TAN(Tetae)/(2*(E1-E3+S2))
8850 I PRINT "E21_exp = "E21,"E22_exp = "E22,"(line 8720)
8860 Dnm=(E1+E21)^2+E22^2
8870 Ao=(E1+E21*(E1+E21)+E1+E22^2)/Dnm
8880 Bo=E22*E1^2/Dnm
8890 A4=E1+E3+E21*(E3-E1)
8900 B4=E22*(E3-E1)
8910 A7=2+E1+E21
8920 B7=2+E1+E22
8930 A8=E21^2-E22^2-E1^2
8940 B8=2+E21+E22
8950 I LOADSUB Cabs FROM "Complex"
8960 I LOADSUB Csqrt FROM "Complex"
8970 CALL Csqrt(E1+E21,E22,A1,B1)
8980 CALL Csqrt(Ao,Bo,K1,K2)
8990 U=C/Wp
9000 Kxor=Ko*K1+U
9010 Kxoi=Ko*K2+U
9020 I LOADSUB Cdivid FROM "Complex"
9030 CALL Cdivid(-2*Ko+H+E22,+2*Ko+H+E21,A1,B1,A2,B2)
9040 I LOADSUB Cexp FROM "Complex"
9050 CALL Cexp(A2,B2,A3,B3)
9060 CALL Csqrt(A4,B4,A5,B5)
9070 CALL Cdivid(E3-A5,-B5,E3+A5,+B5,A6,B6)
9080 I
9090 CALL Cdivid(A7,B7,A8,B8,A9,B9)
9100 I LOADSUB Cmult FROM "Complex"
9110 CALL Cmult(A3,B3,+A6,+B6,A10,B10)
9120 CALL Cmult(A10,B10,A9,B9,A11,B11)
9130 CALL Cmult(Kxor,Kxoi,+A11,+B11,Kxr,Kx1)
9140 I
9150 Kx1i=Kx1-Kxoi
9160 SUBEND

```

```

9180 SUB Opt_n_1(Tetae,Wte,Rme,E1,E3,Hopti)
9190 S2=SIN(Tetae)*SIN(Tetae)
9200 E21e=E1+E3-S2/(E1-E3+S2)      ! Experimentally found E21(w)
9210 K=-1
9220 E22e=Wte*(1+K*SQR(Rme))*E1^2+E3*TAN(Tetae)/(2*(E1-E3+S2)^2)
9230 E22o=Wte*E1^2+E3*TAN(Tetae)/(2*(E1-E3+S2)^2)
9240 Delta=E22o-E22e              ! At H=Hopt
9250 D1(J)=Delta                  ! Lines 1580 - 1670
9260 Dr(J)=D1(J)-D1(J-1)         ! are a switch for Eta
9270 IF Dr(J)>0 AND J>1 THEN K=+1 ! as a function of R min
9280 IF Dr(J)<0 THEN K=-1
9290 IF J=1 THEN K=-1
9300 Prod=Dr(J)*Dr(J-1)
9310 IF Prod<0 AND J>1 THEN Hopti=H
9320 E22e=Wte*(1+K*SQR(Rme))*E1^2+E3*TAN(Tetae)/(2*(E1-E3+S2)^2)
9330 SUBEND

```

Declaration

This thesis is my original work and has not been presented for a degree in any other University.

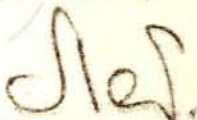
ABDURAHMAN AHMED



Approval

This thesis has been submitted for examination with my approval as University Advisor.

Approved by



Dr. D.A. Letov

Dr. D.A. Letov